Title: Conducting Polymer-Noble Metal Nanoparticle Hybrids: Synthesis Mechanism Application

Authors: Jie Han, Minggui Wang, Yimin Hu, Chuanqiang Zhou, Rong Guo

PII: S0079-6700(17)30083-7
DOI: http://dx.doi.org/doi:10.1016/j.progpolymsci.2017.04.002
Reference: JPPS 1024

To appear in: *Progress in Polymer Science*

Received date: 21-7-2016
Revised date: 14-1-2017

Please cite this article as: Han Jie, Wang Minggui, Hu Yimin, Zhou Chuanqiang, Guo Rong.Conducting Polymer-Noble Metal Nanoparticle Hybrids: Synthesis Mechanism Application.*Progress in Polymer Science* http://dx.doi.org/10.1016/j.progpolymsci.2017.04.002

Conducting Polymer-Noble Metal Nanoparticle Hybrids: Synthesis, Mechanism and Application

Jie Han*, Minggui Wang, Yimin Hu, Chuanqiang Zhou, Rong Guo*

School of Chemistry and Chemical Engineering, Yangzhou University, Yangzhou, 225002, Jiangsu, P. R. China

***Corresponding authors:** hanjie@yzu.edu.cn; guorong@yzu.edu.cn; Fax: +86 514 8797 5568; Tel: +86 514 8797 5590

ABSTRACT

Recent research has established growing research interest in subject of conducting polymer (CP)-based hybrids due to their novel properties and potential applications in diverse fields. The incorporation of CPs with other materials can produce new hybrids showing distinct properties that are not observed in the individual components. Among numerous CP-based hybrids, CP and noble metal nanoparticle (NMNP) hybrids have attracted the most intensive attention in the past few years. The numerous functional groups and tunable chemical structures through redox in the main chains of CPs, make them as ideal supporters for NMNPs. The compact interactions and synergistic effects between CPs and NMNPs contribute to the increased performances in diverse applications. The purpose of this review focuses on state-of-the-art synthetic strategies, mechanisms and applications involved in CP-NMNP hybrids. Herein, CPs used are polyaniline (PANI), polypyrrole (PPY), polythiophene (PTH) and their derivatives; while NMNPs mainly refer to Au, Ag, Pt and Pd nanoparticles. Specifically, the topics include: 1) strategies and mechanisms involved in the synthesis of CP-NMNP hybrids; 2) potential applications of CP-NMNP hybrids in fields of catalysis, sensor, surface-enhanced Roman scattering (SERS), device and others. Finally, prospects and challenges for making advanced CP-NMNP hybrids are discussed.

Keywords: Conducting polymer; Polyaniline; Noble metal nanoparticle; Au, Hybrid; Catalysis; Sensor

Nomenclature

AAO	anodic aluminum oxide
AD	asymmetry degree
4-AP	4-aminophenol
APS	ammonium peroxydisulfate
CMC	critical micelle concentration
CP	conducting polymer
CTAB	cetyltrimethylammoniumbromide
CSA	D-camphor-10-sulfonic acid
DNA	deoxyribonucleic acid
FTIR	Fourier-transform infrared
GO	graphene oxide
GOx	glucose oxidase
HEPES	2-[4-(2-hydroxyethyl)-1-piperazinyl]-ethanesulfonic acid
k_{app}	apparent rate constant
LB	Langmuir-Blodgett
MWNT	multiwall carbon nanotube
NMNP	noble metal nanoparticle
NMP	1-methyl-2-pyrrolidinone
4-NP	4-nitrophenol
OANI	oligoaniline
OFET	organic field effect transistor
ORR	oxygen reduction reaction
P3MeT	poly(3-methylthiophene)
PAA	polyacrylic acid
PANI	polyaniline
PATP	poly(4-aminothiophenol)
PC	polycarbonate
PEDOT	poly(3,4-ethylenedioxythiophene)
POMA	poly(*o*-methoxy aniline)
POPD	poly(*o*-phenylenediamine)
POT	poly(*o*-toluidine)
PPY	polypyrrole
PS	polystyreme
PSPAA	$polystyrene_{154}$-block-$poly(acrylic\ acid)_{60}$
PTFE	poly(tetrafluoroethylent)
PTH	polythiophene
PVP	poly(vinylpyrrolidone)
RNA	ribonucleic acid
SCE	saturated calomel electrode
SDS	sodium dodecyl sulfonate
SERRS	surface-enhanced resonance Raman scattering
SERS	surface-enhanced Raman scattering
m-SiO_2	mesoporous SiO_2
SWNT	single-walled carbon nanotube
TA	thioglycolic acid
Tween-80	polyoxyethylenesorbitan monooleate
TSA	*p*-toluene sulfonic acid

Contents

1. Introduction

Conducting polymers (CPs) have emerged as an attractive subject of great interes in polymer science in the last several decades. They are inherently conducting in nature due to the presence of a conjugated π electron system in their structures. In view of its environmental stability, low cost of monomer, ease of synthesis, and special doping chemistry, polyaniline (PANI) is the most intensively investigated among the family of CPs, followed by polypyrrole (PPY) and polythiophene (PTH). **Fig. 1** shows the oxidative polymerization processes, the reversible acid/base doping/dedoping, and redox chemistry of PANI. PANI is normally prepared by the chemical oxidative polymerization of aniline using a strong oxidant, typically ammonium peroxydisulfate (APS) in an acidic aqueous solution. This produces the acid doped, conductive emeraldine salt form, that may be dedoped by a base to yield the emeraldine base form. In addition to the intermediate oxidation state of emeraldine base, PANI also possesses several other oxidation states, such as the fully oxidized pernigraniline and the fully reduced leucoemeraldine, that may be reversibly changed through chemical or electrochemical routes. Several reviews are available detailing the synthesis, structures, processing and applications of PANI. For example, Kang et al [1] summarized the explicit and quantitative dealings with the various intrinsic oxidation states of PANI and its derivatives and Bhadra et al. [2] reviewed the synthesis, processing and applications of PANI. In addition, nanostructured CPs and their formation mechanisms has also been reviewed [3-7].

Fig. 1

Hybrids of CPs have become an increasing subject in CPs. Hatchett et al. [8] reviewed the hybrids of intrinsically CPs as sensing nanomaterials several years ago. The incorporation of a co-component into CPs may endow them with enhanced properties as compared to the individual ones. Various other functional materials have been introduced into CPs, such as carbon-based materials (carbon nanotubes and graphene), metal and metal oxides, and biological materials [9-11]. In particular, combination of CPs with noble metal nanoparticles (NMNPs) has generated great research interest [12, 13]. NMNPs, such as Au, Ag, Pt, Pd, et. al., have been the research

focus for material scientists for decades because of their unique optical and electronic properties together with their various applications in fields such as electronics, photonics, catalysts, nano- and biotechnology [14-18]. Usually, NMNPs are capped with a stabilizer, involving alkanethiols, amines, nucleotides, and polymers [19]. The basic idea is to direct the nucleation and growth of NMNPs, meanwhile, avoid the aggregation of NMNPs resulted from the van der waals attraction. As mentioned, CPs possess particular multifunctional groups, agree well with the fundamental requirements to stabilize NMNPs.

This review mainly focuses on recent advances in the synthesis and applications of CP-NMNP hybrids. Different strategies are detailed and mechanisms involved are summarized. This review provides a general overview of recent advances in this field and stimulate new research ideals for designed synthesis of CP-based functional hybrids with predominant properties and practical applications. **Table 1** gives an overview of methods for the preparation of CP-NMNP hybrids.

Table 1

2. Strategies and mechanisms involved in the synthesis of CP-NMNP hybrids

2.1. CPs and NMNPs

The most common way make CP-NMNP hybrids is by mixing the pre-synthesized individual components with desired size and morphology. Utilization chemical and electrostatic interactions between CPs and NMNPs, NMNPs are normally adsorbed on surfaces of CPs to form CP-NMNP hybrids.

2.1.1. Electrochemical route

In this approach, CPs are produced by oxidative electropolymerization of monomers and NMNPs are obtained by the reduction of noble metal salts through electrodeposition [20-28]. The number of cycles is varied in order to obtain films of different thickness and NMNPs with different amount. Hatchett et al.[29], synthesized PANI through electropolymerization of aniline in the presence of HBF_4, that was cast on Pt electrode to form dense PANI films with 2-4 μm thick. The addition of $AuCl_4^-$ formed a complex with PANI at the nitrogen linkage subsequently reduced by cyclic voltammetry to form metallic Au clusters (~ 300 nm in diameter) on surfaces of PANI films. The imino groups within PANI show a high affinity for both $AuCl_4^-$ and Au clusters [30].

Atom-by-atom deposition of Au into PANI film through a repeated cyclic pathway have been reported by Jonke and coworkers [31-35]. By controlling the potential, they kept PANI in an oxidized state first while exposing it to a $AuCl_4^-$ solution to form a PANI-$AuCl_4^-$ complex, that was then reduced to atomic Au by sweeping the potential negative. Once reduced, the imine sites on PANI became available for the next Au deposition cycle. The repeated deposition of Au atoms followed a cyclic pathway. The amount of Au deposited using this method was consistent for each repeated cycle. Rinsing the excess $AuCl_4^-$ anions from the film before reduction was a crucial step to avoid uncontrolled $AuCl_4^-$ reduction.

Generally, the morphology of CP-NMNP hybrids by an electrochemical route depends on substrate morphology. In addition to forming PANI dense films, PANI films with granular morphology were obtained by applying cyclic voltammetry scans on Ti electrode in H_2SO_4 solution, following Au nanoparticles dispersed on the PANI/Ti electrode by cathodic electrodeposition under galvanostatic conditions in a bath containing $KAu(CN)_2$ in the presence of a citrate buffer with pH=4 [36]. Au nanoparticles with 60-90 nm diameters were distributed in an almost homogeneous manner at the surface of the PANI films. PANI film with fibrous morphology was deposited by cyclic voltammetry on an ITO coated glass electrode in the presence of $HClO_4$ [37]. The PANI nanofibers (diameter of 150-200 nm) form a cris-cross network running over the entire electrode surface. Then Au nanoparticles were deposited on PANI/ITO coated glass electrode via chronoamperometry with $HAuCl_4$ used as an electrolyte. PANI nanofibers along with Au nanoparticles (less than 100 nm) on their walls were obtained. PANI nanofibers deposited with Au nanoparticles (13 nm) on glassy carbon electrode [38] and PANI nanowires (diameter of 250-320 nm) deposited with Au nanoparticles (70-120 nm) on Au electrode [39] using similar route were also reported.

In a more straightforward way, CPs may be electropolymerized on an electrode surface and then immersed in an NMNPs colloidal solution for a specified duration to capture NMNPs on the CP surface [40]. Cho et al. [41] prepared CP films of PPY, poly(3-methylthiophene) (P3MeT) and poly(3,4-ethylenedioxythiophene) (PEDOT) as electrochemical synthesized on a Au electrode. These were immersed in a Au or Ag colloid solution. A few Au/Ag nanoparticles were seen on the PPY film, whereas Au/Ag nanoparticles were successfully drawn onto the surfaces of P3MeT and PEDOT. Results confirmed that Au and Ag nanoparticles were predominantly linked with the

sulfur atoms via chemical bonding. Similar results have been reported elsewhere [42-46]. In addition to chemical bonds, electrostatic interaction have been used to capture NMNPs. In Guo et al. [47] electrochemically formed PANI nanowires in doped state on glassy carbon electrodes; trisodium citrate-protected negatively charged Au nanoparticles (20 nm) were adsorbed on the surfaces of the PANI nanowires electrostatic interactions. NMNPs could also be introduced before the electropolymerization to form CPs [48]. For example, PANI-Au hybrids were obtained by electropolymerization of aniline in the presence of ˙Au-Nafion [49]; PANI-Pt hybrids were synthesized by electropolymerization of aniline in the presence of phosphododecamolybdate-stabilized Pt nanoparticles [50, 51]; PEDOT-Au hybrids were synthesized by electropolymerization of 3, 4-ethylenedioxythiophene in the presence of 3,4-ethylenedioxythiophene-protected Au nanoparticles (10 nm) [52]; PANI was grafted on the surfaces of a Ag microparticle-modified electrode through electropolymerization of aniline [53]. Unlike adsorbtion on CP surfaces, in this case, NMNPs were normally surrounded and embedded in a CP matrix, to which they were stably attached. Kim et al. [54] prepared a PANI-Au patterned substrate by electrochemical polymerization from a Au-patterned 4-nitrobenzenethiol monolayer with Au nanoparticles selectively adsorbed onto the amine groups of the film; PANI was also found to form exclusively at the amine groups.

PANI chains were grafted onto functionalized multiwall carbon nanotubes (MWNTs) by electropolymerizing a mixture of aniline and MWNTs using cyclic voltammetry [55]. The as-formed hybrid film on electrode contained MWNT and PANI with the presence of PANI over the entire surface of MWNT. Au nanoparticles were uniformly distributed on the film of MWNT/PANI by electrochemical reduction of $HAuCl_4$.

In addition to dissolution in the reaction medium, the monomers may also be cast on electrode or NMNP surfaces [56, 57]. Gopalan et al. [58] reported that inclusion complex of 4-aminothiophenol with β-cyclodextrin was cast on the surface of the glassy carbon electrode as the electroactive layer. Au nanoparticles (10-15 nm) were incorporated into a film of poly(4-aminothiophenol) (PATP) simultaneously by the electrolysis of H_2SO_4 solution of $HAuCl_4$ using a repetitive potential scan between 1.0 and -0.1 V. PATP and Au nanoparticles were simultaneously formed on the glassy carbon electrode. Frasconi et al. [59] reported that Au nanoparticles (4 nm) functionalized with 2-mercaptoethanesulfonic acid and 4-aminothiophenol

were adsorbed on surfaces of Au electrode, and then the surface-tethered 4-aminothiophenol groups were electropolymerized in a 0.1 M 2-[4-(2-hydroxyethyl)-1-piperazinyl]ethanesulfonic acid (HEPES) buffer solution.

As-synthesized CP-NMNP hybrids may be well-shaped by electrochemical reactions at the electrode surface with the aid of a template [60, 61]. In contrast to the solution-based chemical reaction route that normally occurs in a bulk solution, the electrochemical reaction happens at theelectrode/solution interface. In order to shape the resulting deposited CPs and NMNPs, a porous membrane is always attached to electrode surfaces. Porous anodic aluminum oxide (AAO) and polycarbonate track-etched membranes have been well-established as template for CPs nanorods and nanotubes through the electrochemical route [62-67]. In order to form CP-NMNP core-shell nanostructures, Lahav et al. [68] immersed an AAO membrane containing PANI nanotubes in a commercially available Au electroplating solution (pH ≈ 10.2) and electrodeposited Au by reduction starting from the Au cathode. The strongly alkaline Au solution simultaneously caused dissolution and widening of the pores of the AAO template as well as prevented the PANI nanotubes from re-swelling to the width of the pores. An annular space, therefore, formed between the tubes and the membrane. As PANI is an insulator at pH 10.2, the Au deposited on the Au cathode, and not on the PANI tubes, that acted only as templates for formation of the Au shells. The length of the Au shell were controlled by performing a one-step electrodeposition of the Au shell around the polymer tube, and tuning the amount of charge that passed through the electrochemical cell during this deposition, (**Fig. 2**). Moreover, in order to form the segmented structures, Au nanorods were first electrodeposited in an AAO membrane, a self-assembled monolayer of thioaniline nucleated the growth of PANI on top of Au nanorods through electropolymerization to form the PANI nanotube-Au nanorod segmented structures. Zhang et al. [69] reported that Au nanorods was formed by a electrodeposition method using the AAO membrane, and then a thin PANI-poly(4-styrenesulfonate) hybrid layer was electropolymerized on the surface of the Au nanorods after completely removal of the AAO membrane. The study found that by decreasing the thickness of the hybrid layer, a proportion of ordered PANI chains increased on the surface of the Au nanoarray, and fast electron transfer took place between the hybrid layer and the electrode surface.

Fig. 2

Callegari et al. [70] reported an electrochemical template-based strategy using polycarbonate track-etched membrane to prepare well-shaped and mechanically robust tri-segmented Au-PEDOT-Au and tetra-segmented Au-PEDOT-PPY-Au nanowires. Electrodeposition of Au was performed by cycling the potential of the working electrode from 0.7 to 0 V using a cyanide-free solution (KCl, K_2HPO_4, and $HAuCl_4$ in deionized water). Electropolymerization of 3,4-ethylenedioxythiophene was carried out by cyclic voltammetry from an aqueous solution containing $LiClO_4$ and various monomer concentrations. During the whole electrochemical synthesis, the polycarbonate membrane template was not removed, and the formation of CPs was believed to be rooted on the top surfaces of NMNPs, confined in the channel of porous membrane, or *vice versa*. Finally, multisegmented nanowires of CP-NMNP hybrids were controllably formed (**Fig. 3**).

Fig. 3

Use of the nanoporous Au films as an electrode, the electrochemical polymerization of aniline in acid solution led to the formation of three-dimensional bicontinuous nanoporous PANI-Au hybrid films (**Fig. 4**) [71].

Fig. 4

2.1.2. Chemical route

Typically, NMNPs are synthesized and suspended in a solvent and CPs are normally dissolved in another solvent. After the two solutions are mixed, solvents are evaporated, leading to the formation of CP-NMNP hybrid film. The CPs may be prepared using APS or H_2O_2 oxidant agent and the NMNPs may be obtained by reduction of noble metal salts using trisodium citrate, sodium borohydride, hydrazine hydrate, etc., as reducing agents. The compositions of hybrids may be simply varied by controlling the concentration of solutions [72, 73]. As for PANI, it is insoluble in common organic solvents (such as chloroform, xylene, tetrahydrofuran, etc.) and mostly soluble in

1-methyl-2-pyrrolidinone (NMP) and may be cast into a flexible film with residual NMP, about 10-18% by weight, as a plasticizer. As a result, NMP is often chosen as a suitable solvent for dissolving PANI [74, 75]. Afzal et al. [76] mixed the NMP solution of PANI emeraldine base with Au nanoparticles in NMP solution, and then the mixture was poured in Petri dish and the solvent was evaporated at 120 °C for 16 h to cast the PANI-Au hybrid film. Although most of the Au nanoparticles distributed in the polymer matrix had a mean diameter of ≈ 20 nm (similar to that of original Au nanoparticles), some agglomerates were formed, and the number of these aggregated particles increased with increasing concentration of the Au nanoparticles. The authors ascribed the aggregation phenomenon to the synthesis conditions with high temperature and long aging time. Results from Fourier-transform infrared (FTIR) spectroscopy indicated that the Au nanoparticles might reside in the vicinity of the imine nitrogen of PANI. Izumi et al. [77] reported that the emderldine base PANI concentration played a critical role in determining the degree of Au nanoparticles aggregation, and the interaction of emderldine base PANI with Au or Ag colloids were probed by using surface-enhanced resonance Raman scattering (SERRS).

Tanami et al. [78] employed the Langmuir-Blodgett (LB) method to deposit multilayers of PANI and mercaptoethane sulfonate-stabilized Au nanoparticles, where the electrostatic interaction between the negatively charged Au nanoparticles in the subphase and the positively charged PANI at the air-water interface was thought to assist the deposition of PANI-Au hybrid film onto a solid support (**Fig. 5**). They found that the acidity of the subphase as well as the nanoparticles concentration were used to tune the density of Au nanoparticles in the monolayer. Poly(3-hexylthiophene)-Au hybrid film was also maintained using similar method [79]. In addition, PANI-Au [61, 80-82], and PANI-Pt [83] hybrid films were formed through the electrostatic layer-by-layer self-assembly process.

Fig. 5

CPs suspended in a poor solvent maintain their original nanostructure, and the complex with NMNPs will lead to CP-NMNP hybrids with the desired configuration. The driving forces for NMNPs adsorbed on surfaces of CPs also rely on chemical and electrostatic interactions among them [84, 85].

Spherical PANI nanostructures are normally synthesized using polystyreme (PS) as template through a chemical polymerization route. For example, PS nanospheres (400 nm in diameter) were used as template for the formation of PS-PANI core-shell spheres, followed by immersing in Au (20 nm in diameter) colloidal solution for a specified duration to capture Au nanoparticles on surfaces of PANI through electrostatic interactions, leading to the formation of PS-PANI-Au three-component hybrids [86-88]. The PS core in PS-PANI-Au three-component hybrids may be selectively removed through dissolution with tetrahydrofuran, resulting in PANI-Au hollow hybrids (**Fig. 6**) [89].

Fig. 6

For endowing the CP-NMNP hybrids a magnetic property, superparamagnetic Fe_3O_4 microspheres showing dual functionalities of template and magnetism may be chosen as magnetic template for loading CPs and NMNPs. Xuan et al. [90] reported the formation of Fe_3O_4-PANI-Au core-shell hybrids. In the preparation, the superparamagnetic Fe_3O_4-PANI with well-defined core-shell nanostructure was first synthesized via an ultrasound-assisted *in situ* surface polymerization method with poly(vinylpyrrolidone) (PVP) modifier, and then Au nanoparticles (4 nm) were assembled onto the surface of the as-synthesized Fe_3O_4-PANI core-shell microspheres *via* electrostatic attraction (**Fig. 7**). Similar structures could also be found elsewhere [91, 92].

Fig. 7

Magnetic Fe_3O_4 particles with diameters limited to nanometers, may be assembled in a polymer shell. For example, Kong et al. [93] formed PS-Fe_3O_4-PANI core-shell hybrids by coating a layer of PANI on an assembly of Fe_3O_4 nanoparticles (5 nm) on the surfaces of sulfonated PS. Hollow spheres were obtained after Au nanoparticles adsorption and PS template removal, PANI-Fe_3O_4-Au.

CPs with one-dimensional nanostructures of typical nanofiber/nanowire and nanotube have been used to capture NMNPs to form one-dimensional CP-NMNP hybrids. For example, self-doped PANI nanofibers [94, 95], PANI [96-98] and PPY [99] nanotubes, and PANI coated

carbon nanotubes [100-103] were used to immobilize Au nanoparticles through the electrostatic effect to fabricate the CP-NMNP hybrids.

2.2. CPs and noble metal ions

CP-NMNP hybrids may be formed by *in situ* reduction of noble metal ions on pre-synthesized CPs with pre-determined nanostructures. Nanostructured CPs not only supply a support for NMNPs, but also act as an effective reductant for the reduction of noble metal ions to form NMNPs.

The concept of making CP-NMNP hybrids using oxidation-reduction interaction between CPs and noble metal ions was primarily reported by Kang and coworkers, where the CP of PANI was utilized to recover Au from chloroauric acid solution [104]. As shown in **Fig. 1**, PANI possesses several oxidation states, from the fully oxidized pernigraniline to the fully reduced leucoemeraldine. The electrochemical oxidation and reduction in aqueous HCl solution in the pH range of 1-4 involves the following reactions [105]:

Scheme 1

Scheme 2

Scheme 3

Scheme 4

The oxidation of PANI from leucoemeraldine to emeraldine salt (Scheme 1) is pH independent and has an oxidation potential of about 0.1 V *vs* SCE, while the oxidation of PANI from emeraldine salt to pernigraniline (Scheme 2) is pH dependent and has an oxidation of about 0.7 V *vs* SCE. Treatment of pernigraniline with HCl gives rise not to protonated pernigraniline but involves reduction to produce a emeraldine salt (reverse reaction of Scheme 2) [106]. Thus, in chloroauric acid solution, the imine nitrogens of the emeraldine base are first protonated by HCl (Scheme 3). PANI has a reduction potential slightly lower than typical Au, Ag, Pt and Pd ions [107, 108]. As a consequence, for example, the presence of Au ions results in the spontaneous deprotonation *via* oxidation of PANI from emeraldine salt to pernigraniline and reduction of Au ions to metallic state (Scheme 4). The pernigraniline, in turn, is readily reprotonated and reduce to

emeraldine salt in an acidic medium (reverse reaction of Scheme 2), providing a redox reaction recycle [109]. Similar reactions occur with other CP and metal ion pairs. e.g., with PPY and Pd ions [110, 111].

The synthetic parameters that influence the recovery of Au by PANI polymer film were emphasized in early reports. The Au reduction rate was strongly dependent on the intrinsic oxidation state of PANI, pH, reaction temperature and surface area of PANI polymer: 1) PANI in the fully reduced state of leucoemeraldine led to increased Au reduction rate due to addition contribution from Scheme 1; 2) higher pH value resulted in decreased Au reduction rate (referring to PANI emeraldine salt), which agreed well with the electrode potential response with acidity of the solution; 3) higher temperature led to increased Au reduction rate as the redox reaction was endothermic; 4) higher effective contact area between PANI film and chloroauric acid solution led to increased Au reduction rate (implying PANI nanostructures should show enhanced Au reduction rate than PANI film) [104, 112]. The PANI film in leucoemeraldine state could accumulate up to five times its own weight of Au (Au/monomer mole ratio > 2) [104]. During the recovery of Au by PANI film, the PANI underwent degradation, ring substitution by chlorine, and a loss of material into solution. The degradation was due to the higher propensity of the polymers when existing in a higher oxidation state to undergo hydrolysis reactions to soluble products [112].

In the past two decades, more attention has been paid to the rational nanoscale configuration control over CP-NMNP hybrids as morphology and size of their components of CPs and NMNPs and interactions between them play vital roles in determining their properties and applications. In general, the size of NMNPs is largely depended on the nature and morphology, doping state, and even surface texture of CP nanostructures, whereas the morphology of CP-NMNP hybrids mainly lies on the configuration of CP nanostructures.

2.2.1. Without additive

In the standard procedures for the synthesis of PANI *via* the oxidation polymerization of aniline by ammonium persulfate in strong acid solution (such as 0.5 M H_2SO_4) at 0 ºC, PANI powders with irregular agglomerates were normally formed [113]. Wang et al. [114] reported that after alkali dedoping in the emeraldine base state PANI powders were used to obtain Au nanoparticles in PANI *via* the reduction of $AuCl_3$ by PANI in either aqueous or NMP media. The size of the Au

nanoparticles depended on the reaction medium and the initial ratio of metal ions to PANI. The Au nanoparticles were about 20 nm and 50-200 nm when the reduction of $AuCl_3$ was carried out in NMP solutions of PANI and in the powder form of PANI in aqueous media, respectively. Larger Au nanoparticles were obtained with higher molar ratio of $AuCl_3$ to PANI. The limited sites for Au accumulation accounted for the increase in Au size. Moreover, the largest Au nanoparticles were obtained when an acidic medium was used, attributed to possible agglomeration resulted from increased reaction rate. In the case of making Pd nanoparticles, as the reaction of emeraldine base powder with $Pd(NO_3)_2$ was very slow in both aqueous and NMP solutions, PANI in the leucoemeraldine state instead of the emeraldine base state was used to obtain Pd nanoparticles with size of about 150 nm. Using a similar synthesis but with PANI in emeraldine salt state, Pd nanoparticles with size of about 1.5 nm were achieved in PANI and PPY matrix [115], which might be caused by the low reaction rate.

Spherical PANI coated on SiO_2 [116] or PS [117] surfaces was studied for deposition of Au nanoparticles. Although it was not possible to obtain homogeneous Au coatings, PS-PPY core-shell nanospheres randomly decorated with 40–60 nm Au nanoparticles obtained under conditions of dedoped CPs and high pH = 7 [117] were believed to slow down the reaction rate and favor the formation small-sized Au nanoparticles. Spherical PPY nanopsheres (50-150 nm) were also applied as reactive template for loading Au nanoparticles, where 100-200 nm Au nanoparticles were agglomerated on the PPY particle surface [118]. In addition, 1, 5-naphthalene sulfonic acid-doped PEDOT hollow spheres (538 nm in diameter) were treated with Ag ions, and PEDOT-Ag yolk-shell nanostructures were fabricated with Ag size of 80-180 nm. The confinement of Ag inside PEDOT shell might be related to the special treatment of removing unwanted Ag ions outside before redox reaction [119].

In comparison with PANI powders and latex particles, PANI nanofibers show obvious advantageous of high surface area and dispersion ability in aqueous solution, and have been used to prepare Au nanoparticles limited to several nanometers. Several groups [120-127] reported that a relatively uniform distribution of nanometer-sized Au nanoparticles were created by controlling the time and temperature of a reaction between dedoped PANI nanofibers and chloroauric acid. The temperature played the determining role in control the size of Au nanoparticles. For example, when the reaction and dialysis purification were both controlled below 25 ºC, the average size of

Au nanoparticles was in the range of 1-6 nm (**Fig. 8**). However, although PANI nanofibers provide some stabilization for particle growth, the interactions between the PANI chains and Au nanoparticles are not strong enough to guarantee their long-term stability. Therefore, Au nanoparticles with size < 1 nm on PANI nanofibers tend to form sizable aggregates and crystallites [125]. Similar phenomena were also evidenced in the case of using Fe_3O_4-PANI core-shell spheres for Au deposition [128]. When HCl-doped PANI nanofibers were used, Au nanoparticles with similar size of about 2 nm on PANI nanofibers were also attained [129]. In fact, acid protonating PANI was not important for the ability of PANI to reduce Ag ions and also had little effect on the size of Ag nanoparticles [130].

Fig. 8

Moreover, PANI with other morphology and hybrid with other materials, have been applied as reactive support for loading NMNPs. For example, PANI nanotubes were used to load Ag globular and triangular nanoparticles with size of about 50-120 nm [4, 131-133]; sulfonated PANI nanotubes with sulfonic groups introduced in the main chains of PANI were used to load Au nanoplates (80-200 nm) [134, 135]; fibrillar PANI sulfonic acid/ribonucleic acid (RNA) hybrids were used to load Au nanoparticles (~50 nm), where the Au nanoparticles showed as a mixture of different shaped Au nanoparticles (triangular, pentagonal, hexagonal, spherical etc.), and flower like and spherical morphology of Au nanoparticles were maintained by altering the composition between PANI and RNA [136]; HCl-doped PANI-PPY nanofibers (100-200 nm in diameter) were used to load Ag nanocubes (50-200 nm in diameter), and an increased PPY content in PANI-PPY nanofibers led to an increase in Ag particle size accompanied by a decrease in surface coverage [137]; HCl-doped PANI-coated cellulose fibers (20 μm in diameter) were used to load Ag nanoparticles (50 nm in diameter) [138]; phosphotungstic acid-doped PANI-coated multi-wall carbon nanotubes were used to load Pd (10-20 nm), Pt and Rh (2-4 nm) nanoparticles by the microwave-assisted polyol method [100]. Moreover, Au nanoparticles with hexagonal, pentagonal, triangular, rod-like structures were reported through a interfacial redox process using poly(*o*-methoxy aniline) (POMA) polymer, where the transfer of Au nanoparticles from aqueous to organic phase was accomplished using the reducing and solubility properties of POMA in

chloroform. The formation of differently shaped nanoparticles was proposed from catalytic reduction of Au ions by POMA on the Au seed surface followed by the growth of nanoparticles from the exposed Miller planes of seed surfaces [139].

In the case of CP films/membranes, the loaded NMNPs are always shown as micro-sized complex structures. Xia et al. [140] reported that Au quasi microspheres deposited on the PANI/polyacrylonitrile blend films were obtained. Shih et al. reported that fractal-like Pt microparticles conglomerates of many small Pt nanoparticles (<10 nm) were fabricated on camphorsulfonic acid-doped PANI membranes, whereas sheet-like Pt microparticles composed of smaller densely packed Pt nanoparticles were fabricated on undoped PANI membranes [141]. Gao et al. [142] reported that Pd particles grown on top of the porous PANI membrane (Pt size: 200 nm) and on top of the dense PANI film (Pt size: 500 nm) both consisted of many much smaller Pt nanoparticles (13 nm) were obtained. Wang and coworkers [143-145] reported that homogeneous Ag nanosheet assemblies with well-defined three-dimensional nanostructures were fabricated on PANI membranes. They also showed that by varying the nature of the dopant of PANI membranes, Ag nanostructures with fiber, sheet, cube, yarn-ball, and leaf-like morphologies were fabricated. Although the detailed growth mechanism related to the dopant-dependent morphology remain unknown, the morphological difference corresponding to various dopants was ascribed to influence by the surface energy of the membrane (manifested by the water contact angles) that were tuned by the nature of the dopants and the redox states of the PANI membrane [146]. The effect of thickness of the CPs films was also revealed, with thicker PANI films favoring the formation of larger and dense Au nanoparticles [147].

In addition to load a single component of NMNPs on PANI membranes, Au–Ag alloys with hierarchical structure can also been fabricated using a similar strategy. For example, jellyfish-like Au-Ag alloys through sequential chemical deposition on a PANI substrate were developed (**Fig. 9**) [148]. The formation of Au nanoparticles on the PANI membrane by way of self-assembly was simply achieved by immersing the PANI membrane into $AuCl_3$ aqueous solution, followed by immersion in $AgNO_3$ aqueous solution to allow deposition of the Ag metal. PANI was essential for the generation of such jellyfish-like Au–Ag alloys, which served the role of mediating electron transfer to reduce Ag ions and oxidize Au nanoparticles simultaneously.

Fig. 9

2.2.2. With additive

In order to obtain NMNPs with smaller size (< 10 nm) together with higher stability, additional stabilizer are always needed in the synthesis. During the growth process of NMNPs, CPs interact with NMNPs only on the contact side, with the other parts of the NMNPs not effectively protected, so that the neighboring NMNPs will aggregate with each other and result in even, micrometer-sized noble metal particulates. Therefore, the growth of noble metal nuclei will be retarded and the aggregation phenomenon will be prevented if the other surfaces of the as-formed noble metal nanoclusters are effectively capped by additional stabilizer. That is thought to result in evenly deposited nanosized NMNPs on the surfaces of CPs.

2.2.2.1. Functional doping acid

In comparison with undoped CPs, a common acid protonating of PANI has little effect on the size of NMNPs [130]. This may be related to the weak interactions between doping acid and NMNPs that the common doping acid cannot influence the nuclei and growth of NMNPs. However, when a doping acid with functional groups showing strong affinity towards NMNPs is doped to CPs, then the growth and aggregation of noble metal nuclei will be retarded resulting in the formation of NMNPs with smaller size and CP-NMNP hybrids with high uniformity.

For example, the conventional polyelectrolyte polyacrylic acid (PAA) was chosen to hybrid with PANI because PAA not only made the colloidal particles hydrophilic, but it also bound and pulled noble metal ions to the PANI colloids. Li et al. [149] reported that the synthesis of PANI colloid nanoparticles consisted of a spherical outer layer that was PAA rich and an inner core that was a homogeneous mixture of PANI and PAA. The reduction of Ag ions took place either within or on the surface of the PANI colloid nanoparticles. The process involved incrementally adding Ag ions solution to aqueous PANI colloid nanoparticles. The Ag nanoparticles (3 nm in diameter) appeared to form a shell about 10 nm thick around the surface of the PANI colloidal nanoparticles, whereas the core structure of the PANI colloids was free from Ag nanoparticles. When using nitric acid doped PANI colloid nanoparticles instead of undoped PANI colloid nanoparticles to synthesize Ag nanoparticles following the same procedure, all of the Ag nanoparticles resided strictly within the core of the PANI nanoparticles. The difference was explained by the charges on

the polymer chains and the counter ions (dopants) that opened the pores in the doped PANI colloid nanoparticles. As the pores open, Ag ions diffused into the core of PANI colloid nanoparticles and got reduced to form Ag nanoparticles. As for the undoped PANI colloid nanoparticles, most Ag ions were reduced on the surface of the PANI colloid nanoparticles, which then dispersed throughout the solution.

Another example is to introduce thioglycolic acid (TA) in PANI nanofibers for the formation of Au nanoparticles with size limited to 10 nm [150]. Different doping acid, such as citric acid, camphorsulfonic acid, and TA were chosen for comparison. In comparison with the case of dedoped PANI nanofibers, the uniformity of Au nanoaprticles improved when citric acid doped PANI nanofibers were used, and became better when camphorsulfonic acid-doped PANI nanofibers were chosen. However, Au nanoparticles with size exceeds 100 nm apart from PANI nanofibers were still seen in the products, showing that citric acid and camphorsulfonic acid doped in PANI nanofibers could not effectively protect aggregation of Au nanoparticles. In the case of TA-doped PANI nanofibers, almost all Au nanoparticles (2-10 nm in a controlled manner) were evenly deposited on surfaces of PANI nanofibers, and the uniformity of such hybrid nanofibers was near 100% (**Fig. 10**). Therefore, in comparison with the use of dedoped or either citric acid or camphorsulfonic acid-doped PANI nanofibers, in the case of TA-doped PANI nanofibers Au nanoparticles formed during early stage of the reaction would be located on surfaces of PANI nanofibers, and other surfaces in addition to contact sides were effectively protected by TA. It was concluded that a doping acid that showed strong affinity toward Au nanoparticles introduced to PANI nanofibers would effectively prevent aggregation of Au nanoparticles which led to the formation of uniform hybrids with Au nanoparticles evenly deposited on surface of PANI nanofibers. Using a similar method, TA-doped PANI nanotubes were also loaded with Au nanoparticles with size limited to 10 nm [151].

Fig. 10

2.2.2.2. PVP

PVP, as a commonly used protection reagent for Au nanoparticles, shows potential for the formation of Au nanoaprticles on CPs. Han and coworkers [19, 152] reported the synthesis of

well-defined Au nanoparticles with tunable size (3-20 nm) supported on shells of poly(*o*-phenylenediamine) (POPD) microspheres. The choice of POPD was based on the fact that this polymer had higher density of imine groups than PANI. If PVP was not used, besides the formation of Au nanoparticles supported on POPD hollow microspheres some micrometer-sized Au aggregates apart from the microspheres could be seen (**Fig. 11a**), whereas Au nanoparticles of 3 nm exclusively located on surfaces of POPD hollow microspheres were obtained in the presence of PVP (**Fig. 11b**). During the growth process of Au nanoparticles, POPD interacted with Au nanoclusters only on the contact side and the other parts were not effectively protected so that the neighboring Au nanoclusters would aggregate with each other and resulted in even, micrometer-sized Au particulates in the absence of PVP. In the presence of PVP, the other parts of the Au nanoclusters were effectively capped by PVP, which prevented the aggregation phenomenon, resulting in evenly deposited Au nanoparticles on the surfaces of the POPD hollow microspheres. If Au seeds (20 nm) were pre-adsorbed on surfaces of POPD hollow microspheres, addition of PVP and then chloroauric acid into the aqueous solution led to Au nanorods supported on hollow polymer microspheres through a well-known seed-mediated strategy [153-155]. Other NMNPs, such as silver nanoparticles, supported on polymer hollow microspheres could also be obtained by using the same synthetic procedure.

Fig. 11

2.2.2.3. Surfactant

Xu et al. [156] investigated the effect of different surfactant on the formation of Au nanoparticle by an *in situ* reduction reaction of chloroauric acid on the PPY nanotubes. Cationic surfactant cetyltrimethylammoniumbromide (CTAB), the anionic surfactant sodium dodecyl sulfonate (SDS), and the non-ionic surfactant polyoxyethylenesorbitan monooleate (Tween-80) were selected as stabilizers. In the absence of a surfactant, although some small Au nanoparticles with an average diameter of 13 nm were dispersed uniformly on the nanotubes, large Au nanoparticles with an average diameter of 80 nm were also present because of the overgrowth of the Au nanoparticles. In the presence of CTAB, almost no Au nanoparticles were deposited on the PPY nanotubes because of the repulsive electrostatic interactions of CTAB and PPY. When SDS was used as a

stabilizer, large Au nanoparticles with diameters of about 50 nm were formed on the surface of the PPY nanotubes, which indicated that the protecting function of SDS was not quite as good in this case. Using the non-ionic surfactant Tween-80, Au nanoparticles with an average diameter of 13 nm were uniformly distributed on the PPY nanotubes (**Fig. 12**).

Fig. 12

2.2.3. With physical barrier

The addition of a functional stabilizer to control aggregation of NMNPs on CPs has some limitations. For example, the functional doping acid introduced for the formation of nanosized NMNPs only exists in acidic conditions and will be dedoped under basic conditions. As a result, the removal of functional doping acid in basic environment will subsequently cause instability of NMNPs, which eventually limits their application, especially in catalysis in basic conditions. As a result, CP- NMNP hybrids insensitive to pH are highly desirable.

The basic idea is construct nanobarriers on surfaces of CPs. In most reported CPs with spherical, fibrous or tubular nanostructures, the outer surfaces are always smooth. As described in the preceding, during the *in situ* formation of NMNPs, besides the contact sites of noble metal nuclei with polymer matrix, other surfaces are not protected and then the neighboring noble metal nuclei will aggregate leading to overgrowth of NMNPs. If the noble metal nuclei may be effectively isolated by nanobarriers, their overgrowth may be inhibited. One solution is to make rough surface of CPs [157]. As reported, surface-patterned fibrous poly(*o*-toluidine) (POT) were successfully fabricated from fibrous POT with smooth surfaces by a swelling-evaporation strategy [158]. The roughness came from short nanofibers (5-10 nm in diameter) perpendicular to fibrous surfaces (**Fig. 13a**). The rough surfaces of POT nanofibers composing short POT nanofibers on surfaces acted as nanobarriers to isolate noble metal nuclei and therefore prevented their aggregation and overgrowth. The size of Au nanoparticles on POT nanofibers with smooth surfaces was in the range of 80-100 nm, whereas that was mainly 2-5 nm on POT nanofibers with rough surfaces (**Fig. 13b**).

Fig. 13

Another strategy is to introduce mesoporous SiO_2 (*m*-SiO_2) shells with nanochannels on surfaces of CPs [159]. Han et al. [160] developed Fe_3O_4/PANI/*m*-SiO_2 hybrid core/shell spheres as novel and robust reactive supports to produce highly stable and recyclable Au nanoparticles. Specifically, Fe_3O_4/PANI/*m*-SiO_2 hybrid core/shell spheres were first fabricated, followed by the addition of Au ions to initiate the redox reaction between PANI and Au ions to yield Au nanoparticles (5-10 nm) on PANI surfaces (**Fig. 14**). The introduction of *m*-SiO_2 shells not only acted as a barrier to control Au nucleation and further prevented Au coagulation, but also functioned as a channel for mass transfer of reagents involved in catalysis applications.

Fig. 14

2.3. Monomers and NMNPs

In this approach, NMNPs with desirable size and morphology are synthesized in advance, and then the commonly used oxidant is added into the colloidal solution containing NMNPs and monomers, followed by the polymerization of monomers to form CP-NMNP hybrids. During the polymerization, the monomers, oligomers or polymer chains will adsorb onto the surfaces of NMNPs through chemical and/or electrostatic interactions to generate the CP-NMNP hybrids of typical core-shell nanostructures [161-163].

2.3.1. Without additive

The most commonly used NMNPs are citrate-stabilized Au nanoparticles as synthesized through a well-established citrate reduction route [164] due to the simple synthetic conditions, and the fine-tuned diameter (10-25 nm) and morphology of Au nanoparticles. However, only aggregated Au nanoparticles covered with CPs and bare CPs were obtained when APS was added into the colloidal solution containing citrate-stabilized Au nanoparticles and monomers [165]. This may be rationalized as follows: 1) citrate is not an excellent stabilizer for Au nanoparticles, consistent with the observed aggregated Au nanoparticles that develop after ageing for several days; 2) monomers will be present in the whole water phase, but not specifically on the surfaces of Au cores. Thereafter, the polymerization occurs not only on the surfaces of Au nanoparticles but also in the solution phase, which leads to aggregated Au nanoparticles covered with CPs and CPs

without Au nanoparticles embedded, respectively. In order to obtain well-defined uniform CP-NMNP core-shell nanostructures, the surfactant or functional stabilizer is always needed in the synthesis.

2.3.2. With additive

2.3.2.1. Nonionic surfactant F127

Surfactant added to a colloidal solution of Au nanoparticles, will locate on the Au/water solid/liquid interfaces as a monolayer to reduce the interface energy. As such, the stability of Au nanoparticles will be enhanced. After adding monomers, they will locate close to the hydrophobic regions because of the hydrophobic features of most commonly used monomers (with aromatic moiety exhibiting low solubility in water). When initiated by an oxidant, the polymerization will occur on the surfaces of Au nanoparticles where monomers exist, leading to the formation of uniform CP-Au core-shell hybrids.

In the earlier report, Sarma et al. [166] synthesized PANI-Au hybrids using H_2O_2 as oxidizing as well as reducing agents. Au colloids were formed by addition of H_2O_2 to chloroauric acid aqueous solution, followed by the addition of aniline solution (in 1 M HCl solution) in several portions to initiate the polymerization of aniline with excess H_2O_2, leading to the formation of PANI-Au hybrids. In their later report [167], an anionic surfactant SDS was introduced as the stabilizer in a similar synthesis. The morphology of PANI-Au hybrids was not given in either case.

Han et al. [165] systematically studied the effect of surfactant concentration on the resulting morphology of CP-Au hybrids. They chose a nonionic surfactant poly(ethylene oxide)-poly-(propylene oxide)-poly(ethylene oxide) triblock copolymer, Pluronic F127 as an example. First, the surfactant F127 and *o*-toluidine monomers were introduced to citrate-stabilized Au colloids, followed by the chemical polymerization of monomers with APS oxidant to afford a POT shell around each Au nanoparticle. Results showed that the addition of F127 at a concentration lower than critical micelle concentration (CMC) was critical for the synthesis of well-defined uniform POT-Au core-shell hybrids.

It is well known that micelles may form if the surfactant concentration reaches its CMC, whereas only surfactant molecules dispersed in solution when the surfactant concentration is lower than CMC. Therefore, it is believed that the polymerization environments will be completely different at altered surfactant concentration, believed to affect the morphology of hybrids. When a

surfactant is added below its CMC, most surfactant molecules will adsorb on surfaces of Au nanoparticles with its hydrophobic chains heading to surfaces of Au nanoparticles and the hydrophilic chains heading to the water phase. After adding monomers, they will be solubilized in the hydrophobic regions close to Au surfaces. Finally, uniform CP-Au core-shell nanoparticles may be fabricated after polymerization of monomers. If the surfactant concentration exceeds CMC, beside the surfactant molecules adsorbed on surfaces of Au nanoparticles, micelles may be formed in the solution phase. The monomers added will be mostly solubilized in the hydrophobic cores of micelles. Thus, the polymerization of monomers in micelles will result in the formation of POT nanoparticles without Au cores. The concept has been applied to the synthesis of various CP-Au core-shell hybrids with varied chemical structures of CP, and size and shape of Au nanoparticles (**Fig. 15**).

Fig. 15

In their continuing report Han et al. [168], showed that POMA-Au core-shell hybrids synthesized with the aid of F127 may be transformed into yolk-shell hybrids through a novel swelling–evaporation strategy. Specifically, uniform POMA-Au core-shell hybrids with a single Au core (15 nm in diameter) embedded in each polymer particle (100 nm in diameter) were dispersed in a common solvent, such as ethanol. Due to the swelling property of the POMA polymer with ethanol, POMA shells of POMA-Au core-shell hybrids would be in the swollen state. After saturation swelling of the POMA polymer, ethanol solvent was then evaporated under ambient conditions. During the evaporation process, ethanol molecules inside POMA shells, together with POMA polymer chains, moved outside, creating voids between the Au core and POMA shell. The solvent used played the determining role in the formation of POMA-Au yolk-shell hybrids (**Fig. 16**). The proposed sacrificial template-free strategy is in contrast to commonly used sacrificial template strategy for making PANI-Au yolk-shell nanostructures [169].

Fig. 16

In addition to symmetric POMA-Au core–shell hybrids, asymmetric POMA-Au core–shell

hybrids may be synthesized by addition of Au colloids into the polymerizing system containing monomer and APS oxidant, with particular polymerization times [170]. The asymmetry degree (AD) was applied to quantitatively define the eccentricity of the Au core in the POMA bead. Asymmetric POMA-Au core–shell hybrids with different ADs were synthesized by adding Au colloids into the POMA polymerization system after the polymerization proceeded for different times. The AD of POMA-Au core–shell hybrids decreased from 1.0 to 0.8, 0.5, and 0.1 when the addition time of Au colloids was fixed at 60, 50, 10 and 0 s, respectively. After the swelling-evaporation processes, POMA-Au hollow hybrids with a single Au nanoparticle encapsulated in each shell of POMA hollow spheres (yolk-in-shell structure) were found when the AD for POMA-Au core–shell hybrids was higher than 0.8. If the AD decreased to 0.5, the Au cores were encapsulated in both the porous shells and hollow interiors of POMA hollow spheres (**Fig. 17**).

Fig. 17

2.3.2.2. Anionic surfactant SDS

The anionic surfactant SDS is another commonly used surfactant for the synthesis of CP-Au hybrids. Xing et al. [171] prepared CP-Au core-shell hybrids with the aid of SDS. The citrate-stabilized Au colloids (22 nm in diameter) were synthesized in advance, followed by addition of surfactant SDS. The adsorption and *in situ* polymerization of aniline or pyrrole on the surface of Au nanoparticles by APS oxidant gave uniform polymer shells. The shell growth was kinetically controlled, where the PANI was successively grown on Au nanoparticles by multiple growth cycles with shell thickness controlled in the range of 14-92 nm. They also showed that the aggregation of Au nanoparticles were controllably promoted in this system by simply timing SDS addition, to give linearly aggregated cores of 2-20 Au particles (**Fig. 18**). Similar to the synthesis of CP-Au spherical core-shell hybrids in Au colloidal solution with the aid of SDS, CP-Au rod-like core-shell hybrids with Au nanorods as cores, such as PANI-Au nanorod core-shell hybrids [172, 173] and PPY-Au nanorod hybrids [174], have been reported. In addition, if the aniline was introduced from the vapor phase to the solution containing Au colloids, SDS and oxidant H_2O_2, PANI-Au core-shell hybrids with more than one Au nanoparticle were obtained

[175]. If Au nanoparticles were first assembled on surfaces of SiO_2 nanoparticles through electrostatic interaction, the polymerization of aniline in the presence of SDS could lead to the formation of well-defined three-layered SiO_2-Au-PANI core-shell hybrids with numerous Au nanoparticles encapsulated in a single PANI shell [176].

Fig. 18

For polymerization of aniline initiated by oxidant chloroauric acid in Au colloidal solution with the aid of SDS, the simultaneous growth of Au and PANI on Au seeds led to the formation of fractal architectures [177]. By controlling different growth rates of Au and the PANI shell, the anisotropic growth of Au at the exposed tips of the branches (branching growth) were promoted while minimizing the core growth. The PANI shells prevented aggregation and maintained colloidal stability of the hybrids. In addition, pre-fabricated Au seeds of uniform diameter were used to control size distribution of the dendritic hybrids (**Fig. 19**). Using the same reaction system, they showed that seeding were applied to controlling the growth of two-dimensional PANI-Au dendritic nanostructures on sample grids [178].

Fig. 19

During the synthesis of PANI-Au core-shell hybrids in Au colloidal solution with the aid of SDS, if the oxidant is changed from APS to H_2O_2, only oligoaniline (OANI) formed on surfaces of Au nanoparticles (OANI-Au core-shell hybrids) [179]. Since oxidation of monomers by a weak oxidant in neutral pH condition gives oligomers that are rich in amine groups, capable of being oxidized further. When OANI-Au core-shell hybrids were further treated with a stronger oxidant, chloroauric acid, the amine groups of OANI were oxidized to imine groups and form PANI in "pernigraniline" state. If the OANI shell on Au nanoparticles was partially oxidized to PANI, the decrease in solubility allowed the unreacted shell section to be easily dissolved away using 2-propanol, leading to uniform PANI-Au yolk-shell hybrids (**Fig. 20**). The ionic diffusion through the polymer shell was the rate-determining step in the overall process. Conservative estimates showed that the diffusion coefficient of $AuCl_4^-$ was at least 700 times slower than that of the

typical rate values in traditional studies, which was most likely caused by the lack of micropores in the polymer structures.

Fig. 20

If the polymerization of pyrrole is initiated by $AgNO_3$ instead of APS in Au colloidal solution with the aid of SDS, triple-layer PPY-(Au@Ag) core-shell hybrids were fabricated. The Ag and PPY layers were generated simultaneously from the redox reaction between pyrrole and $AgNO_3$, and Ag was found to diffuse through the PPY shell and deposit isotropically on the Au surface due to the close lattice constants of the two NMNPs. The intermediate Ag layer in the triple-layer nanoparticles were easily etched by NH_3 in the presence of O_2, without affecting the Au core, resulting in the formation of PPY-Au yolk-shell hybrids [180].

A novel hybrid vesicle Au@vesicle formed by the polymerization of thiophene initiated by H_2O_2 and $FeCl_3$ in Au colloidal solution with the aid of SDS (**Fig. 21**) [181]. The SDS concentration was found to play the determining role in the hybrid morphology: when the SDS concentration decreased from 5.0 to 2.5 mM while keeping other conditions unchanged, the morphology of the resulting hybrids changed dramatically from PTH-Au core-shell to Au@vesicle nanoparticles. The number of vesicular cavities in one nanohybrid was highly correlated with the size of the seed nanoparticles as larger Au seeds resulted in increase in the number of cavities. The surface polymerization of thiophene to PTH on Au nanoparticles and their simultaneous over-oxidation to thiophene sulfone subunits were proved to give rise to polymers with both hydrophobic and hydrophilic subunits. Phase-segregation of this amphiphilic polymer was proposed to lead to the formation of vesicles.

Fig. 21

It has been demonstrated that completely encapsulated core-shell nanostructures are common, particularly if the shell is made of polymer or amorphous material such as silica [171, 182]. Therefore, through *in situ* polymerization of monomer in NMNP colloid solution with the aid of a surfactant, CPs are well-coated on surfaces of NMNPs as CP-NMNP core-shell hybrids. The

morphology of hybrids is largely determined by the configuration of NMNP seeds, and spherical and rod-like morphology is commonly seen in CP-NMNP core-shell hybrids. If the NMNPs are first coated with other materials and then also may be chosen as seeds for further coating of CPs using similar route, the morphology of the resulting hybrids will be determined by the middle component and the removal of the middle component will lead to the formation of CP-NMNP yolk-shell hybrids. A typical example was reported by Sindoro et al [183]. In their synthesis, citrate-stabilized Au colloids were first coated with single-crystalline phase of perylene to form perylene-Au core-shell nanocuboids, and such perylene-Au core-shell nanocuboids were also regarded as seeds for further PANI coating with the aid of SDS, resulting in the formation of PANI-perylene-Au ternary core-shell hybrids. After release of the perylene, PANI-Au yolk-shell nanostructures were formed (**Fig. 22**).

Fig. 22

2.3.2.3. Anionic surfactant SDS and diblock copolymer

A multiple-petal morphology with the Au nanoparticles encapsulated by hybrid polymers (PANI + PSPAA) by treatment of spherical PANI-Au core-shell hybrids with the diblock copolymer polystyrene$_{154}$-block-poly(acrylic acid)$_{60}$ (PSPAA) (**Fig. 23**) [184]. The inserted PSPAA assembly that led PANI to form a petal-like shell on the Au surface. It was proposed that the morphology of the shell underwent a transformation to decrease the surface energy to the utmost by forming a petal-like shell to increase the volume and finally minimized the surface energy/volume ratio.

Fig. 23

2.3.3. Other methods

In addition to aqueous phase NMNPs seed-growth route with the aid of a surfactant for CP-NMNP hybrids [185], other methods are also available for such hybrids. Dong et al. [186] reported the synthesis of PANI-Au core-shell hybrids by *in situ* polymerization of aniline using poly(N-isopropylacrylamide)-co-poly(acrylic acid)/Au hybrid microgel particles as a template. Surface initiation approach was reported for filament-like PANI attached to Au

nanoparticles/nanorods, where Au nanoparticles stabilized by surfactant 10-bromodecylperoxide carrying peroxide group can initiate aniline polymerization without additional oxidant when the Au nanoparticles were added to an aniline solution [187]. A two-phase polymerization route was reported to generate PANI-Ag hybrids [188]. In the preparation, the dodecanethiol-stabilized Ag nanoparticles were prepared and acted as nucleation centers for PANI growth to obtain the PANI-Ag hybrids through a two-phase water-toluene interfacial reaction. Different structures of the hybrids, such as a thin sheet of PANI around the silver nanoparticles or a PANI mass with nanoparticles homogeneously embedded within it, were obtained by rigorously controlling the reaction time. Interfacial polymerization was also reported to generate PANI nanofibers grafted to Au surfaces by placing the 4-aminothiophenol treated Au substrate at the interface of a biphasic solution of dopant and aniline monomer [189]. Katre et al. [190] synthesized Au nanoparticles by γ-irradiation method using aniline as a stabilizer, and further addition of APS oxidant to initial the polymerization of aniline monomer to obtain PANI-Au core-shell hybrids, where several Au nanoparticles were often seen in a single PANI nanoparticle.

2.4. Monomers and noble metal ions

Co-precipitation of CPs and NMNPs to hybrids means that the reduction of metal ions and oxidation polymerization of organic monomers are simultaneous. For realizing the simultaneous formation of CPs and NMNPs nanostructures, the most commonly-used approach is that oxidation polymerization of monomers to CPs is induced by the reduction of noble metal ions to NMNPs, where CPs and NMNPs will be generated and deposited at the same time, resulting in the formation of CP-NMNP hybrids [191-193]. The polymer oligomers locate on surfaces of newly formed noble metal nuclei to lower down the surface energy. As a consequence, in the CP-NMNP hybrids obtained, normally NMNPs show as core and CPs show as shell. After optimization of synthetic conditions, well-dispersed NMNPs in bulk CPs may be formed. The morphology of the hybrids prepared with this procedure is probably varied from sphere-shaped structure to film, and even to hierarchical nanostructures. The choice of the noble metal salts and the monomers should be such that the noble metal salt can oxidize the monomer to form a polymer as well as utilize the electrons released during the oxidation to reduce the noble metal salt to form NMNPs. It may be predicted whether the amines will function as reducing agents in chloroauric acid reduction based

on their redox properties [194]. In addition, the kinetics of Au nanoparticles formation may be understood in terms of Marcus electron transfer theory, where the slower reactions proceed in the inverted region owing to the difference between the Au reduction potential and the amine oxidation potential [194]. The kinetics of the reaction involving redox reaction between chloroauric acid and aniline in aqueous acidic medium were investigated by the quartz crystal microbalance technique [195]. The results indicated that the kinetics of the reaction were of order 0.5 with respect to chloroauric acid and 1.5 with respect to aniline.

Research has not yielded a definitive view on the formation mechanism of CP-NMNP hybrids. For example, two mechanisms have been proposed for the aniline and chloroauric acid redox system for PANI-Au hybrids. According to one proposal, aniline monomer is first protonated in the protonic acid medium, and then oxidized by chloroauric acid to form aniline radical cation, with chloroauric acid reduced to form Au nanoparticles. The aniline radical cation formed was adsorbed onto the Au nanoparticle surface and the Au nanoparticles served as the catalyst for the polymerization of aniline [195, 196]. In a second proposal, chloroauric acid protonate the aniline hydrochloride with the formation of anilinium cations ($PhNH_3^+$) and the generation of a radical cation accompanied by the release of an electron. Then, $AuCl_4^-$ acted as the oxidizing agent to oxidize $PhNH_3^+$ and form PANI. During polymerization, the process proceeded with the release of an electron that then used to reduce the $AuCl_4^-$ to form Au atoms. The coalescence of these Au atoms ultimately formed Au nanoparticles, which were encapsulated and stabilized by the PANI polymer [197].

2.4.1. Solution polymerization

2.4.1.1. Without additive

In the conventional route for conducting polymer PANI, oxidant APS is added into aqueous acidic solution containing aniline monomers. If the oxidant APS is changed into other noble metal salts, such as $AuCl_4^-$, PANI polymer and NMNPs may be simultaneously formed. In most of the cases, PANI polymers accompanied by microscale Au clusters may be obtained, and a phase separation is normally seen mainly between PANI and Au clusters [196, 198, 199], which is in contrast with radiolysis introduction during synthetic procedure, where NMNP nanoparticles are well embedded in CPs [190, 200-202]. Typically, addition of $HAuCl_4$ aqueous solution to aqueous acidic solution containing aniline results in the reduction of $AuCl_4^-$, accompanied by oxidative

polymerization of aniline, leading to PANI nanofibers with a diameter of 35 nm and aggregated Au nanoparticles that precipitated from the liquid phase during the reaction [203].

The Au nanoparticles aggregated to form microscale Au clusters and capped with a thin layer of PANI. These PANI nanofibers have similar chemical structure and conductivity to the polymer generated from the conventional method using APS to oxidize aniline. The PANI nanofibers might be formed through an Au nanoparticle catalyzed oriented growth mechanism [204-206]. The catalytic effect of as-formed Au nanoparticles to one-dimensional growth of PANI has been extended to the synthesis of nanofibers of PANI derivatives: the reduction of *o*-toluidine [207] and *o*-phenylenediamine [208, 209] with $HAuCl_4$ led to the formation of POT and POPD nanofibers. If the $HAuCl_4$ solution was added drop-wise, the catalytic effect diminished and PANI nanofibers could not be formed. However, Au nanoparticles were sized in the range of 7-15 nm embedded in polymer matrix [210]. In this case, aniline monomers were in excess during the redox reaction. The results were reasonable as large amounts of aniline oligomers were rapidly formed and Au nanoparticles would be well-capped with oligomers, and the further growth of originally formed Au nanoparticles prevented. Meanwhile, the oriented growth of one-dimensional nanostructures of PANI nanofibers driven by the catalysis effect of Au nanoparticles might be inhibited as the originally formed Au nanoparticles were covered with oligomers. When the reaction medium of aqueous solvent was changed to organic or even ionic liquid solutions, similar results with NMNPs with limited size (normally < 20 nm) embedded in CP matrix if the noble metal salt solution was added drop-wise to monomer solution. Such redox systems including aniline/chloroauric acid in methanol/water mixed solution [211-216], *o*-methoxyaniline/$Pd(Ac)_2$ in toluene [217], *o*-phenylenediamine/$Pd(Ac)_2$ in toluene [197], and pyrrole/$AgNO_3$ in ionic liquid solution [218].

The reduction potential of aniline is pH dependent during its initial oxidative stage, decreasing on increasing the pH of the solution due to its deprotonation (p*K*a of aniline is 4.6), possibly making the reduction of $AuCl_4^-$ proceed in a violently way [219]. In the synthesis of Au nanoparticles, with rapid reduction of $AuCl_4^-$ to generate Au atoms, the shape of the final Au product will take the thermodynamically favored one. However, when the reduction rate becomes slow enough, kinetic control will take over in both nucleation and growth and the final Au product will take shapes deviating from the thermodynamically favored one [220]. Guo and co-workers

[221] paid more attention to the morphology of *in situ* formed Au nanoparticles, as layered assemblies of single crystal Au nanoplates were formed by slowing up the reduction process of $AuCl_4^-$ for facilitating the formation of anisotropic Au nanostructures.

Fig. 24

As amino groups interact weakly with noble metal surfaces [221], during the redox reaction between aniline and chloroauric acid, Au nanoparticles always develop as microscale Au clusters. When aniline derivatives with functional groups showing strong affinity towards NMNPs are chosen instead of aniline, highly dispersed Au nanoparticles embedded in PANI matrix may be obtained. For example, when 2-aminothiophenol was chosen instead of aniline under similar synthetic conditions, poly(2-aminothiophenol) stabilized Au nanoparticles, where the Au nanoparticles were estimated to be 1.0 nm in size and in narrow size distribution were fabricated (**Fig. 24**) [222]. The synthesized poly(2-aminothiophenol)-stabilized Au nanoparticles were stable without obvious aggregation for more than 6 months. In addition, by controlling the mechanical stirring speed, the diameter of poly(2-aminothiophenol)-Au hybrid nanofibers were tuned in the range of 80-200 nm, while the diameter of embedded Au nanoparticles remained unchanged [223].

Fig. 25

Uniform raspberry-like or dandelion-like nanospheres PANI-Au hybrids are formed by adding chloroauric acid to aqueous solution containing aniline, followed by agitation, (**Fig. 25**) [224]. The PANI-Au nanospheres comprise many short Au nanorods (about 30 in diameter) wrapped by PANI with the diameter of the entire nanospheres in the range of 150-200 nm [224-226]. A similar structure of PANI-Au hybrids is obtained if the reaction aqueous solution contains critic acid capped Au colloids [227], and similar nanostructures reslut using *o*-toluidine as the monomer. The amount of Au nanoparticles inside each polymer sphere may be adjusted from tens to one (core-shell structure, Au core diameter: 30 nm) by decreasing the amount of chloroauric acid [228]. However, due to strong affinity between Au and sulfur when monomer thiophene or

3,4-ethylenedioxythiophene are used as monomers the reaction is very fast (within a few seconds), and the Au nanoparticles obtained are controlled in several nanometers and well dispersed in polymer matrix with high stability [229, 230].

2.4.1.2. With additive

The addition of functional molecules, such as functional doping acid and surfactant, can affect the configuration of resultant CP-NMNP hybrids involved in the redox reaction between aniline monomer and chloroauric acid. Although the role of additives on the formation of resultant nanostructures has not yet been well-understood (micelles are always proposed as soft template for the formation of different hybrid nanostructures), various intriguing CP-NMNP hybrid nanostructures may be achieved.

During the traditional synthesis of PANI with APS as the oxidant, D-camphor-10-sulfonic acid (CSA) or *p*-toluene sulfonic acid (TSA) is commonly introduced as a functional doping acid for the synthesis of PANI nanotubes or nanofibers [231, 232]. One-dimensional PANI-Au coaxial nanocables with an average diameter of 50-60 nm and lengths of 1-2 μm were synthesized with CSA introduced in the reaction system of aniline monomer with chloroauric acid in aqueous solution [233, 234]. It was proposed that micelles formed by CSA-aniline might act as a soft template in the formation of the PANI-Au nanocables. Results also indicated that high CSA concentration was essential for the formation of nanocables, whereas spherical PANI with Au nanoparticles embedded are formed under low CSA concentration, in accordance with the structure of POMA-Au hybrids under similar synthetic condition except that *o*-methoxy aniline is used as monomer instead of aniline [235]. In contrast, PANI nanospheres (230±22 nm) with Au nanoparticles (6±2 nm) embedded were obtained using added TSA [236], where TSA-aniline micelles were proposed for PANI growth into nanospheres. In another case, spherical dendritic PPY-Au hybrids were prepared with TSA introduced in the reaction system of pyrrole monomer with chloroauric acid in aqueous solution [237]. The morphology was quite similar to that of dandelion-like PANI-Au hybrids synthesized in aniline and chloroauric acid neutral aqueous solution without additive [224].

It is well-known that citric acid is a commonly used stabilizer for Au nanoparticles [164]. Micelles composed of citric acid−aniline salt may also act as soft template, but the resulting morphology is completely different. PANI hollow nanospheres with controllable incontinuous

nanocavities ranging in size from 10 to 50 nm as a novel hollow nanostructure were reported by chemical polymerization of aniline with chloroauric acid as the oxidant in the presence of citric acid (**Fig. 26**) [238]. It was proposed that micelles composed of citric acid−aniline salt acted as template for initial oligomer-Au core-shell structure, and the embedded Au nuclei were inclined to migrate into micelle shells where hydrophilic −COOH groups existed because the interaction between Au nuclei and citric acid are more favorable to that between Au nuclei and PANI with polymerization proceeding, in contrast with the use of CSA and TSA instead of citric acid as the doping acid under similar synthetic conditions. The aggregation and fusion processes of Au nuclei embedded in PANI were attributed to the formation of multicavities in PANI matrix.

Fig. 26

Huang et al. [239] showed that the addition of PVP can dramatically change the morphology of PANI-Au hybrids. It was shown that only mixing $AuCl_3$ with aniline led to homogeneous PANI-Au nanorods; however, upon addition of a small amount of PVP into the reaction system, only PANI-Au nanospheres were obtained (**Fig. 27**). They believed the change in morphology was likely due to the encapsulation of the nuclei (seeds) with PVP, which inhibited the growth of a nanorod. In addition, Sajanlal et al. [227] reported that if raspberry-like OANI-coated Au nanoparticles were pre-introduced in aqueous solution containing PVP, the addition of chloroauric acid led to various PANI-Au hybrid shapes, such as nanoplates, spherical, core-shell nanoparticles and flower-like nanoparticles. The presence of PVP (or surfactant) not only modulated the resulting morphology of CP-Au hybrids, but also endowed them high water solubility and colloidal stability [240, 241]. Their later studies demonstrated the creation of a new class of nano/mesostructures, such as Au/Ag flowers, Au/Pt buds, and Au/Pt beads, through the directed overgrowth of Ag or Pt on OANI-Au nanowires [242].

Fig. 27

The PANI-Au hybrid obtained in the presence of anionic surfactant SDS had a core-shell structure, with individual or multiple Au nanoparticles of 20 nm mean diameter were encapsulated

by PANI of well-defined tetrahedron shape, with 150 nm average edge length [243]. The SDS micelles were believed to template the formation of core-shell structure. A high concentration of SDS and low concentration of anilinium ions suppressed the formation of larger particles, producing nanometer-sized particles only. In contrast, under similar synthetic condition, but at a high anilinium ions concentration, nanoporous Au microsheets enveloped in 10-30 nm thick PANI sheaths were reported [244, 245]. A PANI-Au core-shell structure could also be obtained using the nonionic surfactant Tween 40, [246].

The cationic surfactant CTAB has also been applied. Unlike SDS, it has been well-documented that the selective interaction between CTAB and Au nanocrystals facilitates the formation of anisotropic Au nanostructures [247, 248]. PANI nanotubes and Au nanoplates in separate phases were prepared simultaneously by mixing aniline acidified with glacial acetic acid and chloroauric acid in the presence of CTAB [249]. It was proposed that CTAB and anilinium salt micelles formed during the synthesis. Formation of single crystal fcc Au nanoplates was due to selective growth of (111) side planes, whereas PANI nanotubules might be synthesized via a self-assembly process template by anilinium salt micelles.

In addition to functional doping acid and surfactant, deoxyribonucleic acid (DNA) has also been chosen, and the reduction of chloroauric acid using aniline adsorbed on DNA produced highly branched dendritic Au nanoparticles with concomitant formation of PANI in contrast to the formation of spherical Au nanoparticles in the absence of DNA [250].

2.4.2. Interfacial polymerization

In the interfacial polymerization route, monomers and noble metal salts are dissolved in immiscible solvents, and the redox reaction happens at liquid/liquid interface. In typical, monomer is normally dissolved in organic solvent and noble metal salt is dissolved in aqueous solution. For example, with aniline dissolved in carbon tetrachloride used as the oil phase, and deionized water containing chloroauric acid added to form a water/oil interface, the interface became black immediately after chloroauric acid was added to the water phase, indicating initiation of the aniline polymerization. PANI nanospheres (100-150 nm) evenly decorated with Au nanoparticles (2 nm) were obtained (**Fig. 28**) [251]. With prolonged reaction time, however, Au nanoparticles with larger size were deposited on the PANI surfaces, produced through the chemical reduction of

$AuCl_4^-$ ions by PANI, with the 2 nm Au nanoparticles as growth seeds. The choice of organic phase for aniline includes toluene [252], nitrobenzene [253], chloroform [254-256], ionic liquid 1-butyl-3-methylimidazolium hexafluorophosphate [257], and even aniline itself [258].

Fig. 28

In addition to PANI-Au hybrids synthesized using interfacial polymerization route, other CP-NMNP hybrids have been synthesized using similar route. Lu et al. [259] reported that PEDOT-Au nanocables were obtained with 3,4-ethylenedioxythiophene dissolved in dichloromethane as the oil phase, and chloroauric acid aqueous solution added to form a water–oil interface. The molar ratio between monomer and $HAuCl_4$ determined the formation of hybrid nanocables [260]. The nanocable morphology was quite similar to that of PANI-Au nanocables synthesized with the aid of CSA in aqueous solution [234]. Time-dependent morphological change indicated that one-dimensional aligned buds self-assembled from Au nanosheet first formed at the interface, followed by polymerization of adsorbed monomers to form immature nanocables resulted in breaking up the nanosheet aggregates. Finally, individual nanocables kept growing in one direction with the roots of the nanocables still connected together. Feng et al. [261] reported the synthesis of PPY-Ag core-shell hybrids with pyrrole dissolved in carbon tetrachloride and $AgNO_3$ dissolved in aqueous solution containing PVP, where the presence of PVP could realize the effective coating of PPy on the surface of Ag. Gupta et al. [262] reported the synthesis of polycarbazole-Au hybrids with carbazole dissolved in dichloromethane and chloroauric acid dissolved in acidic aqueous solution, where uniform distribution of Au nanoparticles was observed of the size 2-3 nm embedded in polycarbazole matrix.

In contrast, monomer can also be dissolved in acidic aqueous solution and noble metal salt may be dissolved in organic phase to realize an interfacial polymerization. A typical example was shown by Zheng et al. [263], with the reverse micelles composed of sodium bis(2-ethylhexyl) sulfosuccinate/*p*-xylene/H_2PtCl_6 chosen as the organic phase, and aniline in acidic aqueous solution constructed as the aqueous phase. PANI-Pt nanofilms with Pt nanoparticles (20 nm) dispersed uniformly in the PANI films were fabricated (**Fig. 29**).

Fig. 29

If a solid membrane separates the solutions containing monomer and noble metal salt, liquid/solid/liquid interfaces will be created, and the simultaneous formation of CPs and NMNPs will occur in membrane. For example, PANI-Au were deposited on the surface of the poly(tetrafluoroethylent) (PTFE) membrane via simple diffusing interfacial reaction [264]. The preparation was carried out in a two-compartment system separated by PTFE/Nafion hybrid membranes wetted in 1 M HCl. The upper one contained a chloroauric acid aqueous solution, with the bottom one contained an aqueous solution of aniline and TSA. Aniline monomers together with TSA and oxidizer solutions were allowed to counter-diffuse simultaneously to the membrane. The content of Au in upside surface of the hybrid membrane was higher than that in the bottom side, and on the contrary, the content of PANI in bottom side surface of the hybrid membrane was higher than that in the upside one. Polycarbonate (PC) membranes have been applied in the same manner [265]. In another case, Jiang et al. [266] developed a novel interfacial polymerization route, where PS spheres were first spread on the surface of aqueous solution containing chloroauric acid to form a monolayer, followed by addition of aniline acidic aqueous solution to initial the redox reaction templated by PS monolayer. Finally, removal of PS template led to the formation of PANI-Au nanobowl sheet (**Fig. 30**).

Fig. 30

In addition to liquid/liquid interfacial polymerization, gas/liquid interface polymerization have been proposed with chloroauric acid dissolved in aqueous solution and aniline introduced as a vapor. The polymerization happened at the gas/liquid interfaces, leading to the formation of dendritic PANI-Au hybrids [267].

2.4.3. Template polymerization

Using a hard-template method to synthesize CP-NMNP hybrids is another way to control the morphology of the hybrids. This will lead to ternary hybrids with advanced functionalities. The final morphology of the product is mainly depended on the hard-template.

In Guo's work [221], aniline molecules adsorbed on single-walled carbon nanotubes (SWNTs) in a colloidal solutiondue to the formation of proton-transfer complexes between carboxyl in SWNTs and amine group in aniline. Addition of chloroauric acid into the colloidal solution could readily produce SWNT-PANI-Au hybrids in an *in situ* one-pot fashion. PANI together with Au nanoparticle (3 nm) was well coated on surfaces of SWNTs. Similar results were reported by Chang et al [268]. In a similar way, the two dimensional graphene oxide (GO) nanosheets were utilized for making GO-PANI-Au hybrids [269].

In other cases, mesoporous silica SBA-15 [270] and nickel foam [271] have been used as hard template for the confined formation of PANI-Ag and PPY-Ag hybrids. In a nanofibrillar V_2O_5 seeding approach, the nanofibrillar oligomers, formed due to the reaction between pyrrole monomers and V_2O_5 nanofibers, would further react with the noble metal ions and reduce them to NMNPs, resulting in PPY nanofiber network decorated with Pt, Au or Ag nanoparticles [272].

3. Applications

3.1. Catalysis

Haruta's discovery of CO oxidation catalyzed by supported Au nanoclusters [273] had a great impact on both the scientific and industrial communities; the subsequent activity in this research field may be likened to a "gold rush" in modern science [274]. NMNPs are often supported on activated carbon or metal oxides. In recent years, interest in NMNPs has shifted from activated carbon or metal oxides to polymers [275], because of the merits of mild and simplified synthetic conditions and higher catalytic performances for polymer supported NMNP catalysts, as compared with activated carbon or metal oxides supported NMNP catalysts [276]. Therefore, the synthesis of polymer supported NMNPs is especially attractive. Considering that the conjugated π electrons and heteroatoms (N or S) in the main chain of CPs can bind to metal atoms on the surface of NMNPs, CPs have been chosen as attractive supports for NMNPs. In addition, their easy preparative protocol from non-expensive starting material, controllable doping levels through an acid doping/base dedoping process (**Fig. 1**), inert nature, and non-solubility in most organic solvents and water make them ideal supports in heterogeneous catalysis.

The catalytic activities of NMNPs involved in liquid phase reactions may be examined by choosing the model catalysis reaction involving the reduction of 4-nitrophenol (4-NP) to

4-aminophenol (4-AP) by $NaBH_4$ [277-279]. Such a reaction catalyzed by Au catalysts has been reported intensively because this reaction may be rapidly and easily characterized. It is commonly accepted that when Au nanoparticles are used for catalytic reduction, BH_4^- and 4-NP are first diffused from aqueous solution to the Au surfaces, and then the bare Au nanoparticles serve as catalysts to transfer electrons from BH_4^- to 4-NP, leading to the production of 4-AP. Since excess $NaBH_4$ is present in the reaction solution and the reduction of 4-NP by $NaBH_4$ is negligible in the absence of Au nanoparticles, the reaction may be considered pseudo-first-order with respect to the concentration of 4-NP. The apparent rate constant (k_{app}) is always used to evaluate the catalytic activity of NMNPs. The catalytic activity of NMNPs is affected by various factors, such as catalyst size and surface state, configuration, catalyst-support interaction, et al.

The diameters of NMNPs and CP-NMNP hybrids play the determining role in their catalytic activity [151]. For example, in the case of PANI nanofiber-supported Au nanoparticles where Au nanoparticles were decorated on fiber surface, the reaction catalyzed by smaller Au nanoparticles (2 nm) showed the shorter adsorption time and faster reaction rate (five times higher in k_{app}) as compared with those for larger Au nanoparticles (10 nm) [150]. In another case, diameter of PATP-Au hybrid nanofibers on the catalytic activity was also revealed [223]. When poly(2-aminothiophenol)-Au hybrid nanofibers with diameter of 80 nm and 200 nm both embedded with highly dispersed Au nanoparticles (2 nm) were used as catalyst, the reaction catalyzed by smaller nanofibers (80 nm) showed shorter adsorption time and faster reaction rate possible due to large exposure of Au catalysts on fiber surfaces with smaller diameter. In addition, when surfactant was introduced in poly(2-aminothiophenol)-Au hybrid nanofibers, the catalytic activity was completely lost indicating that the surfactant introduced in poly(2-aminothiophenol)-Au nanofibers might act as a catalyst inhibitor.

In addition, the effect of surface state of NMNPs was also disclosed in the case of PEDOT-Au hybrids [241]. In that study, while the Au content of the dispersion did not show a great influence on the value of k_{app}, the stabilizers showed a variation, in the order of sulfonate PS < SDS < PVP. They speculated that the aggregate size and morphology were likely to play an important role in deciding the reaction rate, however, those issues were not investigated in detailed. As CPs, it was found that dedoping treatment resulted in better catalytic performance due to stronger interaction between –N= groups and 4-NP [88].

The configuration of CP-NMNP hybrids also plays an important role in determining the catalytic performance. In the cases above mentioned, CP-NMNP hybrids with NMNPs decorated on surface of CPs or deeply embedded in CPs were utilized as catalysts. For the former case, high catalytic activity was attributed to the short pathway between reactant molecules and active catalysts; however, NMNPs were inclined to coagulate during reaction processes due to the lack of efficient isolation between nanoparticles, thus showing low stability and recyclability. For the later one, although such hybrids showed high stability, the dense organic coatings made it difficult for reactant molecules to reach buried active catalysts and thus they showed low catalytic activity. Therefore, the synthesis of CP-NMNP hybrids with both improved stability and catalytic activity is highly desirable. Yolk-shell nanostructures with NMNP as the movable core and *m*-SiO_2 as the penetrable shell as advanced catalysts can overcome the drawbacks. For example, PS@PANI@Au/*m*-SiO_2 yolk-shell nanostructures containing numerous sub-10 nm Au nanoparticles in each particle as highly stable/recyclable catalysts have been suggested [159].

In a more straightforward way, CPs themselves can form the penetrable shell due to their amorphous character. For example, PEDOT-Ag [119], PANI-Au [179], and POMA-Au [168] yolk-shell hybrids have been reported. As for CP-NMNP hybrids with CP shell and NMNP yolk, not only the aggregation of NMNP yolk is hindered by CP shell, but NMNP yolk may be also movable in the CP shell, which leads to high surface area. In addition, the CP-NMNP yolk-shell catalyst is stable and may be recycled again for reduction by precipitating, filtering and redispersing processes.

From the catalysis point of view, it should be noted that the introduction of a shell for the active NMNP core will undoubtedly delay the encounter of reaction reagents with catalysts resulting in decreased catalytic efficiency, as compared with bare NMNP catalysts without shell. Besides, the crush of yolk-shell catalysts involved in recyclable catalytic reactions and purification processes may cause the release of the NMNP core and induce their mutual coagulation. If the NMNP core is encapsulated in permeable CP shell, it will be easier for the reagents to encounter the NMNP core, leading to increased catalytic efficiency. Moreover, the stability should be enhanced as partial breakage of shells will not release NMNP core. Han et al. [170] showed that POMA-Au yolk-in-shell hybrids gave the highest catalytic activities, with k_{app} followed the following order: symmetric POMA-Au core–shell hybrids < asymmetric POMA-Au core–shell hybrids <

POMA-Au yolk–shell hybrids < pure Au nanoparticles < POMA-Au yolk-in-shell hybrids (**Fig. 31a**). As for POMA-Au yolk-in-shell hybrids, it was believed that reaction reagents both inside and outside polymer shells were easily accessible to the reactive centers due to porous polymer shells with large pore size and thin shell thickness with active Au cores close to both surfaces. The synergistic effect had been accounted for the result, where the intrinsic conducting nature of POMA favors electron transfer of catalysts due to their effective contact, which was believed to contribute to the improved catalytic efficiency. The synergistic effect between CP and NMNP towards improved catalytic activity was also reported in other cases using CP-NMNP catalysts [85, 90, 93, 115]. The recyclability results (**Fig. 31b**) also merited the high stability of the yolk-in-shell catalysts. As a result, both superior catalytic efficiency and recyclability were established, indicating their potential applications as efficient and recyclable catalysts involved in liquid-phase catalysis.

Fig. 31

In order to improve the recyclability of CP-NMNP hybrid catalysts, superparamagnetic materials may be incorporated. For example, PANI/Fe_3O_4/Au (Pd) hollow spheres [93], $CoFe_2O_4$/PANI/Au nanotubes [98], and Fe_3O_4/PANI/Au/*m*-SiO_2 core-shell spheres [160] were used to catalyze the reduction of 4-NP, with the catalysts recovered through simple magnetic separation.

In comparison with CP-NMNP colloid particles, CP-NMNP hybrid films show obvious advantages of easy and convenient operation in the practical catalytic reaction system. For example, the hybrid film may be processed to different shape according to the practical need, and put into or out from the catalytic reaction system freely. Moreover, the tedious regeneration process including precipitating, filtering and redispersing may be simplified by washing only with excessive water. Therefore, CP-NMNP hybrid films are indeed good catalysts for promoting the practical catalytic application [140, 264].

In addition to the model catalysis reaction of 4-NP to 4-AP by $NaBH_4$ [280], CP-Au hybrids have been applied as heterogeneous catalysts in other catalysis reactions. For example, PANI-Au spherical hybrids were active catalysts towards the reduction of rhodamine B (RhB) dye in the

presence of $NaBH_4$ [251]. Xuan et al. [90] reported that Fe_3O_4/PANI/Au hybrid used as a magnetically recoverable catalyst for the reduction of RhB with $NaBH_4$, was a more effective catalyst than Fe_3O_4/SiO_2/Au catalyst due to effective contact between PANI and Au nanocatalysts. POPD microsphere-supported Au nanoparticles showed high catalytic performance for aerobic oxidation of alcohols under air at room temperature [19, 152]. PANI supported bimetallic nanoparticles of Au and Pd were used as catalysts in the oxidation of benzyl alcohol with oxygen. PANI is expected to be a charge density donor and might have an influence on the electronic properties of the NMNPs [85]. PANI-TiO_2-Pt hybrids used as catalysts for photocatalytic reduction of CO_2 with H_2O vapor to CH_4 and/or CO, where PANI contributed to the enhancement of both the chemisorption of CO_2 and the separation of photogenerated electron–hole pairs [281].

Due to the catalytic activity of Pd nanoparticles towards Suzuki-Miyaura cross-coupling reaction of aryl halides with arylboronic acids, one of the most powerful and convenient synthetic protocols for the generation of biaryl in organic chemistry, CP-Pd hybrids have been intensively investigated as catalysts for such reactions. For example, PANI-Pd [282-286], PPY-Pd [287, 288], and poly(amino acetanilide)-Pd [289] hybrids were used as catalysts for Suzuki-Miyaura cross-coupling reactions. In order to improve the separation efficiency, superparamagnetic materials were incorporated in the hybrids [290, 128]. In particular, poly(2-aminothiophenol)-Au hybrids were established to be highly active towards Suzuki-Miyaura cross-coupling reactions [222].

In addition, CP-Pd hybrids have been used as active catalysts towards other reactions, such as the Heck reaction [283, 287, 291], asymmetric dihydroxylation of olefins to afford optically active vicinal diols [285], phenol formation from aryl halides and potassium hydroxide [286], selective hydrogenation of alkynes, cinnamaldehyde and 2-ethylanthraquinone [142, 292-294]. In some cases, the CP-Pd hybrids show improved catalytic performances over classical metal oxide-Pd hybrids. For example, PANI/Pd and PPY/Pd used as catalysts in a direct reduction of nitrite, showed better catalytic performances than the classical Pd/Al_2O_3 catalyst, with less ammonium ions. These better performances were explained by the redox and ion-exchange properties of the CPs allowing the exchange between the hydroxides produced and the dopant anion of the CPs. The ion-exchange property of the CPs depended on their oxidation states, directly linked to the polymerization conditions and easily modulated [115].

In the electrochemical catalysis, active catalysts of NMNPs should be immobilized on electrode surface. CPs are good candidates for immobilizing NMNPs to electrode surfaces, not only because of their excellent adhesive towards electrode surface and interaction with NMNPs, but also due to their interesting electrochemical properties. The porous structure derived from the amorphous nature of CPs facilitates disperse the NMNPs into the polymer matrix and to generate new electrocatalytic sites. CPs with dispersed NMNPs have shown properties of the individual components with a synergistic effect.

The oxygen reduction reaction (ORR) is one of the typical systems for measuring the catalytic properties of NMNPs and of great importance for fuel cell investigations [295, 296]. Pt nanoparticles are highly electrocatalytically active towards ORR. For example, PANI-Pt film-decorated electrodes were electrocatalytically active towards ORR [57, 83, 297, 298], and the electrocatalytical activity were tuned by controlling the thickness on the PANI-Pt multilayer [83]. In addition, CP-Au hybrids were used as catalysts for ORR, such as PANI-Au [127, 245], PATP-Au [58], and POPD-Au [299].

CP-NMNP hybrids have been frequently applied as electrocatalysts towards the oxidation of glucose to gluconic acid [38, 61, 84, 254, 255, 300]. Majumdar et al. [301] reported the synthesis of PANI-Au hybrids on the cation-exchange resin beads and demonstrated their use in catalyzing the oxidation of glucose to gluconic acid by Au nanoparticles and simultaneously in detecting the formation of the acid by the color change of PANI. The observations demonstrated the possibility of the incorporation of multifunctional components on the surfaces of resins for carrying out a chemical reaction as well as detection of the product. Riskin [25] demonstrated the synthesis and novel functions of a new hybrid material consisting of maghemite-Au core-shell hybrids embedded in PANI. The hybrid system exhibited magnetoswitchable charge transport properties in the absence and presence of an external magnetic field. The magnetic attraction of the hybrids to the electrode facilitated the charge transport across the polymer by shortening the inter-particle electron transfer distances. The magnetoswitchable electron transport properties through the polymer were then employed for the cyclic magnetoswitchable bioelectrocatalyzed oxidation of glucose (**Fig. 32**). In other cases, CP-NMNP hybrids also exhibited good electrochemical activities and electrocatalysis towards oxidation of ascorbic acid [36, 256, 302-304], methanol [34, 42, 55, 305-310], n-propanol [35]; NADH [80], dopamine and uric acid [89, 311, 312], and hydrazine [43,

313].

Fig. 32

3.2. Sensors

Because of its homogeneity, unique redox properties, high electrical conductivity and strong adherence to electrode surface, PANI has been extensively applied in sensors. Beside retaining electrochemical properties of traditional PANI, PANI nanomaterial offers many advantages, such as a large specific surface to allow fast diffusion of target molecules and a unique property to accelerate electron transfer [74]. Therefore, the sensor based on PANI nanomaterials can greatly enhance the sensing sensitivity and selectivity [206]. Addition of NMNPs into CPs will endow more adsorption sites for target molecules and contribute to improved electricity conductivity beneficial for improvement in their sensor performance.

PANI has a distinct doping mechanism. Protonation by acid–base chemistry leads to an internal redox reaction and the conversion from a low conductivity emeraldine base into a highly conducting emeraldine salt (**Fig. 1**). This implies that PANI may be used in highly sensitivity electrochemical sensors for reaction that involve an acid or base [229, 206, 268]. Jiang et al. [266] reported the sensor response to NH_3 using Au nanoparticles-functionalized two-dimensional patterned conducting PANI nanobowl monolayer. The sensor exhibited fast response (5 s) and recovery (7 s) behavior, of great importance in gas detection and control. The sensing mechanism was governed by the protonation/deprotonation phenomena brought by NH_3 gas. The interfused Au nanoparticles played a significant role of catalyst due to their surface activities. The larger surface area provided by the Au nanoparticles present near the nitrogen atom of PANI could enhance the charge transfer between the hybrid and the vapors, so the sensitivity of the sample increased with the increasing percentage of Au. Shirsat et al. [39] reported a sensitive, selective, and fast responding room temperature chemiresistive sensor for H_2S detection and quantification using PANI nanowires-Au nanoparticles hybrid network. Unlike strong acid such as HCl, H_2S is a weak acid and therefore only partially dopes the PANI and does not change conductivity significantly. These chemiresistive sensors show an excellent limit of detection (0.1 ppb), wide dynamic range (0.1-100 ppb), and very good selectivity and reproducibility. The reaction of H_2S

on the Au nanoparticles was obviously a critical step in the detection. The formation of AuS along with the enhancement of doping level of PANI from the donation of electrons to the protons released in the reaction was assumed to change the resistance of the PANI-Au nanoparticles network. PANI and Au nanoparticles acted as a donor and acceptor, respectively, confirming that the transfer of electron from *p*-type PANI network increased the conductance. PANI-Au fibrous hybrids were also used to detect volatile sulfur compounds of human expired breath [126]. The developed sensors, together with a multichannel sensing system, may find use in breath analysis and disease diagnose related to malodor biomarker gases.

Sensors based on CP-NMNP hybrids for dopamine detection have been frequently investigated [52, 81, 314-316] as dopamine is one of the crucial catecholamine neurotransmitter molecules widely distributed in the mammalian central nervous system for message transfer. CP-NMNP hybrids modified electrode possesses a higher active surface area and electrocatalytic activity for the oxidation of dopamine. For example, Song et al. [317] reported a selective dopamine sensor based on overoxidized-PANI-Au hybrids. The overoxidized PANI film enhanced selectivity and sensitivity toward dopamine. The concentration of the dopamine was determined using voltammetry as a non-enzymatic sensor. The Au nanoparticles favored the sensing of dopamine in the presence of ascorbic acid. The combination of the PANI with the Au nanoparticles could create synergetic effects for the performance of the biosensor, such as a fast response time, a lower detection limit, a wider linear range, enhanced selectivity, and higher sensitivity for the determination of dopamine. As the vesicles of catecholamine source have radii on the order of 100 nm, exploring the nanoelectrode is of particular significance. Zhang et al. [318] developed a novel dopamine nanosensor based on the PANI-Au hybrid modified Au nanoelectrode with tip dimensions approximate 200 nm in radius. As a nanosensor, the PANI-Au hybrid modified nanoelectrode exhibited highly electrocatalytic activity toward the oxidations of ascorbic acid and dopamine. Moreover, a large peak separation between ascorbic acid and dopamine allowed the modified nanoelectrode to detect dopamine in the presence of high concentration ascorbic acid. This sensor was sensitive and stable for the detection of dopamine and had a wide linear response. With the good spatial resolution, wide linear response and good selectivity, the proposed nanosensor was hopeful to be applied in detection of dopamine *in vivo*.

Hydrogen peroxide detection is also a hot topic as it may be harmful to biological systems and

appears to be involved in the neuropathology of central nervous system diseases [50, 319, 320]. CP-NMNP hybrids based sensors have been widely studied used for detection of hydrogen peroxide with a low detection limit and rapid response time. Similar to dopamine sensor, CP-NMNP hybrids modified electrode also delivers high electrocatalytic activity for the oxidation and reduction of hydrogen peroxide [94, 102, 129, 257, 321, 322]. As *ex situ* approaches for hydrogen peroxide detection have complicated procedures, use harmful chemicals such as acid, and require extended assay time, *in situ* detection is indeed highly demanded. Guo et al. [47] reported the *in situ* detection using hydrogen peroxide to diagnose ischemia through enhanced protein direct electron transfer on a unique horseradish peroxidase–Au nanoparticle–PANI nanowire biofilm (**Fig. 33**), which showed fast response (3 s), high sensitivity (117.8 μA mM^{-1} cm^{-2}), low detection limit (0.3 μM) and good selectivity and stability. It was discovered that the extracellular hydrogen peroxide molecule released per ischemic cell was 2.7-times of that of a normal cell. They stated that the *in situ* method can significantly reduce the assay time for in-time medical treatments of ischemia.

Fig. 33

DNA electrochemical biosensors based on CP-NMNP hybrids have been reported [44, 323]. In this case, both CP and Au nanostructures afford the high surface area and good electrical conductivity that favoring the transfer of the electrons. In addition, they also play an important role in the immobilization and hybridization of DNA. Feng et al. [324] reported the construction of PANI nanotube-Au nanoparticle (PAN-Au) membranes on the glassy carbon electrode for the electrochemical sensing of DNA. The synergistic effect of Au and PANI enhanced dramatically the sensitivity for the DNA hybridization recognition. DNA sequence-specific of phosphinothricin acetyltransferase gene existing in some transgenic crops was detected by electrochemical impedance spectroscopic measurement. The dynamic detection range of the sequence-specific DNA was from 1.0×10^{-12} to 1.0×10^{-6} M, and the detection limit was 3.1×10^{-13} M. PANI-Au hybrids with fibrous structures were also used for electrochemical sensing of DNA [124]. As PANI is limited redox active only under acidic conditions, normally at pH < 4, this drawback greatly restricts its applicability in bioelectrochemistry, which normally requires a neutral pH

environment. Utilizing self-doped PANI can overcome the problem as it can maintain its electroactivity even up to basic medium [325]. Wang et al. [326] developed self-doped PANI-Au hybrids based biosensors for DNA detection due to the electroactivity in neutral pH range of self-doped PANI. A gene fragment of the cauliflower mosaic virus 35S gene, which is related to one of the screening genes for the transgenically modified plants, was satisfactorily detected. The linear range was from 1.0×10^{-13} to 1.0×10^{-6} M and the detection limit was 1.9×10^{-14} M. In order to improve immobilization efficiency, Nascimento et al. [327] developed a biosensor for detection of dengue serotype at picomolar concentration based on PANI-Au hybrids with SH-terminal groups due to its ability of immobilizing dengue serotype-specific primers. The PANI-Au-serotype system exhibited a highly selectivity response to the complementary target of a human patient's dengue genome.

The advantageous features of PANI and Au nanoparticle have been utilized to construct a nontoxic biocompatible interface for immobilization of tumor cells as sensitive impedance cell sensor. Au nanoparticles with excellent biocompatibility were used to modify leukemia HL-60 cells, which could not only efficiently preserve the activity of tumor cells, but also accelerated the electron transfer between electrode and the immobilized cells. The biosensors based on PS-PANI-Au core-shell hybrids showed the wide detection range, low detection limit, good detection precision and simple fabrication process, which were further developed as a convenient means for the study of cells adhesion, proliferation and apoptosis [87]. PANI nanowire-Au nanoparticle hybrids based mediator free immunosensor were developed for the detection of cancer marker prostate specific antigen (**Fig. 34**). The linear range was from 1 pg mL^{-1} to100 ng mL^{-1}, the detection limit was 0.6 pg mL^{-1} (lower than ELISA), and the sensitivity was 1.4 μA L mol^{-1} (higher than ELISA) along with a regression coefficient of 98.99% [82].

Fig. 34

In addition, CP-NMNP hybrids based sensors have been applied to detect other species, such as glucose [86, 328-331], NADH [69, 80, 97, 332], carcinoembryonic antigen and α-fetoprotein [333], carbohydrate antigen [334-336], salbutamol [48], cortisol [210], glutathione [40], cholesterol [123, 337], chlorpyrifos [338], ascorbic acid [177, 267, 328], uric acid [339], oxalic acid [340],

hypochlorite [341], hydrazine [342], superoxide anion [343], acetone and toluene [344], NO_2 [49] et al. More recently, a pressure sensor consisting of PANI nanofibers and Au-coated polydimethylsiloxane micropillars were reported, where the sensors were operated by the changes in contact resistance between Au-coated micropillars and PANI according to the varying pressure [345].

3.3. Devices

Because of its very low solubility in most solvents, the infusibility, hygroscopic and low conductivity of PANI, its potential applications in devices have been greatly limited. The PANI-only device has not the electrical bistability (reversible transition of device from OFF state to ON state) and negative differential resistance functions. However, when PANI is combined with other components such as NMNPs, it will be meaningful for their application in various aspects with improved properties [241]. The charge-transport phenomena among CP-NMNP films [46, 79, 346] and the interfacial electronic structures of the CP–noble metal interfaces [347-353] have been investigated in detail due to their important role in determining the device performances.

A nonvolatile plastic digital memory device based on PANI-Au hybrids with PANI nanofibers decorated with Au nanoparticles were fabricated by Tseng et al. [122] The device had a simple structure consisting of the plastic hybrid film sandwiched between two electrodes (**Fig. 35**). The Au nanoparticles enhanced the conducting form of PANI which could keep its redox activity. An external bias was used to program the ON and OFF states of the device that were separated by a 3 orders of magnitude difference in conductivity. The hybrids possessed a memory effect via a charge transfer mechanism. The charge transfer happened between the imine nitrogen in the PANI and the Au nanoparticles, where PANI and Au nanoparticles acted as donor and acceptor, respectively. The ON-OFF switching process took less than 25 ns and the device retention time were several days after being programmed. The device was cycled more than 7 times. PANI-Au devices have repeatable conductance switching from room temperature to 121 K [354]. Wei et al. [355] fabricated an air stable nonvolatile memory device based on the PANI-Au hybrids. The synthesis and distribute of Au nanoparticles were conducted at the same time during the electropolymerization of aniline. The Au nanoparticles were embedded in the polymer matrix instead of being confined on the surface which was in favor of the stability of the hybrid in air. In

addition, PANI-Au yolk-shell hybrids been used for flexible memory device [169].

Fig. 35

Patil et al. [37] investigated the emission characteristics of PANI-Au hybrids as a novel and promising material for field emission based applications. From the field emission studies, the value of the turn on field, corresponding to 1 nA emission current, was 0.65 V/μm and emission current density of 1 μA/cm^2 had been drawn at an applied field of 1.1 V/μm. The field emission current stability investigated at 1 μA over duration of more than four hours was good. The superior field emission characteristics were attributed to the nanometric dimensions of the gold and PANI fibers.

Au-doped polyacrylonitrile–PANI core–shell nanofibers, which involved electrospinning of the core and subsequent gas-phase polymerization of the shell, were used as organic field effect transistors (OFETs) [356]. The as-prepared Au-doped PAN-PANI core–shell nanofibers provide a very high field-effect mobility of up to 11.6 cm^2 V^{-1} s^{-1}, without crystallizing the molecular structures of polymers. This high mobility were due to the nanofiber structure, which promoted charge transfer and reduced the grain-boundary effect, and the doping of Au nanoparticles, which served as “conducting bridges” between the PANI semiconducting domains. This approach was also suitable for other conducting polymers. PEDOP–Au/Ag hybrids were fabricated for application as smart window [45]. Electrochemical impedance spectroscopy showed that the easier ion diffusion through the electrode and the reduced charge-transfer resistance in the hybrids were responsible for the larger coloration efficiency shown by the PEDOP–Au/Ag devices. Electrochromic devices based on PEDOP–Ag and PEDOP–Au films, with an ionic-liquid-based polymeric electrolyte, showed a CE_{max} of 270 cm^2 C^{-1} at 458 nm (PEDOP–Au) followed by a second unusually high CE_{max} of 490 cm^2 C^{-1} at 1000 nm, greater than that achieved in neat PEDOP. The hybrids also showed faster switching kinetics while simultaneously maintaining a high optical contrast, thus demonstrating that NMNPs enhanced and modify the electrooptical response of CPs.

The electrical and magnetic properties of PANI-Au-Fe_3O_4-Au sub-microcables bundle as fabricated by combining electrospinning with electroless deposition were investigated [357]. The

conductivity of the bundle of obtained sub-microcables was 17.7 times higher than that of H_2SO_4-doped PANI fibers. Its coercivity was 13.57 times higher than that of H_2SO_4-doped PANI nanoparticles and it showed obvious ferromagnetic property. The sub-microcables bundle had high conductivity (58.4 S/cm), relatively large coercivity (930 G), indicating their potential application in future magnetic storage devices.

3.4. SERS

Surface-enhanced Raman scattering (SERS) is currently recognized as one of the most promising spectroscopic probes for ultrasensitive detection of chemical and biological analytes [358-360]. SERS nanosensors usually consist of NMNPs, which act as SERS substrates. Developing synthetic approaches to making NMNPs with well-defined structures is greatly desired for realizing highly sensitive SERS devices. Xu et al. [143] reported that large-area homogeneous three-dimensional Ag nanostructures on Au-supported PANI membranes displayed uniform SERS responses throughout the whole surface area, with an average enhancement factor of 10^6-10^7. The nanocavities formed by the stereotypical stacking of these Ag nanosheets and the junctions and gaps between two neighboring Ag nanoparticles were believed to be responsible for the strong SERS response upon plasmon absorption. In their continuing research [144], they showed that these ideal conditions typically consisted of Ag nanosheet morphologies with an edge dimension of approximately 50 nm, a size regime that was commensurate with an efficient SERS response from spherical Ag nanoparticle-based SERS substrates. Ag morphologies formed outside of the ideal deposition conditions exhibited relatively weak SERS activity-of approximately an order of magnitude-because they yielded either very thin nanosheets or single-crystal Ag features; neither structure supports efficient plasmon coupling. They also stated that PANI-Ag hybrids benefited from the underlying polymer’s processability to yield SERS-active materials of almost limitless shape and size and showed significant promise for future SERS-based sensing and detection schemes. In addition, thorny Au on PANI membranes for SERS application were also reported [361]. The enhanced Raman effect was used for investigating the structure of CPs near NMNPs. Baibarac et al. [362-364] investigated the SERS spectra of PANI thin films on rough Au, Ag, and Cu supports using the 1064 nm excitation radiation. It was verified that SERS spectra of PANI emeraldine base depended on the oxidizing properties of metallic surface, showing that

chemical reactions took place at polymer/metal interface. Izumi et al. [77] reported that the interaction of PANI emeraldine base with Ag and Au colloids was probed using surface-enhanced resonance Raman scattering (SERRS) at 3 different exciting radiations. Due to the great sensitivity of SERRS technique, the detection limit of PANI emeraldine base concentration was ca. 2×10^{-7} M in Ag and Au colloidal suspensions. Wang et al. [224] demonstrated that dandelion-like PANI-Au hybrid nanospheres were developed as a wonderful sensor for the detection of Hg^{2+} ions, which was based upon the Raman intensity response of PANI to Hg^{2+} ions. In this system, PANI as Raman reporter molecules carried large amounts of amine and imine functional groups, and the N atom had a lone pair of electrons that could involve coordination between N atoms and Au NPs. When Hg^{2+} were added into PANI-Au colloidal solution, the amine and imine groups could act as adsorption sites of Hg^{2+} on PANI chains through forming quadridentate coordination. After addition of Hg^{2+} ions, the 'thorn' of dandelion-like PANI-Au nanospheres shrunk and the surface morphology changed evidently, which demonstrated that there was strong interaction between Hg^{2+} and PANI, and Au nanoparticles in nanospheres aggregated. A large localized electromagnetic field was produced around the aggregated Au nanoparticles due to the electromagnetic coupling between the adjacent Au nanoparticles, so the increase of SERS signal in the intensity were observed. Results from the morphology dependent sensitivity investigations showed that the dandelion-like PANI-Au nanospheres had an ultra sensitive response (as low as 10^{-11} M) compared with other morphologies due to their larger contact area with Hg^{2+} ions.

3.5. Others

CP-NMNP hybrids have been used as electrochemical supercapacitors [365, 366]. Lang et al. [71] reported the synthesis of three-dimensional bicontinuous nanoporous PANI-Au hybrid films made by one-step electrochemical polymerization of PANI shell onto dealloyed nanoporous Au skeletons. The free-standing PANI-Au hybrid films were promising electrode materials for high-performance aqueous and all-solid-state supercapacitors with ultrahigh volumetric capacitance (~1500 F cm^{-3}) and energy density (~0.078 Wh cm^{-3}), seven and four orders of magnitude higher than these of electrolytic capacitors, with the same power density up to ~190 W cm^{-3}. The good capacitive behaviors of PANI-Au supercapacitor devices were arose from the ion and electron transports enhanced by unique bicontinuous nanostructure, where the nanoporosity

facilitated the fast ion diffusion, and provided the large PANI/electrolyte interface to ensure the sufficient redox reaction of PANI during charge/discharge processes, and the three-dimensional interconnected Au network with ultrahigh electrical conductivity harnessed the electron transport by remarkably decreasing the internal resistance of assembled devices. Ye and coworkers [367, 368] reported the fabrication of flexible, in-plane, and all-solid-state micro-supercapacitors on the basis of printed interdigital PANI-Au network hybrid electrodes by the combination of laser printing technology and *in situ* anodic electropolymerization. The micro-supercapacitors acquired a maximum energy density of 5.83 mW h cm^{-3} and a maximum power density of 0.45 W cm^{-3} that were both comparable to or superior to the values obtained for currently available state-of-the-art planar supercapacitors/micro-supercapacitors. In addition, PEDOT-Au hybrids were used as organic thermoelectric materials, where the PEDOT-Au hybrids showed better thermoelectric performance than pristine PEDOT without Au nanoparticles [369]. Addition of Au nanoparticles improved the electrical conductivity of the PEDOT films from 104 S cm^{-1} to 241 S cm^{-1} and the thermoelectric figure of merit from 0.62×10^{-2} to 1.63×10^{-2} at 50 ℃. Microwave absorption property of PANI-Au-GO hybrids was investigated and the electromagnetic interference shielding effectiveness of PANI was enhanced due to the inclusion of Au nanoparticles and GO with increased interaction between the PANI, Au nanoparticles and GO [269].

4. Conclusion and outlook

A variety of CP-NMNP hybrids may be prepared by different methods. The configuration of CP-NMNP hybrids can vary from one-dimensional nanofibers and nanotubes to two-dimensional nanofilms, and to three-dimensional core-shell and yolk-shell nanostructures, and even to hierarchical structures (such as fractal architectures and dandelion-like nanospheres). The location of NMNPs may be supported on surfaces or buried inside CPs, the morphology of NMNPs may be tuned from nanoparticles, nanorods and nanoplates, to complex jellyfish-like nanostructures, and the size of NMNPs may be controlled limited to several nanometers. Control of the nanostructure of both components, PANI and NMNP, has brought promising results with respect to their functions, which is of high importance for their potential applications.

In the last few years, new advances in the preparation, by chemical and electrochemical means,

and characterization of CP-NMNP hybrids, have been seen. Significant progress has been achieved regarding control of the size and morphology of both CP and NMNP nanostructures presented in CP-NMNP hybrids. However, the interfacial interactions between CPs and NMNPs are still not well understood. It is also apparent that studies involving a larger range of NMNPs with CPs of varying lengths will be useful to further understand the effect of a conjugated matrix on the optical and electronic properties of the hybrids. These observations bode well for applications of CP-NMNP hybrids as catalysts, sensors, devices and SERS, which take advantage of the electronic and optical properties of the hybrids. In most cases, the synergistic effect in CP-NMNP hybrids contributes to the improved performances involved in various applications, even though the underlying synergy mechanisms have not been disclosed in detail, inviting future research.

Acknowledgements

The authors gratefully acknowledge financial support from the National Natural Science Foundation of China (21673202 and 21273004), Innovation Program for Graduate Students in Universities of Jiangsu Province (No. KYZZ15_0361), the Priority Academic Program Development of Jiangsu Higher Education Institutions, and Qing Lan Project.

References

[1] Kang ET, Neoh KG, Tan KL. Polyaniline: a polymer with many interesting intrinsic redox states. Prog Polym Sci 1997 ;23:277-324.

[2] Bhadra S, Khastgir D, Singha NK, Lee JH. Progress in preparation, processing and applications of polyaniline. Prog Polym Sci 2009 ;34:783-810.

[3] Palaniappan S, John A. Polyaniline materials by emulsion polymerization pathway. Prog Polym Sci 2008 ;33:732-758.

[4] Stejskal J, Sapurina I, Trchová M. Polyaniline nanostructures and the role of aniline oligomers in their formation. Prog Polym Sci 2010 ;35:1420-1481.

[5] Laslau C, Zujovic Z, Travas-Sejdic J. Theories of polyaniline nanostructure self-assembly: Towards an expanded, comprehensive Multi-Layer Theory (MLT). Prog Polym Sci 2010 ;35:1403-1419.

[6] Lu X, Zhang W, Wang C, Wen TC, Wei Y. One-dimensional conducting polymer nanocomposites: Synthesis, properties and applications. Prog Polym Sci 2011 ;36:671-712.

[7] Long YZ, Li MM, Gu C, Wan M, Duvail JL, Liu Z, Fan Z. Recent advances in synthesis, physical properties and applications of conducting polymer nanotubes and nanofibers. Prog Polym Sci 2011 ;36:1415-1442.

[8] Hatchett DW, Josowicz M. Composites of intrinsically conducting polymers as sensing nanomaterials. Chem Rev 2008 ;108:746-769.

[9] Du Y, Shen SZ, Cai K, Casey PS. Research progress on polymer–inorganic thermoelectric nanocomposite materials. Prog Polym Sci 2012 ;37:820-841.

[10] Oueiny C, Berlioz S, Perrin FX. Carbon nanotube–polyaniline composites. Prog Polym Sci 2014 ;39:707-748.

[11] Janáky C, Rajeshwar K. The role of (photo)electrochemistry in the rational design of hybrid conducting polymer/semiconductor assemblies: From fundamental concepts to practical applications. Prog Polym Sci 2015 ;43:96-135.

[12a] Ćirić-Marjanović G. Recent advances in polyaniline composites with metals, metalloids and nonmetals. Synth Met 2013 ;170:31-56.

[12b] Stejskal J. Polymers of phenylenediamines. Prog Polym Sci 2015 ;41:1-31.

[13] Zhou Q, Shi G. Conducting polymer-based catalysts. J Am Chem Soc 2016 ;138:2868-2876.

[14] Abadeer NS, Murphy CJ. Recent progress in cancer thermal therapy using gold nanoparticles. J Phys Chem C 2016 ;120:4691-4716.

[15] Yang X, Yang M, Pang B, Vara M, Xia Y. Gold nanomaterials at work in biomedicine. Chem Rev 2015 ;115:10410-10488.

[16] Zhou W, Gao X, Liu D, Che X. Gold nanoparticles for in vitro diagnostics. Chem Rev 2015 ;115:10575-10636.

[17] Stratakis M, Garcia H. Catalysis by supported gold nanoparticles: Beyond aerobic oxidative processes. Chem Rev 2012 ;112:4469-4506.

[18] Udayabhaskararao T, Pradeep T. New protocols for the synthesis of stable Ag and Au nanocluster molecules. J Phys Chem Lett 2013 ;4:1553-1564.

[19] Han J, Liu Y, Guo R. Reactive template method to synthesize gold nanoparticles with

controllable size and morphology supported on shells of polymer hollow microspheres and their application for aerobic alcohol oxidation in water. Adv Funct Mater 2009 ;19:1112-1117.

[20] Kessler T, Luna AMC. A catalytic platinum-ruthenium-polyaniline electrode for methanol oxidation. J Appl Electrochem 2002 ;32:825-830.

[21] Pyo M, Bohn CC, Smela E, Reynolds JR, Brennan AB. Direct strain measurement of polypyrrole actuators controlled by the polymer/gold interface. Chem Mater 2003 ;15:916-922.

[22] Smith JA, Josowicz M, Janata J. Gold-polyaniline composite-Part I. Moving electrochemical interface. Phys Chem Chem Phys 2005 ;7:3614-3618.

[23] Smith JA, Josowicz M, Engelhard M, Baer DR, Janata J. Gold-polyaniline composites-Part II. Effects of nanometer sized particles. Phys Chem Chem Phys 2005 ;7:3619-3625.

[24] Lacroix JC, Leroux Y, Emile E, Fave C, Trippe G. Conducting polymer/gold nanoparticle hybrid materials: A step toward electroactive plasmonic devices. Electrochem Commun 2007 ;9:1258-1262.

[25] Riskin M, Basnar B, Huang Y, Willner I. Magnetoswitchable charge transport and bioelectrocatalysis using maghemite-Au core-shell nanoparticle/polyaniline composites. Adv Mater 2007 ;19:2691-2695.

[26] Vorotyntsev MA, Skompska M, Rajchowska A, Borysiuk J, Donten M. A new strategy towards electroactive polymer-inorganic nanostructure composites. Silver nanoparticles inside polypyrrole matrix with pendant titanocene dichloride complexes. J Electroanal Chem 2011 ;662:105-115.

[27] Ali Y, Kumar V, Sonkawade RG, Dhaliwal AS. Effect of swift heavy ion beam irradiation on Au-polyaniline composite films. Vacuum 2013 ;90:59-64.

[28] Ali Y, Kumar V, Sonkawade RG, Shirsat MD, Dhaliwal AS. Two-step electrochemical synthesis of Au nanoparticles decorated polyaniline nanofiber. Vacuum 2013 ;93:79-83.

[29] Hatchett DW, Josowicz M, Janata J, Baer DR. Electrochemical formation of Au clusters in polyaniline. Chem Mater 1999 ;11:2989-2994.

[30] Saheb A, Smith JA, Josowicz M, Janata J, Baer DR, Engelhard MH. Controlling size of gold clusters in polyaniline from top-down and from bottom-up. J Electroanal Chem

2008 ;621:238-244.

[31] Jonke AP, Josowicz M, Janata J, Engelhard MH. Electrochemically controlled atom by atom deposition of gold to Polyaniline. J Electrochem Soc 2010 ;157:P83-P87.

[32] Jonke AP, Josowicz M, Janata J. Polyaniline doped with atomic gold. J Electrochem Soc 2011 ;158:E147-E151.

[33] Jonke AP, Josowicz M, Janata J. Odd-even pattern observed in polyaniline/(Au_0-Au_8) composites. J Electrochem Soc 2012 ;159:P40-P43.

[34] Schwartz IT, Jonke AP, Josowicz M, Janata J. Polyaniline electrodes with atomic Au_nPd_1 alloys: Oxidation of methanol and ethanol. Catal Lett 2013 ;143:636-641.

[35] Jonke AP, Josowicz M, Janata J. Polyaniline electrodes containing tri-atomic Au/Pd clusters: Effect of ordering. Catal Lett 2013 ;143:1261-1265.

[36] Hosseini M, Momeni MM, Faraji M. Electrochemical fabrication of polyaniline films containing gold nanoparticles deposited on titanium electrode for electro-oxidation of ascorbic acid. J Mater Sci 2010 ;45:2365-2371.

[37] Patil SS, Koiry SP, Aswal DK, More MA. Enhanced field emission from the gold-polyaniline (Au-PANI) nanocomposite. AIP Conf Proc 2010 ;1313:295-297.

[38] Guerra-Balcazar M, Ortega R, Castaneda F, Arriaga LG, Ledesma-Garcia J. Synthesis of Au nanoparticles/polyaniline composites by electroreduction for glucose oxidation. Int J Electrochem Sci 2011 ;6:4667-4675.

[39] Shirsat MD, Bangar MA, Deshusses MA, Myung NV, Mulchandani A. Polyaniline nanowires-gold nanoparticles hybrid network based chemiresistive hydrogen sulfide sensor. Appl Phys Lett 2009 ;94:083502/1-3.

[40] Narang J, Chauhan N, Jain P, Pundir CS. Silver nanoparticles/multiwalled carbon nanotube/polyaniline film for amperometric glutathione biosensor. Int J Biol Macromol 2012 ;50:672-678.

[41] Cho SH, Park SM. Electrochemistry of conductive polymers 39. Contacts between conducting polymers and noble metal nanoparticles studied by current-sensing atomic force microscopy. J Phys Chem B 2006 ;110:25656-25664.

[42] Jüttner K, Mangold KM, Lange M, Bouzek K. Preparation and properties of composite polypyrrole/Pt catalyst systems. Russ J Electrochem 2004 ;40:317-325

[43] Ferreira VC, Melato AI, Silva AF, Abrantes LM. Attachment of noble metal nanoparticles to conducting polymers containing sulphur-preparation conditions for enhanced electrocatalytic activity. Electrochim Acta 2011 ;56:3567-3574

[44] Ferreira VC, Melato AI, Silva AF, Abrantes LM. Conducting polymers with attached platinum nanoparticles towards the development of DNA biosensors. Electrochem Commun 2011 ;13:993-996.

[45] Kharkwal A, Deepa M, Joshi AG, Srivastava AK. Red to blue high electrochromic contrast and rapid switching poly(3,4-ethylenedioxypyrrole)-Au/Ag nanocomposite devices for smart windows. ChemPhysChem 2011 ;12:1176-1188.

[46] Deepa M, Kharkwal A, Joshi AG, Srivastava AK. Charge transport and electrochemical response of poly(3,4-ethylenedioxypyrrole) films improved by noble-metal nanoparticles. J Phys Chem B 2011 ;115:7321-7331.

[47] Guo CX, Zheng XT, Ng SR, Lai YC, Lei Y, Li CM. In situ molecular detection of ischemic cells by enhanced protein direct electron transfer on a unique horseradish peroxidase-Au nanoparticles-polyaniline nanowires biofilm. Chem Commun 2011 ;47:2652-2654.

[48] Huang JD, Lin Q, Zhang XM, He XR, Xing XR, Lian WJ, Zuo MM, Zhang QQ. Electrochemical immunosensor based on polyaniline/poly (acrylic acid) and Au-hybrid graphene nanocomposite for sensitivity enhanced detection of salbutamol. Food Res Int 2011 ;44:92-97.

[49] Do JS, Chang WB. Amperometric nitrogen dioxide gas sensor: Preparation of PAn/Au/SPE and sensing behavior. Sens Actuat B 2001 ;72:101-107.

[50] Ernst AZ, Zoladek S, Wiaderek K, Cox JA, Kolary-Zurowska A, Mieunikowski K, Kulesza PJ. Network films of conducting polymer-linked polyoxometalate-modified gold nanoparticles: Preparation and electrochemical characterization. Electrochim Acta 2008 ;53:3924-3931.

[51] Kulesza PJ, Chojak M, Karnicka K, Miecznikowski K, Palys B, Lewera A, Wieckowski A. Network films composed of conducting polymer-linked and polyoxometalate-stabilized platinum nanoparticles. Chem Mater 2004 ;16:4128-4134.

[52] Mathiyarasu J, Senthilkumar S, Phani KLN, Yegnaraman V. PEDOT-Au nanocomposite film for electrochemical sensing. Mater Lett 2008 ;62:571-573.

[53] Koval'chuk EP, Ogenko VM, Reshetnyak OV, Pereviznyk OB, Davydenko N, Marchuk IE. Surface modification of silver microparticles with 4-thioaniline. Electrochim Acta 2010 ;55:5154-5162.

[54] Kim K, Lee I. Chemical lithography by Ag-nanoparticle-mediated photoreduction of aromatic nitro monolayers on Au. Langmuir 2004 ;20:7351-7354.

[55] Santhosh P, Gopalan A, Lee KP. Gold nanoparticles dispersed polyaniline grafted multiwall carbon nanotubes as newer electrocatalysts: Preparation and performances for methanol oxidation. J Catal 2006 ;238:177-185.

[56] Li NF, Lei T, Liu Y, He YH, Zhang YD. Electrochemical preparation and characterization of gold-polyaniline core-shell. Trans Nonferrous Met Soc China 2010 ;20:2314-2319

[57] Kannan P, John SA. Fabrication of conducting polymer-gold nanoparticles film on electrodes using monolayer protected gold nanoparticles and its electrocatalytic application. Electrochim Acta 2011 ;56:7029-7037.

[58] Gopalan AI, Lee KP, Manesh KM, Santhosh P, Kim JH. Gold nanoparticles dispersed into poly(aminothiophenol) as a novel electrocatalyst - Fabrication of modified electrode and evaluation of electrocatalytic activities for dioxygen reduction. J Mol Catal A 2006 ;256:335-345.

[59] Frasconi M, Tel-Vered R, Riskin M, Willner I. Electrified selective "sponges" made of Au nanoparticles. J Am Chem Soc 2010 ;132:9373-9382.

[60] Gao W, Sattayasamitsathit S, Uygun A, Pei A, Ponedal A, Wang J. Polymer-based tubular microbots: role of composition and preparation. Nanoscale 2012 ;4:2447-2453.

[61] Gao E, Granot E, Katz E, Basnar B, Willner I. Enhanced bioelectrocatalysis using Au-nanoparticle/polyaniline hybrid systems in thin films and microstructured rods assembled on electrodes. Chem Mater 2005 ;17:4600-4609.

[62] Parthasarathy RV, Martin CR. Template-synthesized polyaniline microtubules. Chem Mater 1994 ;6:1627-1632.

[63] Cai Z, Martin CR. Electronically conductive polymer fibers with mesoscopic diameters show enhanced electronic conductivities. J Am Chem Soc 1989 ;111:4138-4139.

[64] Martin CR, Dyke LSV, Cai Z, Liang W. Template synthesis of organic microtubules. J Am Chem Soc 1990 ;112:8976-8977.

[65] Martin CR. Template synthesis of polymeric and metal microtubules. Adv Mater 1991 ;3:457-459.

[66] Cai Z, Lei J, Liang W, Menon V, Martin CR. Molecular and supermolecular origins of enhanced electric conductivity in template-synthesized polyheterocyclic fibrils. 1. Supermolecular effects. Chem Mater 1991 ;3:960-967.

[67] Martin BR, Dermody DJ, Reiss BD, Fang M, Lyon LA, Natan MJ, Mallouk TE. Orthogonal self-assembly on colloidal gold-platinum nanorods. Adv Mater 1999 ;11:1021-1025.

[68] Lahav M, Weiss EA, Xu QB, Whitesides GM. Core-shell and segmented polymer-metal composite nanostructures. Nano Lett 2006 ;6:2166-2171

[69] Zhang M, Yamaguchi A, Morita K, Teramae N. Electrochemical synthesis of Au/polyaniline-poly(4-styrenesulfonate) hybrid nanoarray for sensitive biosensor design. Electrochem Commun 2008 ;10:1090-1093.

[70] Callegari V, Gence L, Melinte S, Demoustier-Champagne S. Electrochemically template-grown multi-segmented gold-conducting polymer nanowires with tunable electronic behavior. Chem Mater 2009 ;21:4241-4247.

[71] Lang XY, Zhang L, Fujita T, Ding Y, Chen MW. Three-dimensional bicontinuous nanoporous Au/polyaniline hybrid films for high-performance electrochemical supercapacitors. J Power Sources 2012 ;197:325-329.

[72] Bhandari S, Deepa M, Sharma SN, Joshi AG, Srivastava AK, Kant R. Charge transport and electrochromism in novel nanocomposite films of poly(3,4-ethylenedioxythiophene)-Au nanoparticles-CdSe quantum dots. J Phys Chem C 2010 ;114:14606-14613.

[73] Krutyakov YA, Kudrinsky AA, Olenin AY, Lisichkin GV. Synthesis of highly stable silver colloids stabilized with water soluble sulfonated polyaniline. Appl Surf Sci 2010 ;256:7037-7042.

[74] Kim JH, Cho JH, Cha GS, Lee CW, Kim HB, Paek SH. Conductimetric membrane strip immunosensor with polyaniline-bound gold colloids as signal generator. Biosens Bioelectron 2000 ;14:907-915.

[75] Chen F, Xu GQ, Hor TSA. Preparation and assembly of colloidal gold nanoparticles in CTAB-stabilized reverse microemulsion. Mater Lett 2003 ;57:3282-3286.

[76] Afzal AB, Akhtar MJ, Nadeem M, Hassan MM. Investigation of structural and electrical properties of polyaniline/gold nanocomposites. J Phys Chem C 2009 ;113:17560-17565.

[77] Izumi CMS, Andrade GFS, Temperini MLA. Surface-enhanced resonance Raman scattering of polyaniline on silver and gold colloids. J Phys Chem B 2008 ;112:16334-16340.

[78] Tanami G, Gutkin V, Mandler D. Thin nanocomposite films of polyaniline/Au nanoparticles by the Langmuir-Blodgett technique. Langmuir 2010 ;26:4239-4245.

[79] Nicholson PG, Ruiz V, Macpherson JV, Unwin PR. Effect of composition on the conductivity and morphology of poly (3-hexylthiophene)/gold nanoparticle composite Langmuir-Schaeffer films. Phys Chem Chem Phys 2006 ;8:5096-5105.

[80] Tian S, Liu J, Zhu T, Knoll W. Polyaniline/gold nanoparticle multilayer films: assembly, properties, and biological applications. Chem Mater 2004 ;16:4103-4108.

[81] Stoyanova A, Ivanov S, Tsakova V, Bund A. Au nanoparticle-polyaniline nanocomposite layers obtained through layer-by-layer adsorption for the simultaneous determination of dopamine and uric acid. Electrochim Acta 2011 ;56:3693-3699.

[82] Dey A, Kaushik A, Arya SK, Bhansali S. Mediator free highly sensitive polyaniline–gold hybrid nanocomposite based immunosensor for prostate-specific antigen (PSA) detection. J Mater Chem 2012 ;22:14763-14772.

[83] Yuan JH, Han DX, Zhang YJ, Shen YF, Wang ZJ, Zhang QX, Niu L. Electrostatic assembly of polyaniline and platinum-poly(amidoamine) dendrimers hybrid nanocomposite multilayer, and its electrocatalysis towards CO and O_2. J Electroanal Chem 2007 ;599:127-135.

[84] Ishida T, Kuroda K, Kinoshita N, Minagawa W, Haruta M. Direct deposition of gold nanoparticles onto polymer beads and glucose oxidation with H_2O_2. J Colloid Interface Sci 2008 ;323:105-111.

[85] Marx S, Baiker A. Beneficial interaction of gold and palladium in bimetallic catalysts for the selective oxidation of benzyl alcohol. J Phys Chem C 2009 ;113:6191-6201.

[86] Liu Y, Feng X, Shen J, Zhu JJ, Hou W. Fabrication of a novel glucose biosensor based on a highly electroactive polystyrene/ polyaniline/Au nanocomposite. J Phys Chem B 2008 ;112:9237-9242.

[87] Gu MM, Zhang JJ, Li Y, Jiang LP, Zhu JJ. Fabrication of a novel impedance cell sensor based on the polystyrene/polyaniline/Au nanocomposite. Talanta 2009 ;80:246-249.

[88] Yu J, Guo W, Yang M, Luan Y, Tao J, Zhang X. Synthesis of hierarchical Polystyrene/Polyaniline@Au nanostructures of different surface states and studies of their catalytic properties. Sci China Chem 2014 ;57:1211-1217.

[89] Feng XM, Mao CJ, Yang G, Hou WH, Zhu JJ. Polyaniline/Au composite hollow spheres: Synthesis, characterization, and application to the detection of dopamine. Langmuir 2006 ;22:4384-4389.

[90] Xuan SH, Wang YXJ, Yu JC, Leung KCF. Preparation, characterization, and catalytic activity of core/shell Fe_3O_4@polyaniline@Au nanocomposites. Langmuir 2009 ;25:11835-11843.

[91] Yu Q, Shi M, Cheng Y, Wang M, Chen H. Fe_3O_4@Au/polyaniline multifunctional nanocomposites: their preparation and optical, electrical and magnetic properties. Nanotechnology 2008 ;19:265702/1-6.

[92] Zhang H, Zhong X, Xu JJ, Chen HY. Fe_3O_4/polypyrrole/Au nanocomposites with core/shell/shell structure: Synthesis, characterization, and their electrochemical properties. Langmuir 2008 ;24:13748-13752.

[93] Kong L, Lu X, Jin E. Jiang S, Bian X, Zhang W, Wang C, Constructing magnetic polyaniline/metal hybrid nanostructures using polyaniline/Fe_3O_4 composite hollow spheres as supports. J Solid State Chem 2009 ;182:2081-2087.

[94] Chen XJ, Chen ZX, Zhu JW, Xu CB, Yan W, Yao C. A novel H_2O_2 amperometric biosensor based on gold nanoparticles/self-doped polyaniline nanofibers. Bioelectrochemistry 2011 ;82:87-94.

[95] Sanches EA, Soares JC, Iost RM, Marangoni VS, Trovati G, Batista T, Mafud AC, Zucolotto V, Mascarenhas YP. Structural characterization of emeraldine-salt polyaniline/gold nanoparticles complexes. J Nanomater 2011 ;2011:697071/1-7.

[96] Huang H, Feng X, Zhu JJ. Synthesis, characterization and application in electrocatalysis of polyaniline/Au composite nanotubes. Nanotechnology 2008 ;19:145607/1-7.

[97] Feng X, Zhang Y, Yan Z, Ma Y, Shen Q, Liu X, Fan Q, Wang L, Huang W. Synthesis of

polyaniline/Au composite nanotubes and their high performance in the detection of NADH. J Solid State Electrochem. 2014 ;18:1717-1723.

[98] Zhang Z, Jiang Y, Chi M, Yang Z, Nie G, Lu X, Wang C. Fabrication of Au nanoparticles supported on $CoFe_2O_4$ nanotubes by polyaniline assisted self-assembly strategy and their magnetically recoverable catalytic properties. Appl Surf Sci 2016 ;363:578-585.

[99] Zhang J, Liu X, Zhang L, Cao B, Wu S. Reactive template synthesis of polypyrrole nanotubes for fabricating metal/conducting polymer nanocomposites. Macromol Rapid Commun 2013 ;34:528-532.

[100] Sapurina I, Stejskal J. Ternary composites of multi-wall carbon nanotubes, polyaniline, and noble-metal nanoparticles for potential applications in electrocatalysis. Chem Papers 2009 ;63:579-585.

[101] Kumar NA, Jeong YT. Fabrication of conducting polyaniline-multiwalled carbon nanotube nanocomposites and their use as templates for loading gold nanoparticles. Polym Int 2010 ;59:1367-1374

[102] Feng XM, Li RM, Ma YW, Fan QL, Huang W. The synthesis of highly electroactive N-doped carbon nanotube/polyaniline/Au nanocomposites and their application to the biosensor. Synth Met 2011 ;161:1940-1945.

[103] Reddy KR, Sin BC, Ryu KS, Kim JC, Chung H, Lee Y. Conducting polymer functionalized multi-walled carbon nanotubes with noble metal nanoparticles: Synthesis, morphological characteristics and electrical properties. Synth Met 2009 ;159:595-603.

[104] Ting YP, Neoh KG, Kang ET, Tan KL. Recovery of gold by electroless precipitation from acid solutions using polyaniline. J Chem Technol Biotechnol 1994 ;59:31-36.

[105] MacDiarmid AG, Yang LS, Huang WS, Humphrey BD. Polyaniline: Electrochemistry and application to rechargeable batteries. Synth Met 1987 ;18:393-398.

[106] MacDiarmid AG, Manohar SK, Masters JG, Sun Y, Weiss H, Epstein AJ. Polyaniline: Synthesis and properties of pernigraniline base. Synth Met 1991 ;41:621-626.

[107] Li D, Huang J, Kaner RB. Polyaniline nanofibers: A unique polymer nanostructure for versatile applications. Acc Chem Res 2009 ;42:135-145.

[108] Xu P, Jeon SH, Chen HT, Luo H, Zou G, Jia Q, Anghel M, Teuscher C, Williams DJ, Zhang B, Han X, Wang HL. Facile synthesis and electrical properties of silver wires

through chemical reduction by polyaniline. J Phys Chem C 2010 ;114:22147-22154.

[109] O'Mullane AP, Dale SE, Macpherson JV, Unwin PR. Fabrication and electrocatalytic properties of polyaniline/Pt nanoparticle composites. Chem Commun 2004 :1606-1607.

[110] Kang ET, Ting YP, Neoh KG, Tan KL. Electroless recovery of precious metals from acid solutions by N-containing electroactive polymers. Synth Met 1995 ;69:477-478.

[111] Ma ZH, Tan KL, Kang ET. Electroless plating of palladium and copper on polyaniline films. Synth Met 2000 ;114:17-25.

[112] Neoh KG, Young TT, Looi NT, Kang ET, Tan KL. Oxidation-reduction interactions between electroactive polymer thin films and Au(III) ions in acid solutions. Chem Mater 1997 ;9:2906-2912.

[113] Huang J, Kaner RB. Nanofiber formation in the chemical polymerization of aniline: A mechanistic study. Angew Chem Int Ed 2004 ;43:5817-5821.

[114] Wang JG, Neoh KG, Kang ET. Preparation of nanosized metallic particles in polyaniline. J Colloid Interface Sci 2001 ;239:78-86.

[115] Dodouche I, Epron F. Promoting effect of electroactive polymer supports on the catalytic performances of palladium-based catalysts for nitrite reduction in water. Appl Catal B 2007 ;76:291-299.

[116] Neoh KG, Tan KK, Goh PL, Huang SW, Kang ET, Tan KL. Electroactive polymer-SiO_2 nanocomposites for metal uptake. Polymer 1999 ;40:887-893.

[117] Khan MA, Perruchot C, Armes SP, Randall DP. Synthesis of gold-decorated latexes via conducting polymer redox templates. J Mater Chem 2001 ;11:2363-2372.

[118] Ding J, Wang HX, Lin T, Lee B. Electroless synthesis of nano-structured gold particles using conducting polymer nanoparticles. Synth Met 2008 ;158:585-589.

[119] Xia Y, Xu L. Fabrication and catalytic property of an Ag@poly(3,4-ethylenedioxythiophene) yolk/shell structure. Synth Met 2010 ;160:545-548.

[120] Smith JA, Josowicz M, Janata J. Polyaniline-gold nanocomposite system. J Electrochem Soc 2003 ;150:E384-E388.

[121] Huang J, Virji S, Weiller BH, Kaner RB. Nanostructured polyaniline sensors. Chem Eur J 2004 ;10:1314-1319.

[122] Tseng RJ, Huang JX, Ouyang J, Kaner RB, Yang Y. Polyaniline nanofiber/gold

nanoparticle nonvolatile memory. Nano Lett 2005 ;5:1077-1080.

[123] Huang J. Syntheses and applications of conducting polymer polyaniline nanofibers. Pure Appl Chem 2006 ;78:15-27.

[124] Spain E, Kojima R, Kaner RB, Wallace GG, O'Grady J, Lacey K, Barry T, Keyes TE, Forster RJ. High sensitivity DNA detection using gold nanoparticle functionalised polyaniline nanofibers. Biosens Bioelectron 2011 ;26:2613-2618.

[125] Baker CO, Shedd B, Tseng RJ, Martinez-Morales AA, Ozkan CS, Ozkan M, Yang Y, Kaner RB. Size control of gold nanoparticles grown on polyaniline nanofibers for bistable memory devices. ACS Nano 2011 ;5:3469-3474.

[126] Liu CJ, Hayashi K, Toko K. Au nanoparticles decorated polyaniline nanofiber sensor for detecting volatile sulfur compounds in expired breath. Sens Actuat B 2012 ;161:504-509.

[127] Liu S, Xu HM, Ou JF, Li ZP, Yang SR, Wang JQ. A feasible approach to the fabrication of gold/polyaniline nanofiber composites and its application as electrocatalyst for oxygen reduction. Mater Chem Phys 2012 ;132:500-504.

[128] Chen Y, Lu S, Liu W, Han J. Redox-induced in-situ formation of Pd nanoparticles on surfaces of Fe3O4/PANI core/shell hybrids as high performance catalysts for Suzuki cross-coupling reactions. Colloid Polym Sci 2015 ;293:2301-2309.

[129] Hung CC, Wen TC, Wei Y. Site-selective deposition of ultra-fine Au nanoparticles on polyaniline nanofibers for H_2O_2 sensing. Mater Chem Phys 2010 ;122:392-396.

[130] Stejskal J, Trchová M, Kovářová J, Brožová L, Prokeš J. The reduction of silver nitrate with various polyaniline salts to polyaniline–silver composites. React Funct Polym 2009 ;69:86-90.

[131] Stejskal J, Trchová M, Brožová L, Prokeš J. Reduction of silver nitrate by polyaniline nanotubes to produce silver-polyaniline composites. Chem Papers 2009 ;63:77-83

[132] Stejskal J, Prokeš J, Sapurina I. The reduction of silver ions with polyaniline: The effect of the type of polyaniline and the mole ratio of the reagents. Mater Lett 2009 ;63:709-711

[133] Ayad MM, Prastomo N, Matsuda A, Stejskal J. Sensing of silver ions by nanotubular polyaniline film deposited on quartz-crystal in a microbalance. Synth Met 2010 ;160:42-46

[134] Yuan J, Wang Z, Zhang Q, Han D, Zhang Y, Shen Y, Niu L. Controlled synthesis of 2D Au nanostructure assembly with the assistance of sulfonated polyaniline nanotubes.

Nanotechnology 2006 ;17:2641-2648.

[135] Xia Y, Xiao H. Room temperature conductive sulfonated polyaniline-promoted reductive synthesis of gold nanoplates. Mater Chem Phys 2010 ;122:.333-335.

[136] Routh P, Garai A, Nandi AK. Optical and electronic properties of polyaniline sulfonic acid-ribonucleic acid-gold nanobiocomposites. Phys Chem Chem Phys 2011 ;13:13670-13682.

[137] Xu P, Han X, Wang C, Zhang B, Wang X, Wang HL. Facile synthesis of polyaniline-polypyrrole nanofibers for application in chemical deposition of metal nanoparticles. Macromol Rapid Commun 2008 ;29:1392-1397.

[138] Stejskal J, Trchová M, Kovářová J, Prokeš J, Omastová M. Polyaniline-coated cellulose fibers decorated with silver nanoparticles. Chem Papers 2008 ;62:181-186.

[139] Mukherjee P, Nandi AK. Growth of different shape Au nanoparticles through an interfacial redox process using a conducting polymer. Langmuir 2010 ;26:2785-2790.

[140] Xia YY, Xiao HP. Hierarchical gold microspheres catalyst: Simultaneous synthesis and immobilization. J Mol Catal A 2010 ;331:35-39.

[141] Shih HH, Williams D, Mack NH, Wang HL. Conducting polymer-based electrodeless deposition of Pt nanoparticles and its catalytic properties for regioselective hydrosilylation reactions. Macromolecules 2009 ;42:4-16.

[142] Gao Y, Chen CA, Gau HM, Bailey JA, Akhadov E, Williams D, Wang HL. Facile synthesis of polyaniline-supported Pd nanoparticles and their catalytic properties toward selective hydrogenation of alkynes and cinnamaldehyde. Chem Mater 2008 ;20:2839-2844.

[143] Xu P, Mack NH, Jeon SH, Doorn SK, Han XJ, Wang HL. Facile fabrication of homogeneous 3D silver nanostructures on gold-supported polyaniline membranes as promising SERS substrates. Langmuir 2010 ;26:8882-8886.

[144] Mack NH, Bailey JA, Doorn SK, Chen CA, Gau HM, Xu P, Williams DJ, Akhadov EA, Wang HL. Mechanistic study of silver nanoparticle formation on conducting polymer surfaces. Langmuir 2011 ;27:4979-4985

[145] Xu P, Zhang B, Mack NH, Doorn SK, Han X, Wang HL. Synthesis of homogeneous silver nanosheet assemblies for surface enhanced Raman scattering applications. J Mater Chem 2010 ;20:7222-7226.

[146] Wang HL, Li W, Jia QX, Akhadov E. Tailoring conducting polymer chemistry for the chemical deposition of metal particles and clusters. Chem Mater 2007 ;19:520-525.

[147] Sheffer M, Martina V, Seeber R, Mandlera D. Deposition of gold nanoparticles on thin polyaniline films. Israel J Chem 2008 ;48:349-357.

[148] Xu P, Akhadov E, Wang LY, Wang HL. Sequential chemical deposition of metal alloy jellyfish using polyaniline: redox chemistry at the metal-polymer interface. Chem Commun 2011 ;47:10764-10766.

[149] Li W, Jia QX, Wang HL. Facile synthesis of metal nanoparticles using conducting polymer colloids. Polymer 2006 ;47:23-26.

[150] Han J, Li L, Guo R. Novel approach to controllable synthesis of gold nanoparticles supported on polyaniline nanofibers. Macromolecules 2010 ;43:10636-10644.

[151] Han J, Dai J, Zhou C, Guo R. Dilute cationic surfactant-assisted synthesis of polyaniline nanotubes and application as reactive support for various noble metal nanocatalysts. Polym Chem 2013 ;4:313-321.

[152] Han J, Liu Y, Li L, Guo R. Poly(*o*-phenylenediamine) submicrosphere-supported gold nanocatalysts: Synthesis, characterization and application in selective oxidation of benzyl alcohol. Langmuir 2009 ;25:11054-11060.

[153] Jana NR, Gearheart L, Murphy CJ. Wet chemical synthesis of high aspect ratio cylindrical gold nanorods. J Phys Chem B 2001 ;105:4065-4067.

[154] Jana NR, Gearheart L, Murphy CJ. Seed-mediated growth approach for shape-controlled synthesis of spheroidal and rod-like gold nanoparticles using a surfactant template. Adv Mater 2001 ;13:1389-1393.

[155] Nikoobakht B, El-Sayed MA. Preparation and growth mechanism of gold nanorods (NRs) using seed-mediated growth method. Chem Mater 2003 ;15:1957-1962.

[156] Xu JJ, Hu JC, Quan BG, Wei ZX. Decorating polypyrrole nanotubes with Au nanoparticles by an in situ reduction process. Macromol Rapid Commun 2009 ;30:936-940.

[157] Han J, Wang L, Guo R. Facile synthesis of hierarchical conducting polymer nanotubes derived from nanofibers and their application for controlled drug release. Macromol Rapid Commun 2011 ;32:729-735.

[158] Han J, Song G, Guo R. Fabrication of polymer hollow nanospheres by a

swelling-evaporation strategy. J Polym Sci Part A Polym Chem 2007 ;45:2638-2645.

[159] Han J, Wang L, Guo R. Reactive polyaniline-supported sub-10 nm noble metal nanoparticles protected by a mesoporous silica shell: controllable synthesis and application as efficient recyclable catalysts. J Mater Chem 2012 ;22:5932-5935.

[160] Han J, Lu S, Jin C, Wang M, Guo R. Fe_3O_4/PANI/*m*-SiO_2 as robust reactive catalyst supports for noble metal nanoparticles with improved stability and recyclability. J Mater Chem A 2014 ;2:13016-13023.

[161] Boomi P, Prabu HG. Synthesis, characterization and antibacterial analysis of polyaniline/Au-Pd nanocomposite. Colloids Surf A 2013 ;429:51-59.

[162] Zhang H, Liu R, Zheng J. Seed-mediated synthesis of polyaniline/Au nanocomposite and its application for a cholesterol biosensor. Synth Met 2013 ;167:5-9.

[163] Sharma B, Mandani S, Sarma TK. Enzymes as bionanoreactors: glucose oxidase for the synthesis of catalytic Au nanoparticles and Au nanoparticle-polyaniline nanocomposites. J Mater Chem B 2014 ;2:4072-4079.

[164] Turkevich J, Stevenson PC, Hillier J. A study of the nucleation and growth processes in the synthesis of colloidal gold. Discuss Faraday Soc 1951 ;11:55-75.

[165] Han J, Liu Y, Wang L, Guo R. A versatile surfactant mediated synthetic route to gold/polyaniline derivative core/shell nanocomposites. J Polym Sci Part A Polym Chem 2010 ;48:3903-3912.

[166] Sarma TK, Chowdhury D, Paul A, Chattopadhyay A. Synthesis of Au nanoparticle–conductive polyaniline composite using H_2O_2 as oxidising as well as reducing agent. Chem Commun 2002 :1048-1049.

[167] Sarma TK, Chattopadhyay A. Reversible encapsulation of nanometer-size polyaniline and polyaniline-Au-nanoparticle composite in starchReversible encapsulation of nanometer-size polyaniline and polyaniline-Au-nanoparticle composite in starch. Langmuir 2004 ;20:4733-4737.

[168] Han J, Chen R, Wang M, Lu S, Guo R. Core-shell to yolk-shell nanostructure transformation by a novel sacrificial template-free strategy. Chem Commun 2013 ;49:11566-11568.

[169] Zhang B, Cai T, Li S, Zhang X, Chen Y, Neoh KG, Kang ET, Wang C. Yolk-shell

nanorattles encapsulating a movable Au nanocore in electroactive polyaniline shells for flexible memory device. J Mater Chem C 2014 ;2:5189-5197.

[170] Han J, Wang M, Chen R, Han N, Guo R. Beyond yolk-shell nanostructure: A single Au nanoparticle encapsulated in the porous shell of polymer hollow spheres with remarkably improved catalytic efficiency and recyclability. Chem Commun 2014 ;50:8295-8298.

[171] Xing S, Tan LH, Yang M, Pan M, Lv Y, Tang Q, Yang Y, Chen H. Highly controlled core/shell structures: tunable conductive polymer shells on gold nanoparticles and nanochains. J Mater Chem 2009 ;19:3286-3291.

[172] Hou H, Chen L, He H, Chen L, Zhao Z, Jin Y. Fine-tuning the LSPR response of gold nanorod–polyaniline core–shell nanoparticles with high photothermal efficiency for cancer cell ablation. J Mater Chem B 2015 ;3:5189-5196.

[173] Jiang N, Shao L, Wang J. (Gold nanorod core)/(polyaniline shell) plasmonic switches with large plasmon shifts and modulation depths. Adv Mater 2014 ;26:3282-3289.

[174] Du C, Wang A, Fei J, Zhao J, Li J. Polypyrrole-stabilized gold nanorods with enhanced photothermal effect towards two-photon photothermal therapy. J Mater Chem B 2015 ;3:4539-4545.

[175] Sarma TK, Chattopadhyay A. One pot synthesis of nanoparticles of aqueous colloidal polyaniline and its Au-nanoparticle composite from monomer vapor. J Phys Chem A 2004 ;108:7837-7842.

[176] Hou T, Gai P, Song M, Zhang S, Li F. Synthesis of a three-layered SiO_2@Au nanoparticle@polyaniline nanocomposite and its application in simultaneous electrochemical detection of uric acid and ascorbic acid. J Mater Chem B 2016 ;4:2314-2321.

[177] Pan M, Xing S, Sun T, Zhou W, Sindoro M, Teo HH, Yan Q, Chen H. 3D dendritic gold nanostructures: Seeded growth of multi-generation fractal architecture. Chem Commun 2010 ;46:7112-7114.

[178] Pan M, Sun H, Lim JW, Bakaul SR, Zeng Y, Xing S, Wu T, Yan Q, Chen H. Seeded growth of two-dimensional dendritic gold nanostructures. Chem Commun 2012 ;48:1440-1442.

[179] Sun H, Shen X, Yao L, Xing S, Wang H, Feng Y, Chen H. Measuring the unusually slow

ionic diffusion in polyaniline via study of yolk-shell nanostructures. J Am Chem Soc 2012 ;134:11243-11250.

[180] Xing S, Tan LH, Chen T, Yang Y, Chen H. Facile fabrication of triple-layer (Au@Ag)@polypyrrole core–shell and (Au@H_2O)@polypyrrole yolk–shell nanostructures. Chem Commun 2009 :1653-1654.

[181] Sun H, He J, Xing S, Zhu L, Wong YJ, Wang Y, Zhai H, Chen H. One-step synthesis of composite vesicles: Direct polymerization and in situ over-oxidation of thiophene. Chem Sci 2011 ;2:2109-2114.

[182] Ge J, Zhang Q, Zhang T, Yin Y. Core–satellite nanocomposite catalysts protected by a porous silica shell: Controllable reactivity, high stability, and magnetic recyclability. Angew Chem Int Ed 2008 ;47:8924-8928.

[183] Sindoro M, Feng Y, Xing S, Li H, Xu J, Hu H, Liu C, Wang Y, Zhang H, Shen Z, Chen H. Triple-layer (Au@perylene)@polyaniline nanocomposite: unconventional growth of faceted organic nanocrystals on polycrystalline Au. Angew Chem Int Ed 2011 ;50:9898-9902.

[184] Xing SX, He J, Liu XC, Chen H. A symmetry-adapted shell transformation of core–shell nanoparticles for binary nanoassembly. Chem Commun 2011 ;47:12533-12535.

[185] Berzina T, Pucci A, Ruggeri G, Erokhin V, Fontana MP. Gold nanoparticles-polyaniline composite material: Synthesis, structure and electrical properties. Synth Met 2011 ;161:1408-1413.

[186] Dong Y, Ma Y, Zhai TY, Zeng Y, Fu HB, Yao JN. A novel approach to the construction of core-shell gold-polyaniline nanoparticles. Nanotechnology 2007 ;18:455603/1-6.

[187] Pillalamarri SK, Blum FD, Bertino MF. Synthesis of polyaniline–gold nanocomposites using “grafting from” approach. Chem Commun 2005 ;4584-4585.

[188] Oliveira MM, Castro EG, Canestraro CD, Zanchet D, Ugarte D, Roman LS, Zarbin AJG. A simple two-phase route to silver nanoparticles/polyaniline structures. J Phys Chem B 2006 ;110:17063-17069.

[189] Sawall DD, Villahermosa RM, Lipeles RA, Hopkins AR. Interfacial polymerization of polyaniline nanofibers grafted to Au surfaces. Chem Mater 2004 ;16:1606-1608.

[190] Katre PP, Athawale AA. Au-polyaniline nanocomposite synthesized using γ-ray induced

Au nanoparticles. Synth React Inorg 2007 ;37:363-366.

[191] Selvan ST, Nogami M. Novel gold-polypyrrole anisotropic colloids: a TEM investigation. J Mater Sci Lett 1998 ;17:1385-1388.

[192] Henry MC, Hsueh CC, Timko BP, Freund MS. Reaction of pyrrole and chlorauric acid a new route to composite colloids. J Electrochem Soc 2001 ;148:D155-D162.

[193] Selvakannan PR, Mandal S, Pasricha R, Sastry M. Hydrophobic, organically dispersible gold nanoparticles of variable shape produced by the spontaneous reduction of aqueous chloroaurate ions by hexadecylaniline molecules. J Colloid Interface Sci 2004 ;279:124-131.

[194] Newman JDS, Blanchard GJ. Formation of gold nanoparticles using amine reducing agents. Langmuir 2006 ;22:5882-5887.

[195] Qiu W, Huang HA, Zeng S, Xue T, Liu JX. A kinetic study of in situ polyaniline-gold composite film formation. J Polym Res 2011 ;18:19-23.

[196] Kinyanjui JM, Hatchett DW, Smith JA, Josowicz M. Chemical synthesis of a polyaniline/gold composite using tetrachloroaurate. Chem Mater 2004 ;16:3390-3398.

[197] Mallick K, Witcomb MJ, Scurrell MS. Palladium nanoparticles in poly(*o*-phenylenediamine): Synthesis of a nanostructured 'metal-polymer' composite material. J Macromol Sci Part A 2006 ;43:1469-1476.

[198] Kinyanjui JM, Hanks J, Hatchett DW, Smith A, Josowicz M. Chemical and electrochemical synthesis of polyaniline/gold composites. J Electrochem Soc 2004 ;151:D113-D120.

[199] Gedanken A, Sivakumar M. A sonochemical method for the synthesis of polyaniline and Au-polyaniline composites using H_2O_2 for enhancing rate and yield. Synth Met 2005 ;148:301-306.

[200] Breimer MA, Yevgeny G, Sy S, Sadik OA. Incorporation of metal nanoparticles in photopolymerized organic conducting polymers: A mechanistic insight. Nano Lett 2001 ;1:305-308.

[201] Pillalamarri SK, Blum FD, Tokuhiro AT, Bertino MF. One-pot synthesis of polyaniline-metal nanocomposites. Chem Mater 2005 ;17:5941-5944.

[202] Lee KP, Gopalan AY, Santhosh P, Lee SH, Nho YC. Gamma radiation induced distribution

of gold nanoparticles into carbon nano tube-polyaniline composite. Compos Sci Technol 2007 ;67:811-816.

[203] Wang Y, Liu Z, Han B, Sun Z, Huang Y, Yang G. Facile synthesis of polyaniline nanofibers using chloroaurate acid as the oxidant. Langmuir 2005 ;21:833-836.

[204] Chen Z, Pina CD, Falletta E, Faro ML, Pasta M, Rossi M, Santo N. Facile synthesis of polyaniline using gold catalyst. J Catal 2008 ;259:1-4.

[205] Feng X, Yang G, Xu Q, Hou W, Zhu JJ. Self-assembly of polyaniline/Au composites: From nanotubes to nanofibers. Macromol Rapid Commun 2006 ;27:31-36.

[206] Hasan M, Ansari MO, Cho MH, Lee M. Electrical conductivity, optical property and ammonia sensing studies on HCl doped Au@polyaniline nanocomposites. Electron Mater Lett 2015 ;11:1-6.

[207] Han J, Liu Y, Guo R. A novel templateless method to nanofibers of polyaniline derivatives with size control. J Polym Sci Part A Polym Chem 2008 ;46:740-746.

[208] Sun X, Dong S, Wang E. Large scale, templateless, surfactantless route to rapid synthesis of uniform poly(*o*-phenylenediamine) nanobelts. Chem Commun 2004 :1182-1183.

[209] Han J, Song G, Guo R. Synthesis of poly(*o*-phenylenediamine) hollow spheres and nanofibers using different oxidizing agents. Eur Polym J 2007 ;43:4229-4235.

[210] Arya SK, Dey A, Bhansali S. Polyaniline protected gold nanoparticles based mediator and label free electrochemical cortisol biosensor. Biosens Bioelectron 2011 ;28:166-173.

[211] Mallick K, Witcomb MJ, Dinsmore A, Scurrell MS. Polymerization of aniline by auric acid: Formation of gold decorated polyaniline nanoballs. Macromol Rapid Commun 2005 ;26:232-235.

[212] Mallick K, Witcomb MJ, Scurrell MS. Polyaniline stabilized highly dispersed gold nanoparticle: an in-situ chemical synthesis route. J Mater Sci 2006 ;41:6189-6192.

[213] Mallick K, Witcomb MJ, Scurrell MS, Strydom AM. In-situ chemical synthesis route for a fiber shaped gold-polyaniline nanocomposite. Gold Bull 2008 ;41:246-250.

[214] Mallick K, Witcomb M, Scurrell M, Strydom A. Optical, microscopic and low temperature electrical property of one-dimensional gold-polyaniline composite networks. J Phys D Appl Phys 2009 ;42:095409/1-9.

[215] Mallick K, Witcomb MJ, Strydom AM. Charge transport property of one-dimensional

gold-polyaniline composite networks. Phys Status Solidi A 2009 ;206:2245-2248.

[216] Luong ND, Oh J, Lee Y, Huh J, Park JJ, Kim JM, Nam JD. Self-assembled tetramethylbenzidine conductive nanofibers synchronized with gold nanoparticle formation. Appl Surf Sci 2011 ;257:3233-3235.

[217] Mallick K, Witcomb MJ, Scurrell MS. Formation of palladium nanoparticles in poly (*o*-methoxyaniline) macromolecule fibers: An in-situ chemical synthesis method. Eur Phys J E 2006 ;19:149-154.

[218] Pringle JM, Winther-Jensen O, Lynam C, Wallace GG, Forsyth M, MacFarlane DR. One-step synthesis of conducting polymer-noble metal nanoparticle composites using an ionic liquid. Adv Funct Mater 2008 ;18:2031-2040.

[219] Gospodinova N, Terlemezyan L. Conducting polymers prepared by oxidative polymerization: polyaniline. Prog Polym Sci 1998 ;23:1443-1484.

[220] Xiong Y, McLellan JM, Chen J, Yin Y, Li ZY, Xia Y. Kinetically controlled synthesis of triangular and hexagonal nanoplates of palladium and their SPR/SERS properties. J Am Chem Soc 2005 ;127:17118-17127.

[221] Guo LM, Peng ZQ. One-pot synthesis of carbon nanotube-polyaniline-gold nanoparticle and carbon nanotube-gold nanoparticle composites by using aromatic amine chemistry. Langmuir 2008 ;24:8971-8975.

[222] Han J, Liu Y, Guo R. Facile synthesis of highly stable gold nanoparticles and their unexpected high catalytic activity for Suzuki-Miyaura cross-coupling reaction in water. J Am Chem Soc 2009 ;131:2060-2061.

[223] Han J, Dai J, Li L, Guo R. Highly uniform self-assembled conducting polymer/gold fibrous nanocomposites: additive-free controllable synthesis and application as efficient recyclable catalysts. Langmuir 2011 ;27:2181-2187.

[224] Wang X, Shen Y, Xie A, Li S, Cai Y, Wang Y, Shu H. Assembly of dandelion-like Au/PANI nanocomposites and their application as SERS nanosensors. Biosens Bioelectron 2011 ;26:3063-3067.

[225] Shiigi H, Yamamoto Y, Yoshi N, Nakao H, Nagaoka T. One-step preparation of positively-charged gold nanoraspberry. Chem Commun 2006 :4288-429.

[226] Morita R, Inoue R, Tokonami S, Yamamoto Y, Nakayama M, Nakao H, Shiigi H, Nagaoka

T. Organic-inorganic hybrid nanoraspberry consisted of gold nanoparticle and aniline oligomer. J Electrochem Soc 2011 ;158:K95-K100.

[227] Sajanlal PR, Sreeprasad TS, Nair AS, Pradeep T. Wires, plates, flowers, needles, and core-shells: Diverse nanostructures of gold using polyaniline templates. Langmuir 2008 ;24:4607-4614.

[228] Han J, Liu Y, Guo R. A simple one-step chemical route to gold/polymer core/shell composites and polymer hollow spheres. J Appl Polym Sci 2009 ;112:1244-1249.

[229] Panda BR, Chattopadhyay A. A water-soluble polythiophene-Au nanoparticle composite for pH sensing. J Colloid Interface Sci 2007 ;316:962-967.

[230] Ventosa E, Colina A, Heras A, Ruiz V, Garoz J, Lopez-Palacios J. One-pot synthesis of gold/poly(3,4-ethylendioxythiophene) nanocomposite. J Nanopart Res 2012 ;14:661/1-7.

[231] Yan Y, Yu Z, Huang YW, Yuan WX, Wei ZX. Helical polyaniline nanofibers induced by chiral dopants by a polymerization process. Adv Mater 2007 ;19:3353-3357.

[232] Zhang L, Wan M. Polyaniline/TiO_2 composite nanotubes. J Phys Chem B 2003 ;107:6748-6753.

[233] Huang K, Zhang YJ, Long YZ, Yuan JH, Han DX, Wang ZJ, Niu L, Chen Z. Preparation of highly conductive, self-assembled gold/polyaniline nanocables and polyaniline nanotubes. Chem Eur J 2006 ;12:5314-5319.

[234] Long YZ, Huang K, Yuan JH, Han DX, Niu L, Chen ZJ, Gu CZ, Jin AZ, Duvail JL. Electrical conductivity of a single Au/polyaniline microfiber. Appl Phys Lett 2006 ;88:162113/1-3.

[235] Dai XH, Tan YW, Xu J. Formation of gold nanoparticles in the presence of *o*-anisidine and the dependence of the structure of poly(*o*-anisidine) on synthetic conditions. Langmuir 2002 ;18:9010-9016.

[236] Zhang L, Peng H, Kilmartin PA, Soeller C, Tilley R, Travas-Seidic J. Self-assembled hollow polyaniline/Au nanospheres obtained by a one-step synthesis. Macromol Rapid Commun 2008 ;29:598-603.

[237] Huang K, Zhang YJ, Han DX, Shen YF, Wang ZJ, Yuan JH, Zhang QX, Niu L. One-step synthesis of 3D dendritic gold/polypyrrole nanocomposites via a self-assembly method. Nanotechnology 2006 ;17:283-288.

[238] Han J, Fang P, Dai J, Guo R. One-pot surfactantless route to polyaniline hollow nanospheres with incontinuous multicavities and application for the removal of lead ions from water. Langmuir 2012 ;28:6468-6475.

[239] Huang YF, Park YI, Kuo C, Xu P, Williams DJ, Wang J, Lin CW, Wang HL. Low-temperature synthesis of Au/polyaniline nanocomposites: Toward controlled size, morphology, and size dispersity. J Phys Chem C 2012 ;116:11272-11277.

[240] Lenhart N, Crowley K, Killard AJ, Smyth MR, Morrin A. Inkjet printable polyaniline-gold dispersions. Thin Solid Films 2011 ;519:4351-4356.

[241] Kumar SS, Kumar CS, Mathiyarasu J, Phani KL. Stabilized gold nanoparticles by reduction using 3,4-ethylenedioxythiophene-polystyrenesulfonate in aqueous solutions: Nanocomposite formation, stability, and application in catalysis. Langmuir 2007 ;23:3401-3408.

[242] Sajanlal PR, Pradeep T. Bimetallic flowers, beads, and buds: Synthesis, characterization, and Raman imaging of unique mesostructures. Langmuir 2010 ;26:456-465.

[243] Peng ZQ, Guo LM, Zhang ZH, Tesche B, Wilke T, Ogermann D, Hu SH, Kleinermanns K. Micelle-assisted one-pot synthesis of water-soluble polyaniline-gold composite particles. Langmuir 2006 ;22:10915-10918.

[244] Bu X, Yuan J, Song J, Han D, Niu L. Controlled synthesis of nanoporous Au microsheet via surfactant emulsion template. Mater Chem Phys 2009 ;116:153-157.

[245] Song JX, Yuan JH, Li F, Han DX, Song JF, Niu L. Tunable activity in electrochemical reduction of oxygen by gold-polyaniline porous nanocomposites. J Solid State Electrochem 2010 ;14:1915-1922.

[246] Wang ZJ, Yuan JH, Han DX, Niu L, Ivaska A. One-step synthesis of gold-polyaniline core-shell particles. Nanotechnology 2007 ;18:115610/1-5.

[247] Chen S, Wang ZL, Ballato J, Foulger SH, Carroll DL. Monopod, bipod, tripod, and tetrapod gold nanocrystals. J Am Chem Soc 2003 ;125:16186-16187.

[248] Sau TK, Murphy CJ. Room temperature, high-yield synthesis of multiple shapes of gold nanoparticles in aqueous solution. J Am Chem Soc 2004 ;126:8648-8649.

[249] Wang Z, Yuan J, Han D, Zhang Y, Shen Y, Kuehner D, Niu L, Ivaska A. Simultaneous synthesis of polyaniline nanotubules and gold nanoplates. Cryst Growth Des

2008 ;8:1827-1832.

[250] Mukherjee P, Nandi AK. Concomitant synthesis of polyaniline and highly branched gold nanoparticles in the presence of DNA. J Colloid Interface Sci 2011 ;356:145-150.

[251] Zhang B, Zhao BT, Huang SH, Zhang RY, Xu P, Wang HL. One-pot interfacial synthesis of Au nanoparticles and Au-polyaniline nanocomposites for catalytic applications. CrystEngComm 2012 ;14:1542-1544.

[252] Mallick K, Witcomb MJ, Scurrell MS. Directional assembly of polyaniline functionalized gold nanoparticles. J Phys Condens Matter 2007 ;19:196225/1-8.

[253] Gniadek M, Bak E, Stojek Z, Donten M. Metal ion-driven synthesis of polyaniline composite doped with metallic nanocrystals at the boundary of two immiscible liquids. J Solid State Electrochem 2010 ;14:1303-1310.

[254] Grace AN, Pandian K. Synthesis of gold and platinum nanoparticles using tetraaniline as reducing and phase transfer agent-A brief study and their role in the electrocatalytic oxidation of glucose. J Phys Chem Solids 2007 ;68:2278-2285.

[255] Grace AN, Pandian K. Organically dispersible gold and platinum nanoparticles using aromatic amines as phase transfer and reducing agent and their applications in electro-oxidation of glucose. Colloids Surf A 2007 ;302:113-120.

[256] Tang Y, Pan K, Wang X, Luo S. Enhancing electrochemical and electrocatalytic activities of polyaniline via co-doping with poly(styrene sulfonate) and gold. J Electroanal Chem 2010 ;639:123-129.

[257] Yang W, Liu J, Zheng R, Liu Z, Dai Y, Chen G, Ringer S, Braet F. Ionic liquid-assisted synthesis of polyaniline/gold nanocomposite and its biocatalytic application. Nanoscale Res Lett 2008 ;3:468-472.

[258] Kim T, Heo K, Jeon KS, Park J, Byun KE, Kim M, Suh YD, Hong S, Kim NJ. A facile, one-pot synthesis of ultra-long nanoparticle-chained polyaniline wires. J Mater Chem 2011 ;21:17304-17308.

[259] Lu GW, Li C, Shen JY, Chen ZJ, Shi GQ. Preparation of highly conductive gold-poly(3,4-ethylenedioxythiophene) nanocables and their conversion to poly(3,4-ethylenedioxythiophene) nanotubes. J Phys Chem C 2007 ;111:5926-5931.

[260] Harish S, Mathiyarasu J, Phani KLN. Generation of gold-PEDOT nanostructures at an

interface between two immiscible solvents. Mater Res Bull 2009 ;44:1828-1833.

[261] Feng XM, Huang HP, Ye QQ, Zhu JJ, Hou WH. Ag/polypyrrole core-shell nanostructures: Interface polymerization, characterization, and modification by gold nanoparticles. J Phys Chem C 2007 ;111:8463-8468.

[262] Gupta B, Joshi L, Prakash R. Novel synthesis of polycarbazole-gold nanocomposite. Macromol Chem Phys 2011 ;212:1692-1699.

[263] Zheng LZ, Li JH. Platinum-polyaniline nanofilms synthesized at a liquid|liquid interface with enhanced conductivity. J Electroanal Chem 2005 ;577:137-144.

[264] Shi ZQ, Zhou H, Lu Y. Poly(tetrafluoroethylene)@polyaniline/gold composite membranes: Preparation, characterization and application. Colloids Surf A 2012 ;393:153-159.

[265] Sharma MK, Ambolikar AS, Aggarwal SK. In situ synthesis of gold-polyaniline composite in nanopores of polycarbonate membrane. J Mater Sci 2011 ;46:5715-5722.

[266] Jiang S, Chen J, Tang J, Jin E, Kong L, Zhang W, Wang C. Au nanoparticles-functionalized two-dimensional patterned conducting PANI nanobowl monolayer for gas sensor. Sens Actuat B 2009 ;140:520-524.

[267] Zhang H, Huang F, Xu S, Xia Y, Huang W, Li Z. Fabrication of nanoflower-like dendritic Au and polyaniline composite nanosheets at gas/liquid interface for electrocatalytic oxidation and sensing of ascorbic acid. Electrochem Commun 2013 ;30:46-50.

[268] Chang QF, Zhao K, Chen X, Li MQ, Liu JH. Preparation of gold/polyaniline/multiwall carbon nanotube nanocomposites and application in ammonia gas detection. J Mater Sci 2008 ;43:5861-5866.

[269] Basavaraja C, Kim WJ, Kim YD, Huh DS. Synthesis of polyaniline-gold/graphene oxide composite and microwave absorption characteristics of the composite films. Mater Lett 2011 ;65:3120-3123.

[270] Han J, Fang P, Jiang W, Li L, Guo R. Ag nanoparticles loaded mesoporous silica: spontaneous formation of Ag nanoparticles and mesoporous silica SBA-15 by a one-pot strategy and their catalytic applications. Langmuir 2012 ;28:4768-4755.

[271] Wei J, Xing G, Gao L, Suo H, He X, Zhao C, Li S, Xing S. Nickel foam based polypyrrole–Ag composite film: a new route toward stable electrodes for supercapacitors. New J Chem 2013 ;37:337-341.

[272] Liu Z, Poyraz S, Liu Y, Zhang XY. Seeding approach to noble metal decorated conducting polymer nanofiber network. Nanoscale 2012 ;4:106-109.

[273] Haruta M, Yamada N, Kobayashi T, Iijima S. Gold catalysts prepared by coprecipitation for low-temperature oxidation of hydrogen and of carbon monoxide. J Catal 1989 ;115:301-309.

[274] Tsunoyama H, Sakurai H, Negishi Y, Tsukuda T. Size-specific catalytic activity of polymer-stabilized gold nanoclusters for aerobic alcohol oxidation in water. J Am Chem Soc 2005 ;127:9374-9375.

[275] Ishida T, Haruta M. Gold catalysts: Towards sustainable chemistry. Angew Chem Int Ed 2007 ;46:7154-7156.

[276] Miyamura H, Matsubara R, Miyazaki Y, Kobayashi S. Aerobic oxidation of alcohols at room temperature and atmospheric conditions catalyzed by reusable gold nanoclusters stabilized by the benzene Rings of polystyrene derivatives. Angew Chem Int Ed 2007 ;46:4151-4154.

[277] Hervés P, Pérez-Lorenzo M, Liz-Marzán LM, Dzubiella J, Lu Y, Ballauff M. Catalysis by metallic nanoparticles in aqueous solution: model reactions. Chem Soc Rev 2012 ;41:5577-5587.

[278] Xiao H, Xia Y, Cai C. Conducting polymer hydrogel reactor for synthesizing Au nanoparticles and its use in the reduction of *p*-nitrophenol. J Nanopart Res 2013 ;15:1521/1-7.

[279] Xia Y, Li T, Ma C, Gao C, Chen J. Au/montmorillonite/polyaniline nanoflakes: facile fabrication by self-assembly and application as catalyst. RSC Adv 2014 ;4:20516-20520.

[280] Xue Y, Lu X, Bian X, Lei J, Wang C. Facile synthesis of highly dispersed palladium/polypyrrole nanocapsules for catalytic reduction of *p*-nitrophenol. J Colloid Interface Sci 2012 ;379:89-93.

[281] Liu G, Xie S, Zhang Q, Tian Z, Wang Y. Carbon dioxide-enhanced photosynthesis of methane and hydrogen from carbon dioxide and water over Pt-promoted polyaniline-TiO_2 nanocomposites. Chem Commun 2015 ;51:13654-13657.

[282] Kantam ML, Roy M, Roy S, Sreedhar B, Madhavendra SS, Choudary BM, De RL. Polyaniline supported palladium catalyzed Suzuki-Miyaura cross-coupling of bromo- and

chloroarenes in water. Tetrahedron 2007 ;63:8002-8009.

[283] Houdayer A, Schneider R, Billaud D, Ghanbaja J, Lambert J. Heck and Suzuki–Miyaura couplings catalyzed by nanosized palladium in polyaniline. Appl Organomet Chem 2005 ;19:1239-1248.

[284] Islam RU, Witcomb MJ, Lingen E, Scurrell MS, Otterlo WV, Mallick K. In-situ synthesis of a palladium-polyaniline hybrid catalyst for a Suzuki coupling reaction. J Organomet Chem 2011 ;696:2206-2210.

[285] Choudary BM, Roy M, Roy S, Kantam ML, Sreedhar B, Kumar KV. Preparation, characterization and catalytic properties of polyaniline-supported metal complexes. Adv Synth Catal 2006 ;348:1734-1742.

[286] Gallon BJ, Kojima RW, Kaner RB, Diaconescu PL. Palladium nanoparticles supported on polyaniline nanofibers as a semi-heterogeneous catalyst in water. Angew Chem Int Ed 2007 ;46:7251-7254.

[287] Ohtaka A, Kono Y, Teratani T, Fujii S, Matsuzawa S, Nakamura Y, Nomura R. Polypyrrole–palladium nanocomposite-coated latex particles as a heterogeneous catalyst in water. Catal Lett 2011 ;141:1097-1103.

[288] Fujii S, Matsuzawa S, Nakamura Y, Ohtaka A, Teratani T, Akamatsu K, Tsuruoka T, Nawafune H. Synthesis and characterization of polypyrrole−palladium nanocomposite-coated latex particles and their use as a catalyst for Suzuki coupling reaction in aqueous media. Langmuir 2010 ;26:6230-6239.

[289] Islam RU, Witcomb MJ, Scurrell MS, Lingen E, Otterlo WV, Mallick K. Conjugated polymer stabilized palladium nanoparticles as a versatile catalyst for Suzuki cross-coupling reactions for both aryl and heteroaryl bromide systems. Catal Sci Technol 2011 ;1:308-315.

[290] Fujii S, Hamasaki H, Abe H, Yamanaka S, Ohtaka A, Nakamura E, Nakamura Y. One-step synthesis of magnetic iron–conducting polymer–palladium ternary nanocomposite microspheres with applications as a recyclable catalyst. J Mater Chem A 2013 ;1:4427-4430.

[291] Likhar PR, Roy M, Roy S, Subhas MS, Kantam ML, Sreedhar B. Highly efficient and reusable polyaniline-supported palladium catalysts for open-air oxidative Heck reactions

under base- and ligand-free conditions. Adv Synth Catal 2008 ;350:1968-1974.

[292] Hasik M, Drelinkiewicz A, Choczyriski M, Quillard S, Proń A. Polyaniline containing palladium-new conjugated polymer supported catalysts. Synth Met 1997 ;84:93-94.

[293] Drelinkiewicz A, Stejskal J, Waksmundzka A, Sobczak JW. Physicochemical and catalytic properties of palladium deposited on polyaniline-coated silica gel. Synth Met 2004 ;140:233-246.

[294] Drelinkiewicz A, Hasik M, Choczyński M. Preparation and properties of polyaniline containing palladium. Mater Res Bull 1998 ;33:739-762.

[295] Shao M, Chang Q, Dodelet JP, Chenitz R. Recent advances in electrocatalysts for oxygen reduction reaction. Chem Rev 2016 ;116:3594-3657.

[296] Dai L, Xue Y, Qu L, Choi HJ, Baek JB. Metal-free catalysts for oxygen reduction reaction. Chem Rev 2015 ;115:4823-4892.

[297] Kulesza PJ, Karnicka K, Miecznikowski K, Chojak M, Kolary A, Barczuk PJ, Tsirlina G, Czerwinski W. Network electrocatalytic films of conducting polymer-linked polyoxometallate-stabilized platinum nanoparticles. Electrochim Acta 2005 ;50:5155-5162.

[298] Wu RH, Tsai MJ, Ho KS, Wei TE, Hsieh TH, Han YK, Kuo CW, Tseng PH, Wang YZ. Sulfonated polyaniline nanofiber as Pt-catalyst conducting support for proton exchange membrane fuel cell. Polymer 2014 ;55:2035-2043.

[299] Thangavel S, Ramaraj R. Electroless synthesis of multibranched gold nanostructures encapsulated by poly(o-phenylenediamine) in Nafion. J Colloid Interface Sci 2011 ;355:293-299.

[300] Guerra-Balcazar M, Morales-Acosta D, Castaneda F, Ledesma-Garcia J, Arriaga LG. Synthesis of Au/C and Au/Pani for anode electrodes in glucose microfluidic fuel cell. Electrochem Commun 2010 ;12:864-867.

[301] Majumdar G, Goswami M, Sarma TK, Paul A, Chattopadhyay A. Au nanoparticles and polyaniline coated resin beads for simultaneous catalytic oxidation of glucose and colorimetric detection of the product. Langmuir 2005 ;21:1663-1667.

[302] Niu L, Wang Z, Yuan J, Li M, Han D, Zhang Y, Shen Y, Ivaska A. Electropolymerization and catalysis of well-dispersed polyaniline/carbon nanotube/gold composite. J Electroanal

Chem 2007 ;599:121-126.

[303] Mao H, Lu XF, Liu XC, Tang J, Wang C, Zhang WJ. One-step synthesis of Au/PEDOT/β-$Fe^{3+}O$(OH, Cl) nanospindles in aqueous solution. J Phys Chem C 2009 ;113:9465-9472.

[304] Zanfrognini B, Zanardi C, Terzi F, Aaritalo T, Viinikanoja A, Lukkari J, Seeber R. Layer-by-layer deposition of a polythiophene/Au nanoparticles multilayer with effective electrochemical properties. J Solid State Electrochem 2011 ;15:2395-2400.

[305] Wang Z, Gao G, Zhu H, Sun Z, Liu H, Zhao X. Electrodeposition of platinum microparticle interface on conducting polymer film modified nichrome for electrocatalytic oxidation of methanol. Int J Hydrogen Energy 2009 ;34:9334-9340.

[306] Patten HV, Ventosa E, Colina A, Ruiz V, Lopez-Palacios J, Wain AJ, Lai SCS, Macpherson JV, Unwin PR. Influence of ultrathin poly-(3,4-ethylenedioxythiophene) (PEDOT) film supports on the electrodeposition and electrocatalytic activity of discrete platinum nanoparticles. J Solid State Electrochem 2011 ;15:2331-2339.

[307] Saheb AH, Seo SS. Polyaniline/Au electrodes for direct methanol fuel cells. Anal Lett 2011 ;44:2221-2228.

[308] Amani M, Kazemeini M, Hamedanian M, Pahlavanzadeh H, Gharibi H. Investigation of methanol oxidation on a highly active and stable Pt-Sn electrocatalyst supported on carbon-polyaniline composite for application in a passive direct methanol fuel cell. Mater Res Bull 2015 ;68:166-178.

[309] Li X, Wei J, Chai Y, Zhang S, Zhou M. Different polyaniline/carbon nanotube composites as Pt catalyst supports for methanol electro-oxidation. J Mater Sci 2015 ;50:1159-1168

[310] Yang F, Ma L, Gan M, Zhang J, Yan J, Huang H, Yu L, Li Y, Ge C, Hu H. Polyaniline-functionalized TiO_2-C supported Pt catalyst for methanol electro-oxidation. Synth Met 2015 ;205:23-31.

[311] Zhang L, Zhang C, Lian J. Electrochemical synthesis of polyaniline nano-networks on p-aminobenzene sulfonic acid functionalized glassy carbon electrode: Its use for the simultaneous determination of ascorbic acid and uric acid. Biosens Bioelectron 2008 ;24:690-695.

[312] Tsakova V, Ivanov S, Lange U, Stoyanova A, Lyutov V, Mirsky VM. Electroanalytical

applications of nanocomposites from conducting polymers and metallic nanoparticles prepared by layer-by-layer deposition. Pure Appl Chem 2011 ;83:345-358.

[313] Ivanov S, Lange U, Tsakova V, Mirsky VM. Electrocatalytically active nanocomposite from palladium nanoparticles and polyaniline: Oxidation of hydrazine. Sens Actuat B 2010 ;150:271-278

[314] Wang AJ, Feng JJ, Li YF, Xi JL, Dong WJ. In-situ decorated gold nanoparticles on polyaniline with enhanced electrocatalysis toward dopamine. Microchim Acta 2010 ;171:431-436.

[315] Huang KJ, Zhang JZ, Liu YJ, Wang LL. Novel electrochemical sensing platform based on molybdenum disulfide nanosheets-polyaniline composites and Au nanoparticles. Sens Actuat B 2014 ;194:303-310.

[316] Saha S, Sarkar P, Turner APF. Interference-free electrochemical detection of nanomolar dopamine using doped polypyrrole and silver nanoparticles. Electroanalysis 2014 ;26:2197-2206.

[317] Song MJ, Lee SK, Kim JH, Lim DS. Dopamine sensor based on a boron-doped diamond electrode modified with a polyaniline/Au nanocomposites in the presence of ascorbic acid. Anal Sci 2012 ;28:58[473-587.

[318] Zhang Y, Lin LL, Feng ZF, Zhou JZ, Lin ZH. Fabrication of a PANI/Au nanocomposite modified nanoelectrode for sensitive dopamine nanosensor design. Electrochim Acta 2009 ;55:265-270.

[319] Mazzio EA, Soliman KFA. Glioma cell antioxidant capacity relative to reactive oxygen species produced by dopamine. J Appl Toxicol 2004 ;24:99-106.

[320] Jamal R, Xu F, Shao W, Abdiryim T. The study on the application of solid-state method for synthesizing the polyaniline/noble metal (Au or Pt) hybrid materials. Nanoscale Res Lett 2013 ;8:117/1-8.

[321] Tanori J, Del Castillo-Castro T, Larios-Rodriguez E, Molina-Arenas Z, Castillo-Ortega MM. Synthesis and characterization of metallic nanoparticles and their incorporation into electroconductive polymer composites. Composites Part A 2007 ;38:107-113.

[322] Li F, Yang L, Zhao C, Du Z. Electroactive gold nanoparticles/polyaniline/polydopamine hybrid composite in neutral solution as high-performance sensing platform. Anal Methods

2011 ;3:1601-1606.

[323] Wang XX, Yang T, Jiao K. Controllable fabrication of Au micro/nanostructures on self-doped polyaniline nanofibers via electrochemical deposition and its application for DNA immobilization. Chin Sci Bull 2010 ;55:4125-4131.

[324] Feng YY, Yang T, Zhang W, Jiang C, Jiao K. Enhanced sensitivity for deoxyribonucleic acid electrochemical impedance sensor: Gold nanoparticle/polyaniline nanotube membranes. Anal Chim Acta 2008 ;616:144-151.

[325] Yue J, Epstein AJ. Synthesis of self-doped conducting Polyaniline. J Am Chem Soc 1990 ;112:2800-2801.

[326] Wang X, Yang T, Li X, Jiao K. Three-step electrodeposition synthesis of self-doped polyaniline nanofiber-supported flower-like Au microspheres for high-performance biosensing of DNA hybridization recognition. Biosens Bioelectron 2011 ;26:2953-2959.

[327] Nascimento HPO, Oliveira MDL, Melo CP, Silva GJL, Cordeiro MT, Andrade CAS. An impedimetric biosensor for detection of dengue serotype at picomolar concentration based on gold nanoparticles-polyaniline hybrid composites. Colloids Surf B 2011 ;86:414-419.

[328] Zhou H, Chen H, Luo S, Chen J, Wei W, Kuang Y. Glucose biosensor based on platinum microparticles dispersed in nano-fibrous polyaniline. Biosens Bioelectron 2005 ;20:1305-1311.

[329] Jin L, Xian Y, Hu Y, Liu F, Xian Y, Wang H. Glucose biosensor based on Au nanoparticles-conductive polyaniline nanocomposite. Biosens Bioelectron 2006 ;21:1996-2000.

[330] Yan W, Feng X, Chen X, Hou W, Zhu JJ. A super highly sensitive glucose biosensor based on Au nanoparticles-AgCl@polyaniline hybrid material. Biosens Bioelectron 2008 ;23:925-931.

[331] Kong FY, Gu SX, Li WW, Chen TT, Xu Q, Wang W. A paper disk equipped with graphene/polyaniline/Au nanoparticles/glucose oxidase biocomposite modified screen-printed electrode: Toward whole blood glucose determination. Biosens Bioelectron 2014 ;56:77-82.

[332] Mao H, Li YX, Liu XC, Zhang WJ, Wang C, Al-Deyab SS, El-Newehy M. The application of novel spindle-like polypyrrole hollow nanocapsules containing Pt

nanoparticles in electrocatalysis oxidation of nicotinamide adenine dinucleotide (NADH). J Colloid Interface Sci 2011 ;356:757-762.

[333] Li L, Li W, Yang H, Ma C, Yu J, Yan M, Song X. Sensitive origami dual-analyte electrochemical immunodevice based on polyaniline/Au-paper electrode and multi-labeled 3D graphene sheets. Electrochim Acta 2014 ;120:102-109.

[334] Fan H, Guo Z, Gao L, Zhang Y, Fan D, Ji G, Du B, Wei Q. Ultrasensitive electrochemical immunosensor for carbohydrate antigen 72-4 based on dual signal amplification strategy of nanoporous gold and polyaniline-Au asymmetric multicomponent nanoparticles. Biosens Bioelectron 2015 ;64:51-56.

[335] Wang L, Feng F, Ma Z. Novel electrochemical redox-active species: one-step synthesis of polyaniline derivative-Au/Pd and its application for multiplexed immunoassay. Sci Rep 2015 ;5:3127-3145.

[336] Wang L, Shan J, Feng F, Ma Z. Novel redox species polyaniline derivative-Au/Pt as sensing platform for label-free electrochemical immunoassay of carbohydrate antigen199. Anal Chim Acta 2016 ;911:108-113.

[337] Srivastava M, Srivastava SK, Nirala NR, Prakash R. A chitosan-based polyaniline-Au nanocomposite biosensor for determination of cholesterol. Anal Methods 2014 ;6:817-824.

[338] Sun X, Qiao L, Wang X. A novel immunosensor based on Au nanoparticles and polyaniline/multiwall carbon nanotubes/chitosan nanocomposite film functionalized interface. Nano-Micro Lett 2013 ;5:191-201.

[339] Rawal R, Chawla S, Chauhan N, Dahiya T, Pundir CS. Construction of amperometric uric acid biosensor based on uricase immobilized on PBNPs/cMWCNT/PANI/Au composite. Int J Biol Macromol 2012 ;50:112-118.

[340] Devi R, Relhan S, Pundir CS. Construction of a chitosan/polyaniline/graphene oxide nanoparticles/polypyrrole/Au electrode for amperometric determination of urinary/plasma oxalate. Sens Actuators B 2013 ;186:17-26.

[341] Tsai TH, Lin KC, Chen SM. Electrochemical synthesis of poly(3,4-ethylenedioxythiophene) and gold nanocomposite and its application for hypochlorite sensor. Int J Electrochem Sci 2011 ;6:2672-2687.

[342] Xin M, Lin H, Yang J, Chen M, Ma X, Liu J. Preparation of polyaniline/Au_0

nanocomposites modified electrode and application for hydrazine detection. Electroanalysis 2014 ;26:2216-2223.

[343] Santhosh P, Manesh KM, Lee SH, Uthayakumar S, Gopalan AI, Lee KP. Sensitive electrochemical detection of superoxide anion using gold nanoparticles distributed poly(methyl methacrylate)-polyaniline core-shell electrospun composite electrode. Analyst 2011 ;136:1557-1561.

[344] Vaddiraju S, Gleason KK. Selective sensing of volatile organic compounds using novel conducting polymer-metal nanoparticle hybrids. Nanotechnology 2010 ;21:125503/1-9.

[345] Park H, Jeong YR, Yun J, Hong SY, Jin S, Lee SJ, Zi G, Ha JS. Stretchable array of highly sensitive pressure sensors consisting of polyaniline nanofibers and Au-coated polydimethylsiloxane micropillars. ACS Nano 2015 ;9:9974-9985.

[346] Huang R, Cao Y, Qiu H. Structural and electrical properties of Au films sputter-deposited on HCl-doped polyaniline substrates. Thin Solid Films 2015 ;583:158-162.

[347] Bianchi R, Cunha HN, Faria RM, Ferreira GFL, Net JMG. Electrical studies on the doping dependence and electrode effect of metal-PANI-metal structures. J Phys D Appl Phys 2005 ;38:1437-1443.

[348] Mello RMQ, Hummelgenü IA. Ohmic contacts between sulfonated polyaniline and metals. J Solid State Electrochem 2001 ;5:546-549.

[349] Takashima W, Kawamura S, Kaneto K. Diffusion-limited characteristics of mechanically induced currents in polypyrrole/Au-membrane composites. Electrochim Acta 2011 ;56:4603-4610.

[350] Sünel N, Sedef AG, Parlak M, Toppare L. Electronic properties of polyamide-PPy/metal junction and electrical conductivity of a typical sample at low temperatures. Mater Chem Phys 2005 ;91:227-232

[351] Boyarbay B, Cetin H, Uygun A, Ayyildiz E. Electrical characterization and fabrication of organic/inorganic semiconductor heterojunctions. Appl Phys A 2011 ;103:89-96.

[352] Angappane S, Kini NR, Natarajan TS, Rangarajan G, Wessling B. PAni-PMMA blend/metal Schottky barriers. Thin Solid Films 2002 ;417:202-205.

[353] Abthagir PS, Saraswathi R. Junction properties of metal/polypyrrole Schottky barriers. J Appl Polym Sci 2001 ;81:2127-2135.

[354] Tseng RJ, Baker CO, Shedd B, Huang J, Kaner RB, Ouyang J, Yang Y. Charge transfer effect in the polyaniline-gold nanoparticle memory system. Appl Phys Lett 2007 ;90:053101/1-3.

[355] Wei D, Baral JK, Osterbacka R, Ivaska A. Electrochemical fabrication of a nonvolatile memory device based on polyaniline and gold particles. J Mater Chem 2008 ;18:1853-1857.

[356] Wang W, Li Z, Xu X, Dong B, Zhang H, Wang Z, Wang C, Baughman RH, Fang S. Au-doped polyacrylonitrile-polyaniline core-shell electrospun nanofibers having high field-effect mobilities. Small 2011 ;7:597-600.

[357] Yu QZ. Polyaniline/Au&Fe_3O_4@Au sub-microcables fabricated by electrospinning and electroless deposition. Mater Sci Eng B 2010 ;167:26-30.

[358] Lane LA, Qian X, Nie S. SERS nanoparticles in medicine: from label-free detection to spectroscopic tagging. Chem Rev 2015 ;115:10489-10529.

[359] Rycenga M, Camargo PHC, Li W, Moran CH, Xia Y. Understanding the SERS effects of single silver Nanoparticles and their dimers, one at a time. J Phys Chem Lett 2010 ;1:696-703.

[360] Willets KA. Super-resolution imaging of SERS hot spots. Chem Soc Rev 2014 ;43:3854-3864

[361] Li S, Xu P, Ren Z, Zhang B, Du Y, Han X, Mack NH, Wang HL. Fabrication of thorny Au nanostructures on polyaniline surfaces for sensitive surface-enhanced Raman spectroscopy. ACS Appl Mater Interfaces 2013 ;5:49-54.

[362] Baibarac M, Cochet M, Łapkowski M, Mihut L, Lefrant S, Baltog I. SERS spectra of polyaniline thin films deposited on rough Ag, Au and Cu. Polymer film thickness and roughness parameter dependence of SERS spectra. Synth Met 1998 ;96:63-70.

[363] Baibarac M, Mihut L, Louarn G, Mevellec JY, Wery J, Lefrant S, Baltog I. Interfacial chemical effect evidenced on SERS spectra of polyaniline thin films deposited on rough metallic supports. J Raman Spectrosc 1999 ;30:1105-1113

[364] Baibarac M, Mihut L, Louarn G, Lefrant S, Baltog I. Doping and metallic-support effect evidenced on SERS spectra of polyaniline thin films. J Polym Sci Part B Polym Phys 2000 ;38:2599-2609.

[365] Sharma MK, Ambolikar AS, Aggarwal SK. A hybrid electrochemical-chemical synthesis of a polyaniline film on a Au electrode. RSC Adv 2013 ;3:25674-25676.

[366] Wang L, Wu T, Du S, Pei M, Guo W, Wei S. High performance supercapacitors based on ternary graphene/Au/polyaniline (PANI) hierarchical nanocomposites. RSC Adv 2016 ;6:1004-1011.

[367] Hu H, Zhang K, Li S, Ji S, Ye C. Flexible, in-plane, and all-solid-state micro-supercapacitors based on printed interdigital Au/polyaniline network hybrid electrodes on a chip. J Mater Chem A 2014 ;2:20916-20922.

[368] Zhang K, Hu H, Yao W, Ye C. Flexible and all-solid-state supercapacitors with long-time stability constructed on PET/Au/polyaniline hybrid electrodes. J Mater Chem A 2015 ;5:617-623.

[369] Toshima N, Jiravanichanun N, Marutani H. Organic thermoelectric materials composed of conducting polymers and metal nanoparticles. J Electron Mater 2012 ;41:1735-1742.

Fig. 1. The oxidative polymerization processes, reversible acid/base doping/dedoping, and redox chemistry of PANI.

Fig. 2. (a) Procedure for the preparation of the core-shell polymer-metal manostructures within the pores of a AAO membrane. (B-E) SEM images of nanostructures grown in the AAO membrane (after dissolution of the membrane in 1 M NaOH for 1.5 h): (b) PANI fiber only; (c-e) PANI-Au core-shell structures, where the Au was deposited for 1 h (c), 1.5 h (d), and 2.5 h (e). [68], Copyright 2006. Reproduced with permission from the American Chemical Society.

Fig. 3. SEM pictures of 110 nm diameter tri-segmented Au-PEDOT-Au nanowires presenting two different polymer junction lengths: (a) 200 nm (20 scans) and (b) 1 μm (100 scans). The good contrast between the metallic and the polymer segments on SEM pictures allows for growth calibration. Scale bars: 1 μm. [70], Copyright 2009. Reproduced with permission from the American Chemical Society.

Fig. 4. (a) Schematic diagram showing the fabrication of three-dimensional nanoporous

PANI-Au hybrid films by electrochemical polymerization. (b) SEM image of nanoporous Au dealloyed for 8 h in HNO_3. Inset: the wrinkled films illustrating that nanoporous Au films exhibit excellent flexibility. (c) Typical top-view and cross-section (inset) SEM micrographs of nanoporous PANI-Au hybrid films electroplated for 10-cycle plating. [71], Copyright 2012. Reproduced with permission from Elsevier Ltd.

Fig. 5. Possible arrangements of the Au-NPs within the PANI: (a) homogeneous layers, (b) condensed assembly, and (c) extrusion across the polymer. [78], Copyright 2010. Reproduced with permission from the American Chemical Society.

Fig. 6. (a) Scheme of the preparation and (b) TEM image of PANI-Au hollow spheres. [89], Copyright 2006. Reproduced with permission from the American Chemical Society.

Fig. 7. (a-d) TEM images of the as-prepared Fe_3O_4-PANI-Au hybrid with core/shell nanostructure with different magnifications. [90], Copyright 2009. Reproduced with permission from the American Chemical Society.

Fig. 8. TEM images of autoreduced Au nanoparticles of (a) <1, (b) 2, (c) 6, and (d) >20 nm grown on PANI nanofibers. Inset scale bars = 10 nm. (e) Au crystal with its TEM diffraction pattern (inset). [125], Copyright 2011. Reproduced with permission from the American Chemical Society.

Fig. 9. Schematic illustration of the formation process of Au-Ag jellyfish on PANI membranes. [148], Copyright 2011. Reproduced with permission from the Royal Society of Chemistry.

Fig. 10. (a) Schematic illustration for the formation of PANI Nanofiber/Au Nanoparticle hybrids. (b-d) TEM images Au nanoparticles supported on PANI nanofibers with different dopin acids: (b) citric acid, (c) camphorsulfonic acid, and (d) TA. [150], Copyright 2010. Reproduced with permission from the American Chemical Society.

Fig. 11. TEM images of POPD hollow microspheres supporting Au nanoparticles (a) without and (b) with PVP. [19], Copyright 2009. Reproduced with permission from John Wiley & Sons Inc.

Fig. 12. (a) SEM and (b) TEM images of the PPY-Au hybrids using Tween-80 as a stabilizer. [156], Copyright 2009. Reproduced with permission from John Wiley & Sons Inc.

Fig. 13. TEM images of surface-patterned fibrous POT (a) before and (b) after Au deposition, [157], Copyright 2011. Reproduced with permission from John Wiley & Sons Inc.

Fig. 14. (a) Schematic illustration of the formation of Fe_3O_4/PANI/noble metal nanoparticle/*m*-SiO_2 core/shell spheres and (b) a typical TEM image of Fe_3O_4/PANI/Au/*m*-SiO_2 core/shell spheres. [160], Copyright 2014. Reproduced with permission from the Royal Society of Chemistry.

Fig. 15. Schematic illustration of the formation of POT-Au core-shell hybrids at different concentrations of surfactant. [165], Copyright 2010. Reproduced with permission from John Wiley & Sons Inc.

Fig. 16. (a) Schematic illustration of the transformation of POMA-Au core-shell into yolk–shell nanostructures by a swelling–evaporation strategy. TEM images of POMA-Au (b and c) core–shell and (d and e) yolk–shell nanostructures. [168], Copyright 2014. Reproduced with permission from the Royal Society of Chemistry.

Fig. 17. (a) Schematic illustration of the AD of asymmetric POMA–Au core–shell hybrids. (b–g) TEM images of asymmetric POMA–Au core–shell hybrids (b, d, f) before and (c, e, g) after swelling–evaporation processes with different ADs: (b, c) 0.8, (d, e) 0.5 and (f, g) 0.1. [170], Copyright 2014. Reproduced with permission from the Royal Society of Chemistry.

Fig. 18. Illustrations of ideal core-shell nanoparticles (a), in contrast to nanoparticles that experiences aggregation before (b) or after (c) the encapsulation process; and proposed mechanisms of our encapsulation methods: (d) addition of SDS before aniline prevents Au nanoparticle aggregation and allows single encapsulation upon polymerization; (e) in the absence of SDS, aniline-Au nanoparticles mixture leads to linear aggregation that can be controllably terminated by SDS addition. Subsequent polymerization encapsulates the linearly aggregated cores. [171], Copyright 2009. Reproduced with permission from the Royal Society of Chemistry.

Fig. 19. (a) Schematics illustrating multi-generation growth of Au dendritic nanoparticles by using Au nanoparticles and Au nanorods as seeds, respectively; (b–d) TEM images of G1, G2, and G3 dendritic nanoparticles, respectively, by sequential growth from Au nanoparticles seeds; (e–g) TEM images of G1, G2, and G3 dendritic nanoparticles

grown from Au nanoparticles. Scale bars: 100 nm. [177], Copyright 2010. Reproduced with permission from the Royal Society of Chemistry.

Fig. 20. (a) Schematics illustrating the fabrication of PANI-Au yolk-shell nanoparticles. TEM images of (b, c) OANI-Au core-shell hybrids at low and high magnification, respectively. (d) IR spectra of (1) Au-OANI and (2) Au-PANI hybrids (asterisks indicate peaks of interest). (e, f) After treating sample (b) with chloroauric acid for 6 h, imaged at low and high magnification, respectively; and (g) after etching sample (e) with 2-propanol for 2 h. [179], Copyright 2012. Reproduced with permission from the American Chemical Society.

Fig. 21. (a) Schematic illustrations of the PTH-Au core-shell nanoparticles and the Au@vesicle nanoparticles. TEM images of (b) the Au@PTH nanoparticles, [SDS] = 5.0 mM, t = 12 h and (c) Au@vesicle nanoparticles, [SDS] = 2.5 mM, t = 12 h. [181], Copyright 2011. Reproduced with permission from the Royal Society of Chemistry.

Fig. 22. Triple-layer PANI-perylene-Au nanohybrids: (a) Schematics of the two-step synthesis; (b, c) TEM images of nanohybrids grown from 60 nm Au nanoparticles; (d) nanohybrids grown from 100 nm Au nanoflowers. Controlled perylene release: (e) schematic illustration; (f, g) TEM images of yolk-shell PANI-Au after complete release of perylene; (h) TEM image of PANI-perylene-Au after partial release. [183], Copyright 2011. Reproduced with permission from John Wiley & Sons Inc.

Fig. 23. (a) Transformation of PANI-Au into (PANI+PSPAA)-Au in DMF/H_2O solution; (b) and (c) TEM images of the typical (PANI+PSPAA)-Au with multiple petals at low and high magnification. [184], Copyright 2011. Reproduced with permission from the Royal Society of Chemistry.

Fig. 24. (a) TEM and (b) HR-TEM images of poly(2-aminothiophenol)-stabilized Au nanoparticles. Scale bar: (a) 20 nm, (b) 4 nm [222]. Copyright 2009. Reproduced with permission from the American Chemical Society.

Fig. 25. (a) SEM images of the PANI-Au hybrids (inset: larger scale magnification SEM image); (b) A photograph of native dandelion spheres; TEM images of the dandelion-like PANI-Au hybrids: (c) at low magnification; (d) at high magnification (inset: an SAED pattern). [224], Copyright 2011. Reproduced with permission from Elsevier Ltd.

Fig. 26. (a) Illustration of the proposed formation mechanism of PANI hollow nanospheres with incontinuous multicavities. (b) FE-SEM and (c) TEM images of PANI hollow nanospheres. [238], Copyright 2012. Reproduced with permission from the American Chemical Society.

Fig. 27. SEM images showing the size and morphology of PANI-Au hybrids prepared by mixing 2.5 mM $AuCl_3$ and 0.05 M aniline (a) and with additional 0.05 M PVP (b). [239], Copyright 2012. Reproduced with permission from the American Chemical Society.

Fig. 28. (a) Low- and (b) high-magnification TEM images, HR-TEM images taken (c) at the edge and (d) on the body of the prepared PANI-Au hybrids. Reaction time: 1 h. [251], Copyright 2012. Reproduced with permission from the Royal Society of Chemistry.

Fig. 29. Proposed mechanism of the formation of PANI-Pt nanofilms. [263], Copyright 2005. Reproduced with permission from Elsevier Ltd.

Fig. 30. (a) Schematic illustration of the process for fabrication 2D patterned conducting PANI-Au hybrid nanobowl sheet with PS spheres as template. (b) TEM image of the PANI-Au nanobowl sheet. [266], Copyright 2009. Reproduced with permission from Elsevier Ltd.

Fig. 31. (a) Plot of $\ln(c_t/c_0)$ of 4-NP against time using different catalysts. (b) Synthesis yield of 4-AP in the successive reactions with different catalysts. [170], Copyright 2014. Reproduced with permission from the Royal Society of Chemistry.

Fig. 32. (a) Magnetic control of the charge transport across the PANI/Au-γ-Fe_2O_3 hybrids. (b) Electrical contacting of glucose oxidase (GOx) by the PANI-modified electrode and the bioelectrocatalytic activation of the oxidation of glucose. (c) Cyclic voltammograms corresponding to the PANI/Au-γ-Fe_2O_3 hybrids: a) in the presence of GOx, without glucose; b) in the presence of GOx and glucose, 80 mM, in the absence of the external magnet; c) in the presence of GOx and glucose, 80 mM, in the presence of the external magnet. All data were recorded in 0.2 M phosphate buffer, pH 7.3, in the presence of GOx (2 mg mL^{-1}), scan rate 5 mV s^{-1}, under argon. [25], Copyright 2007. Reproduced with permission from John Wiley & Sons Inc.

Fig. 33. Schematics of construction of the horseradish peroxidase–Au nanoparticle–PANI

nanowire sensing biofilm and the *in situ* detection. [47], Copyright 2011. Reproduced with permission from the Royal Society of Chemistry.

Fig. 34. Proposed schematics for the fabrication of Au nanoparticle–PANI–Au hybrids to immobilize anti-PSA to detect PSA. [82], Copyright 2012. Reproduced with permission from the Royal Society of Chemistry.

Fig. 35. The structure of the PANI nanofiber-Au nanoparticle bistable memory device (a). Schematic structure of a PANI nanofiber-Au nanoparticle after the application of +3 V (b). An increase in charge transfer from PANI to the Au nanoparticles is believed to occur. [122], Copyright2005. Reproduced with permission from the American Chemical Society.

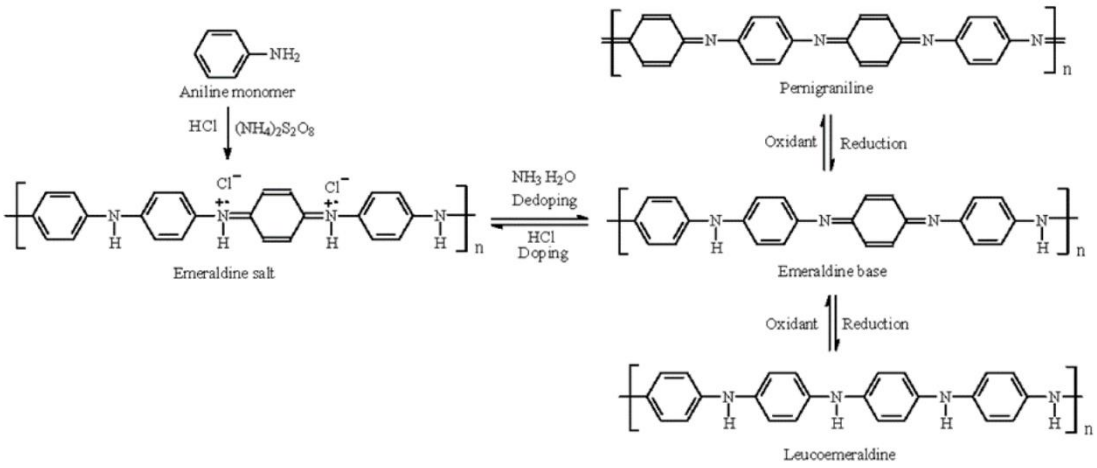

Figure 1

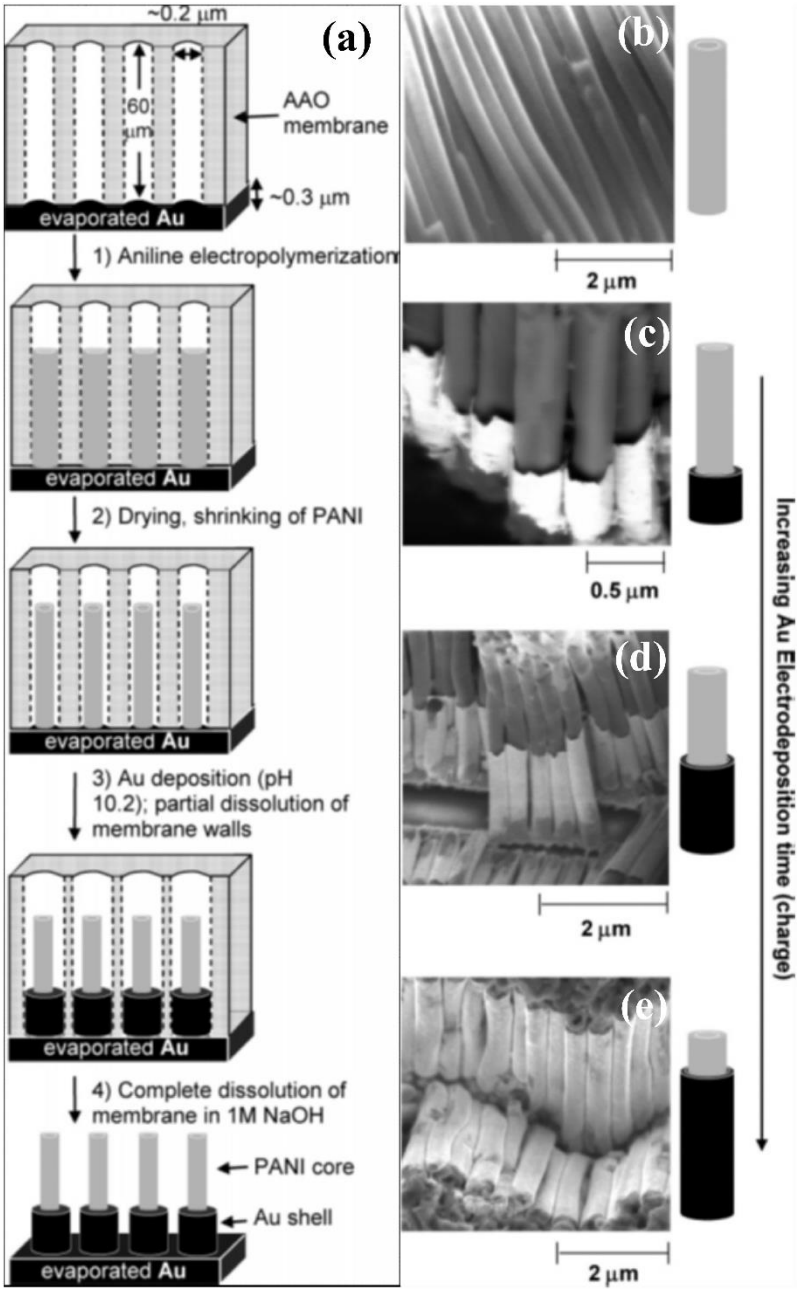

Figure 2

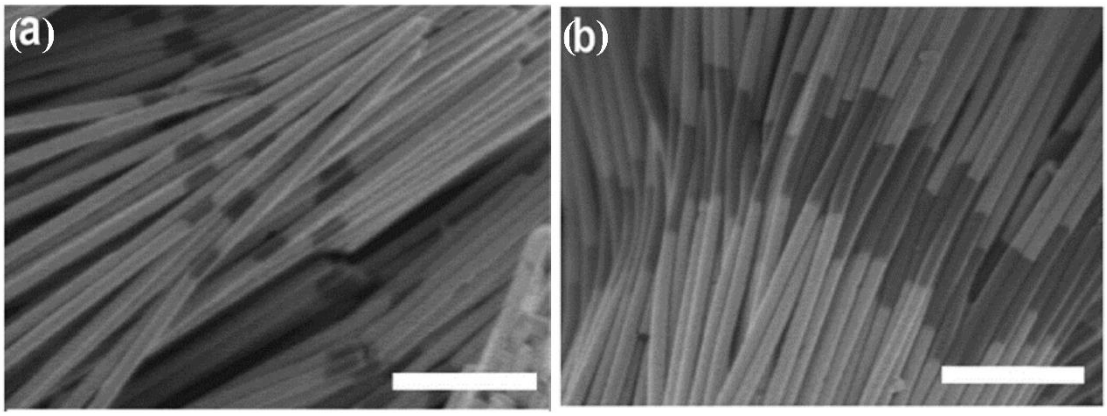

Figure 3

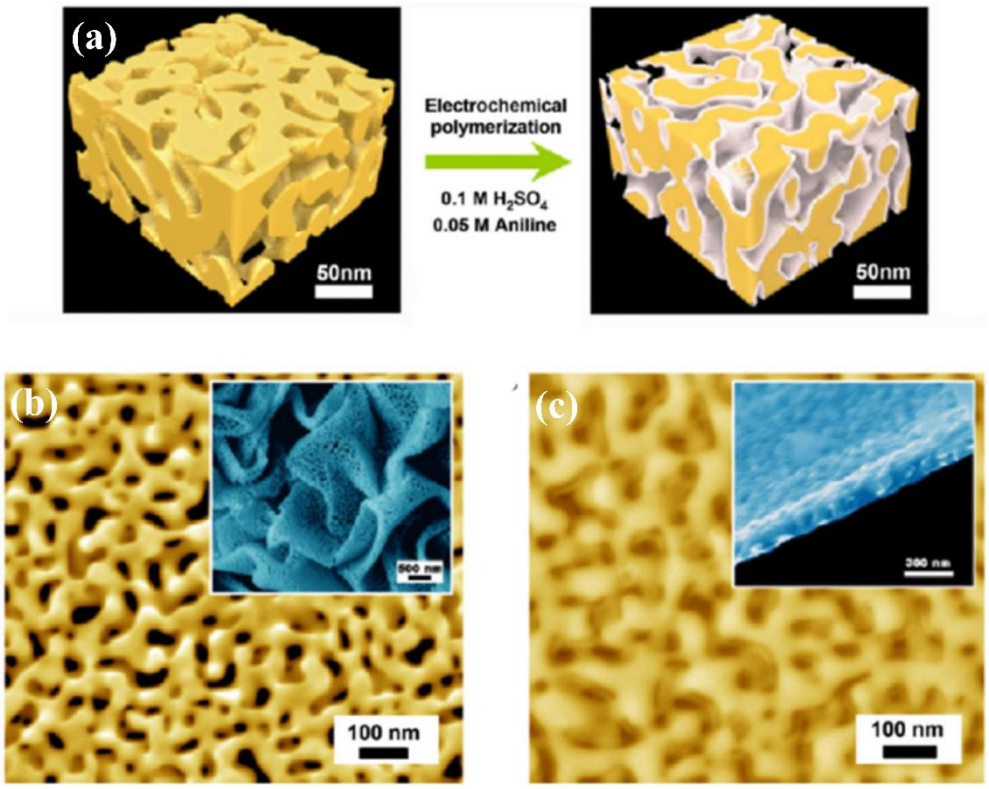

Figure 4

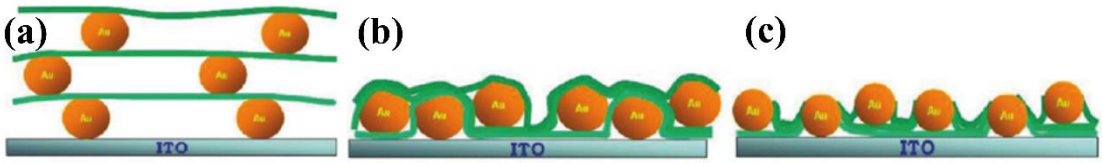

Figure 5

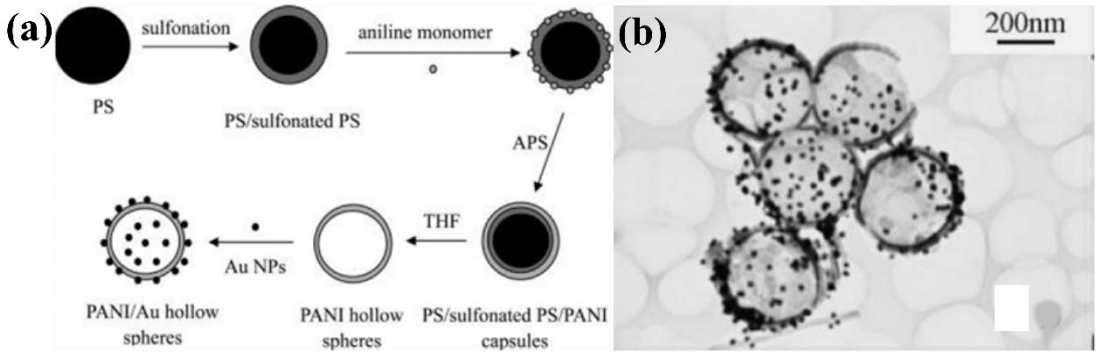

Figure 6

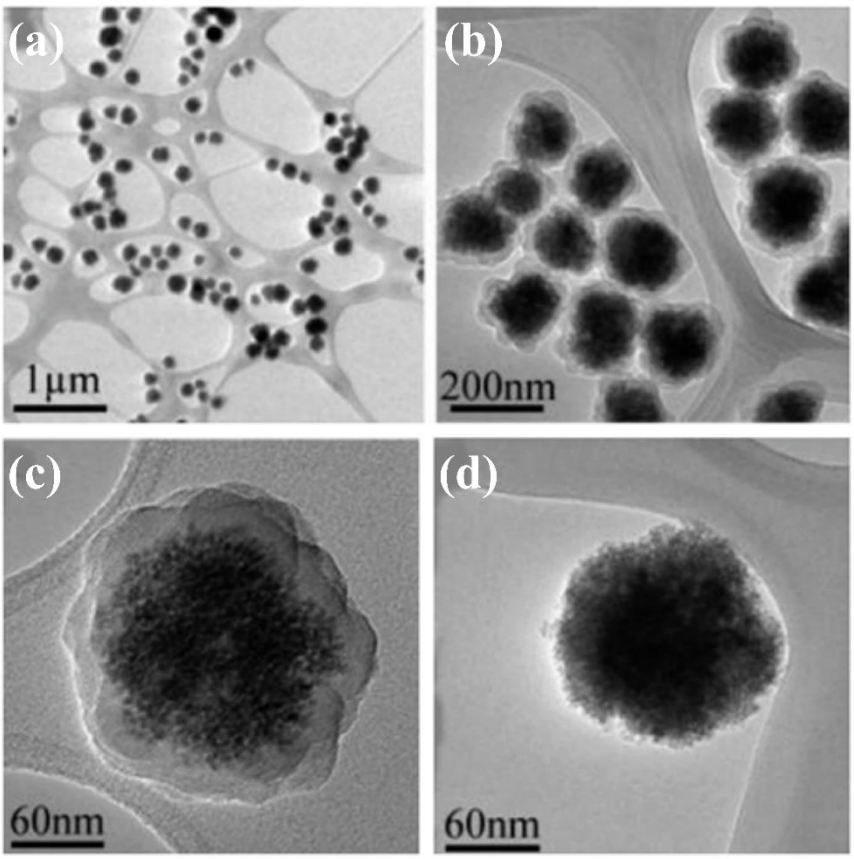

Figure 7

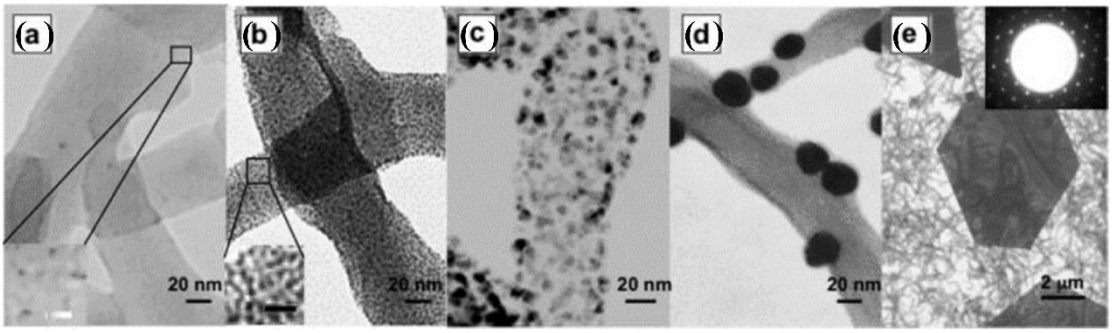

Figure 8

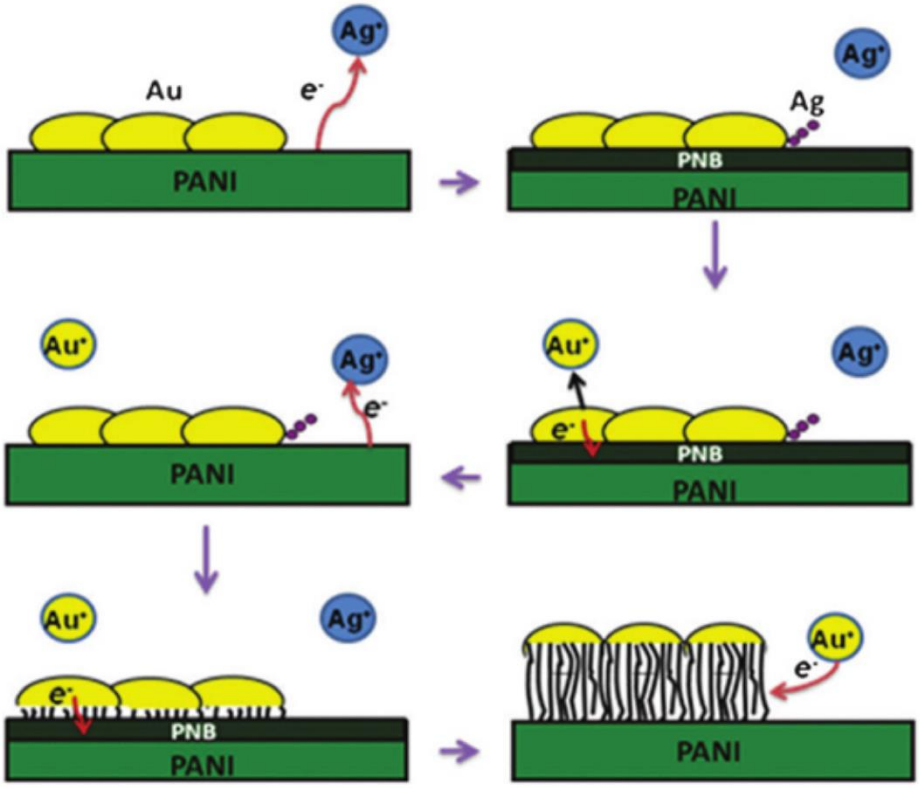

Figure 9

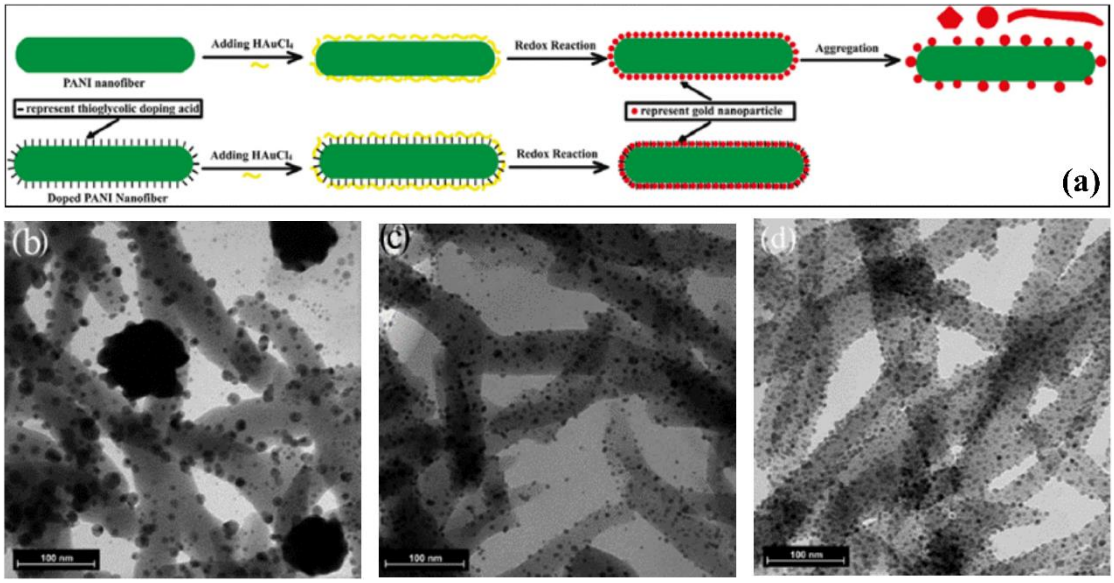

Figure 10

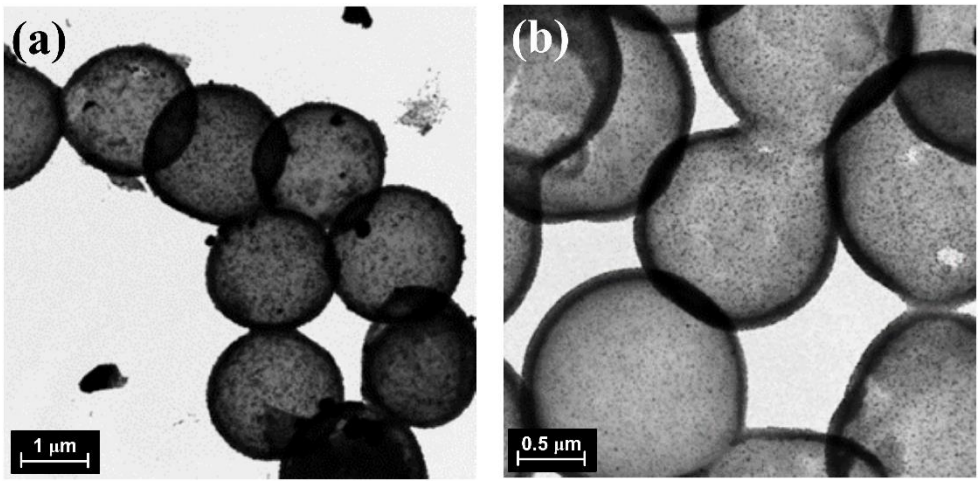

Figure 11

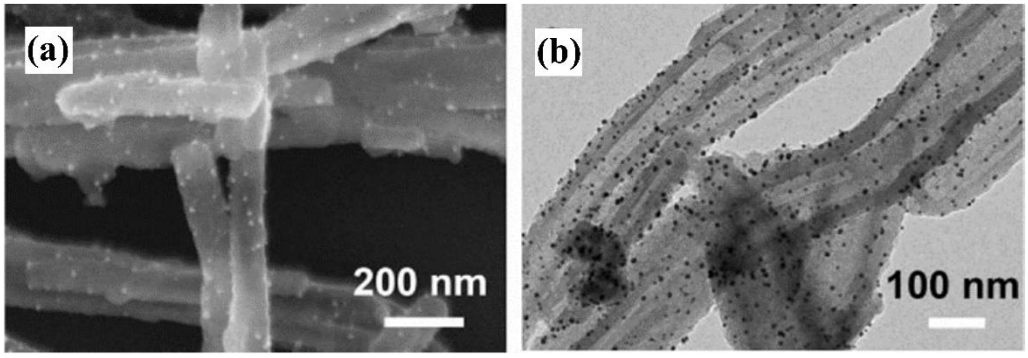

Figure 12

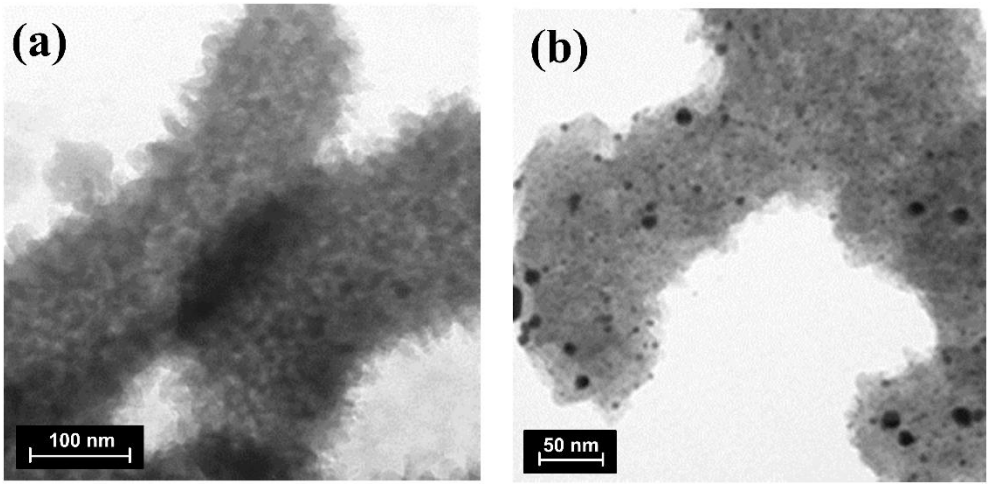

Figure 13

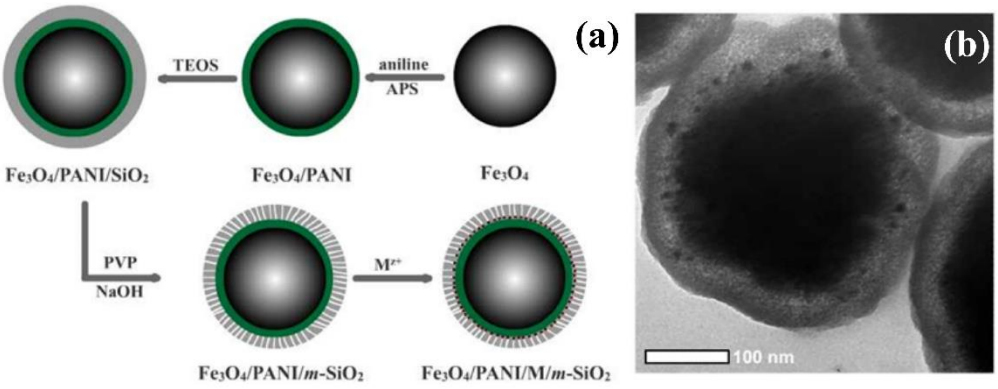

Figure 14

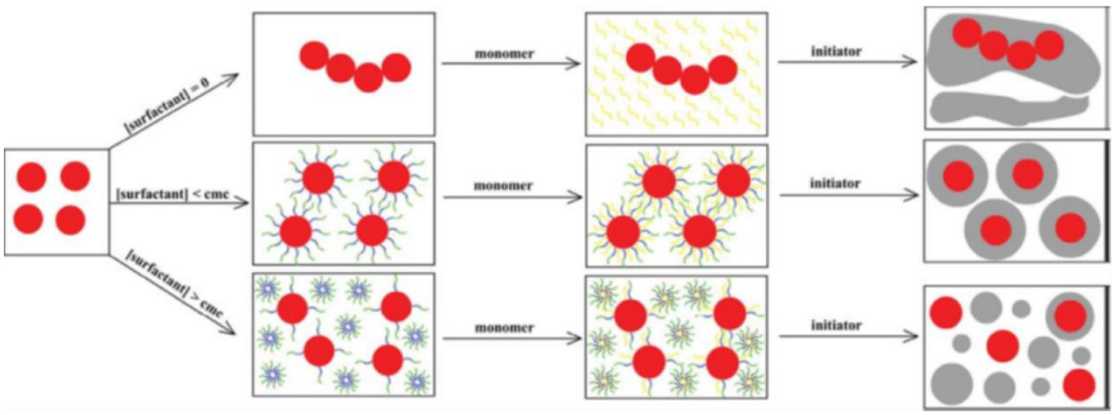

Figure 15

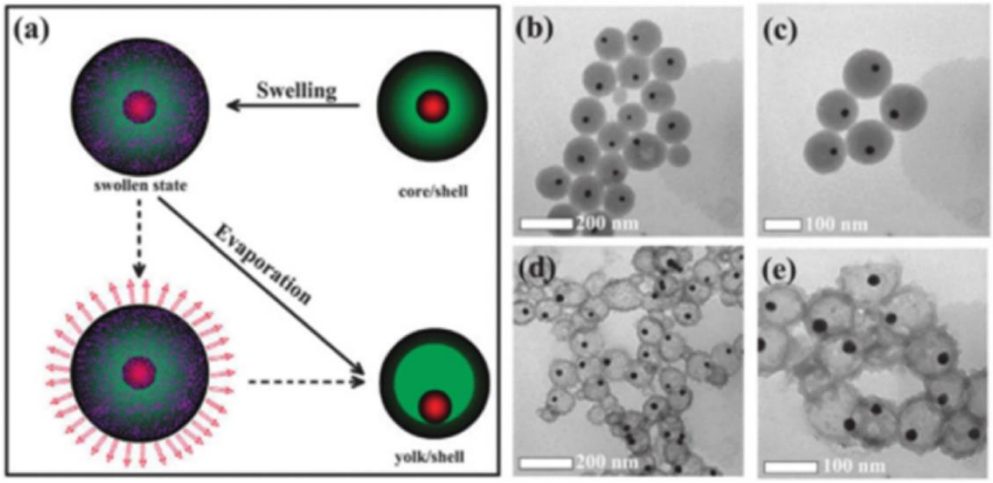

Figure 16

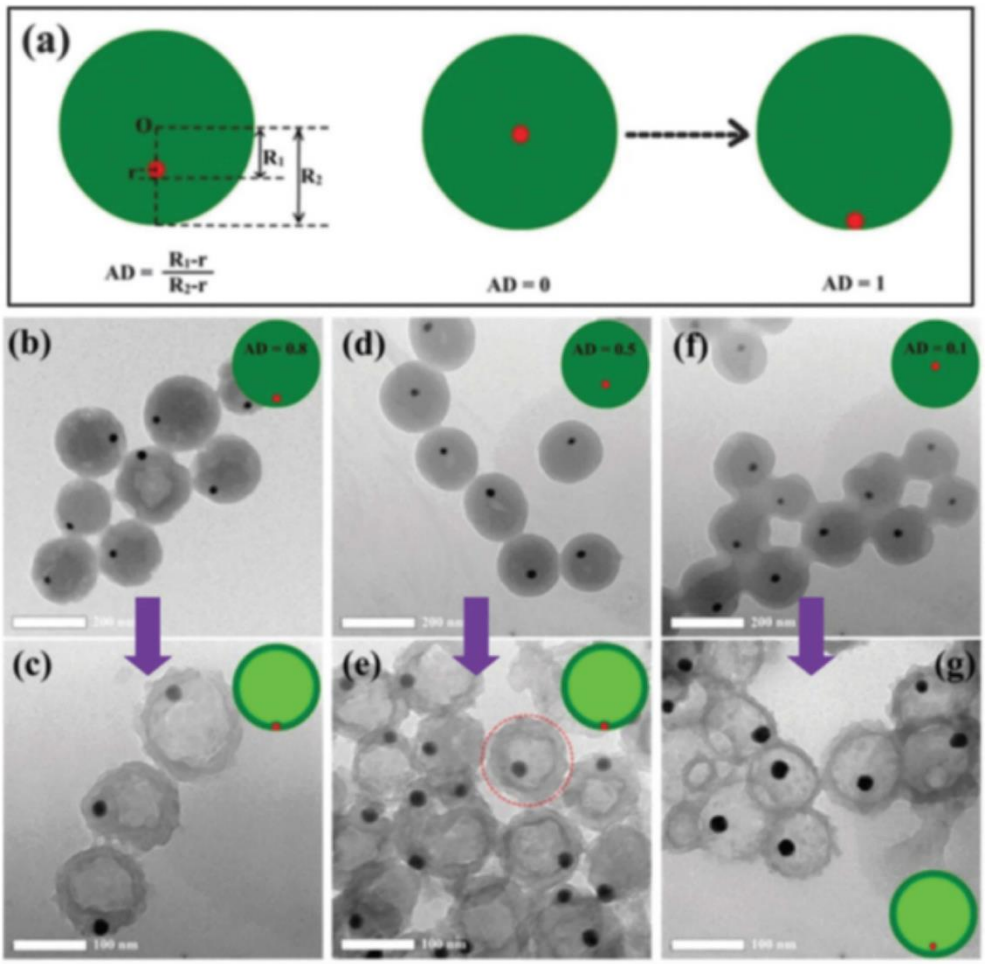

Figure 17

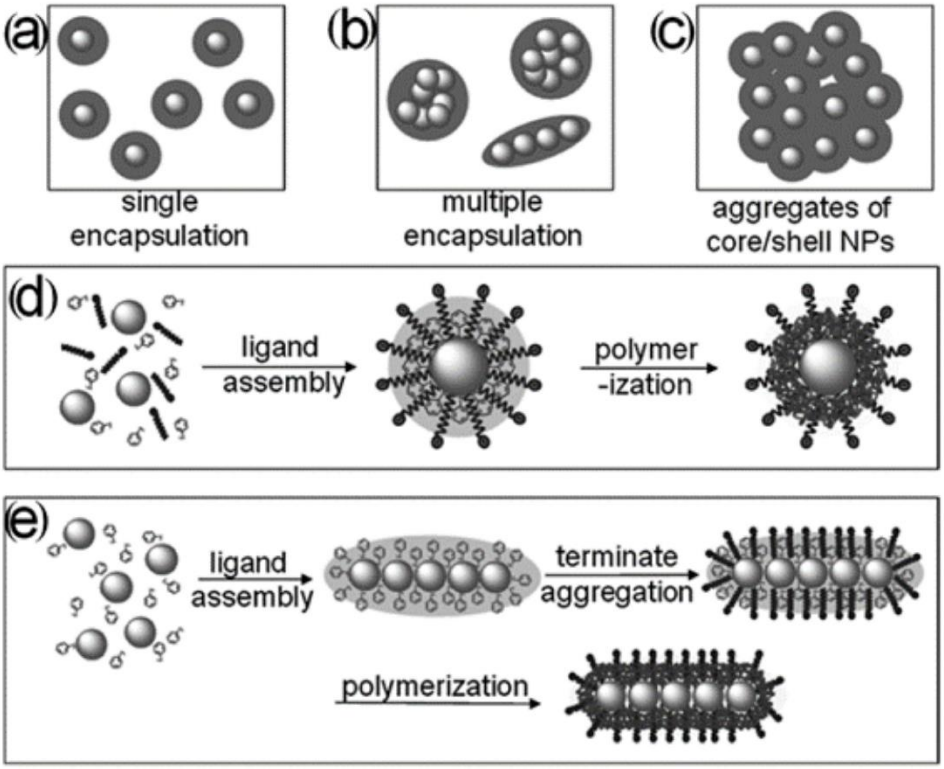

Figure 18

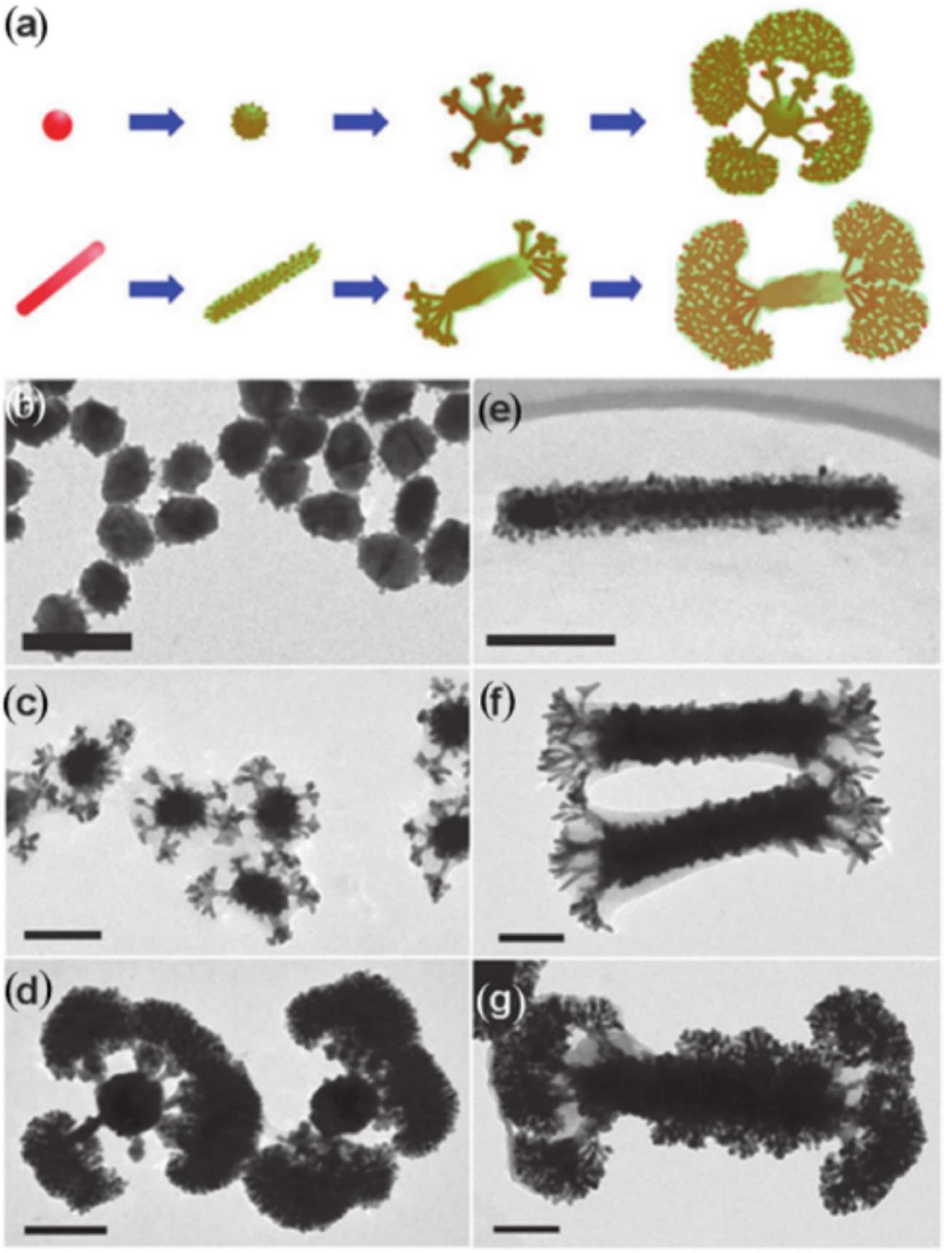

Figure 19

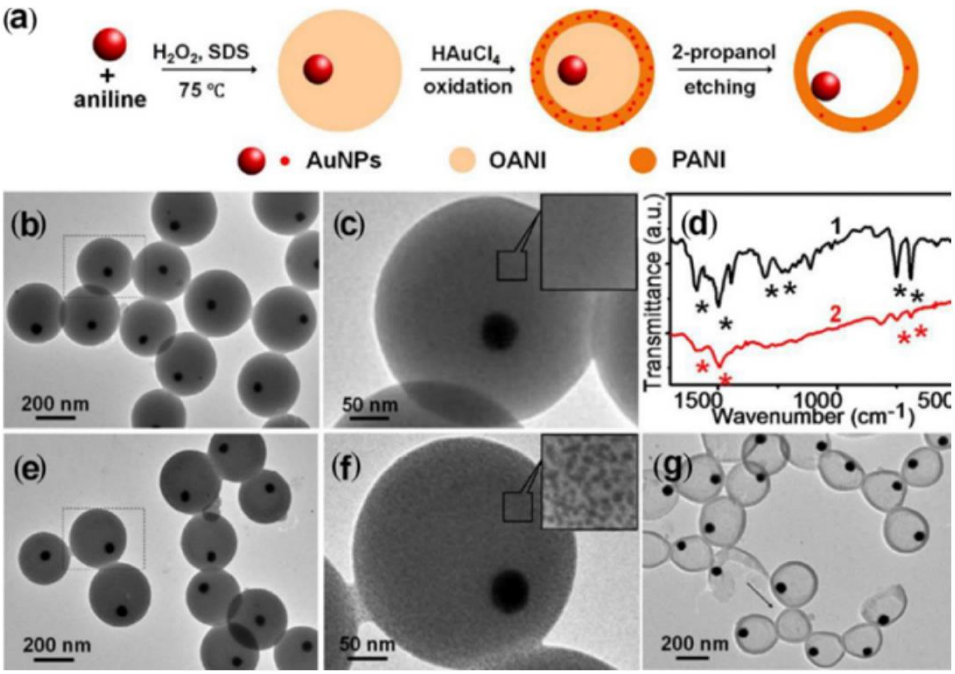

Figure 20

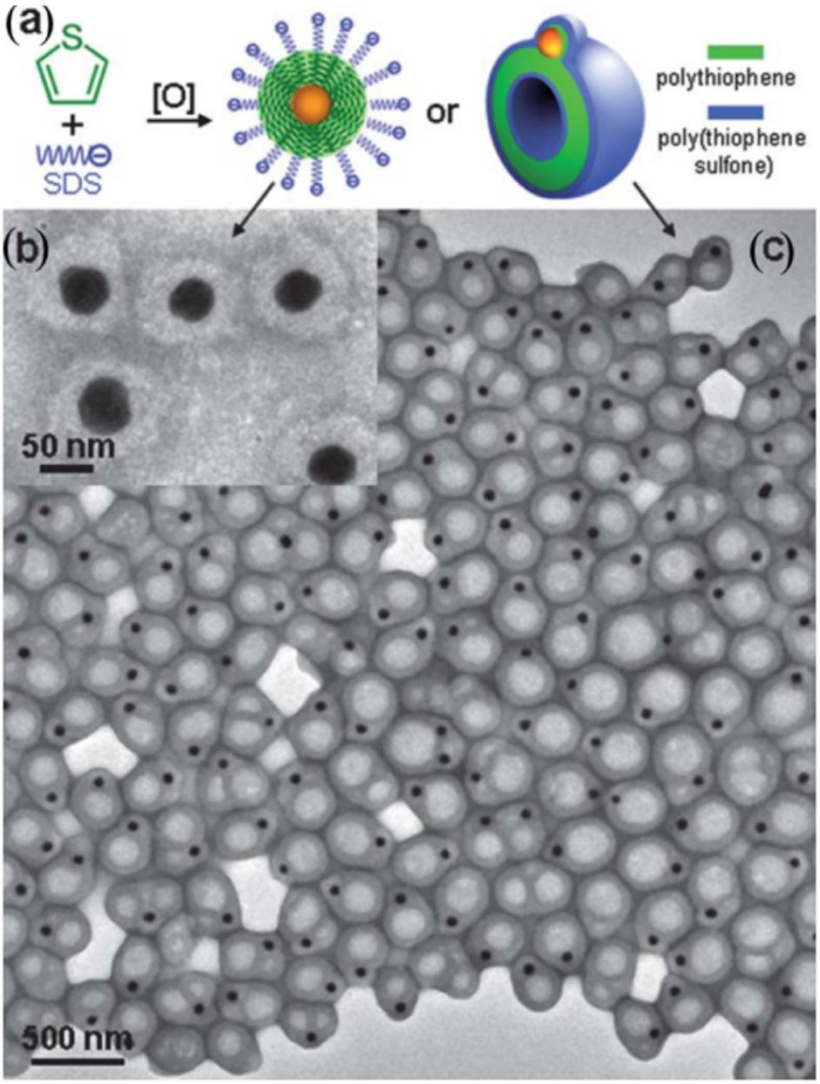

Figure 21

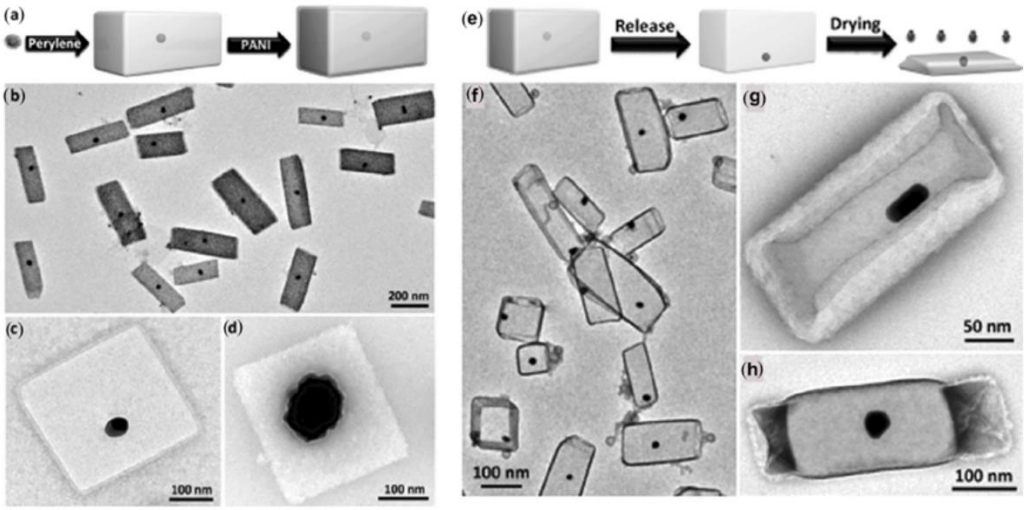

Figure 22

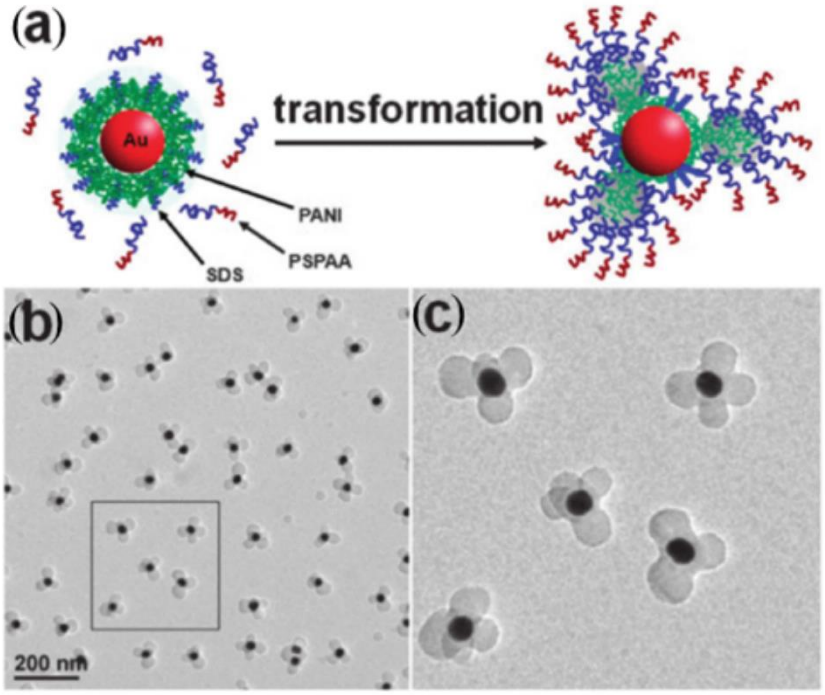

Figure 23

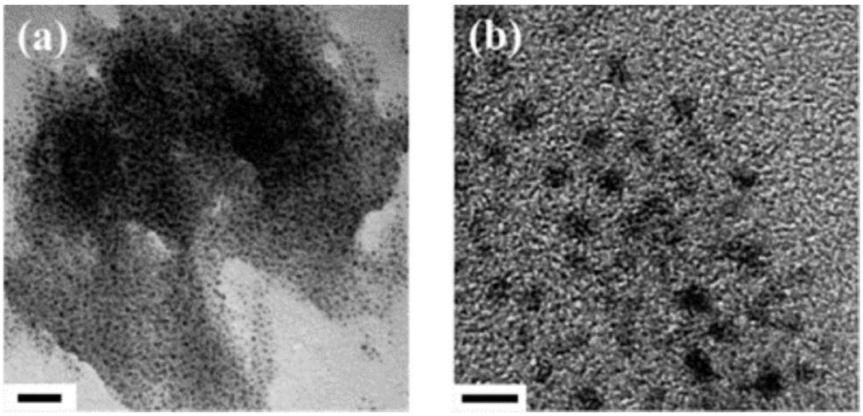

Figure 24

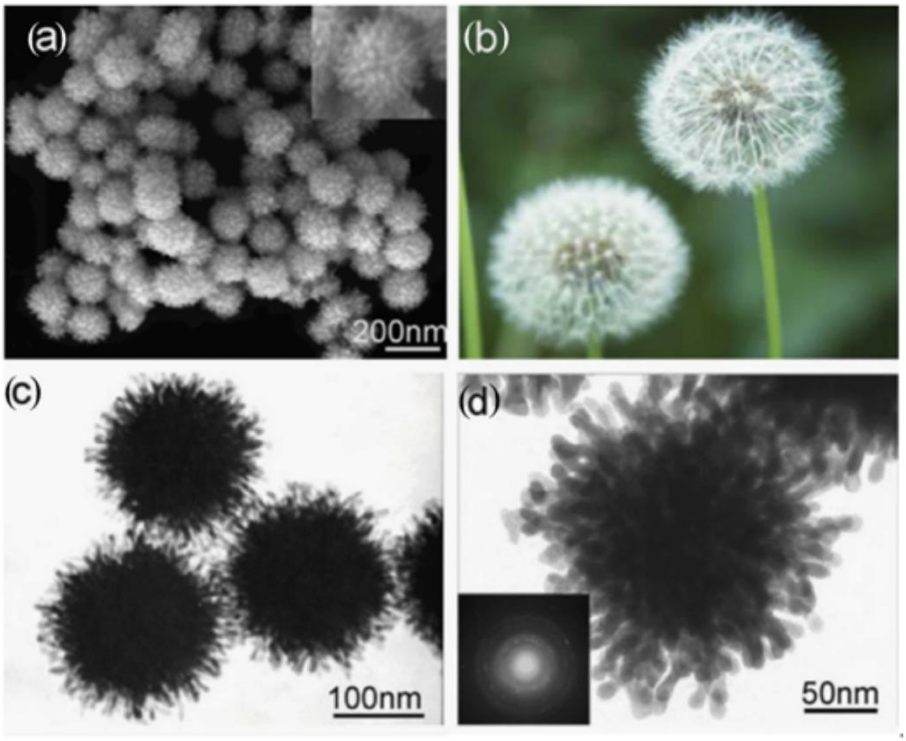

Figure 25

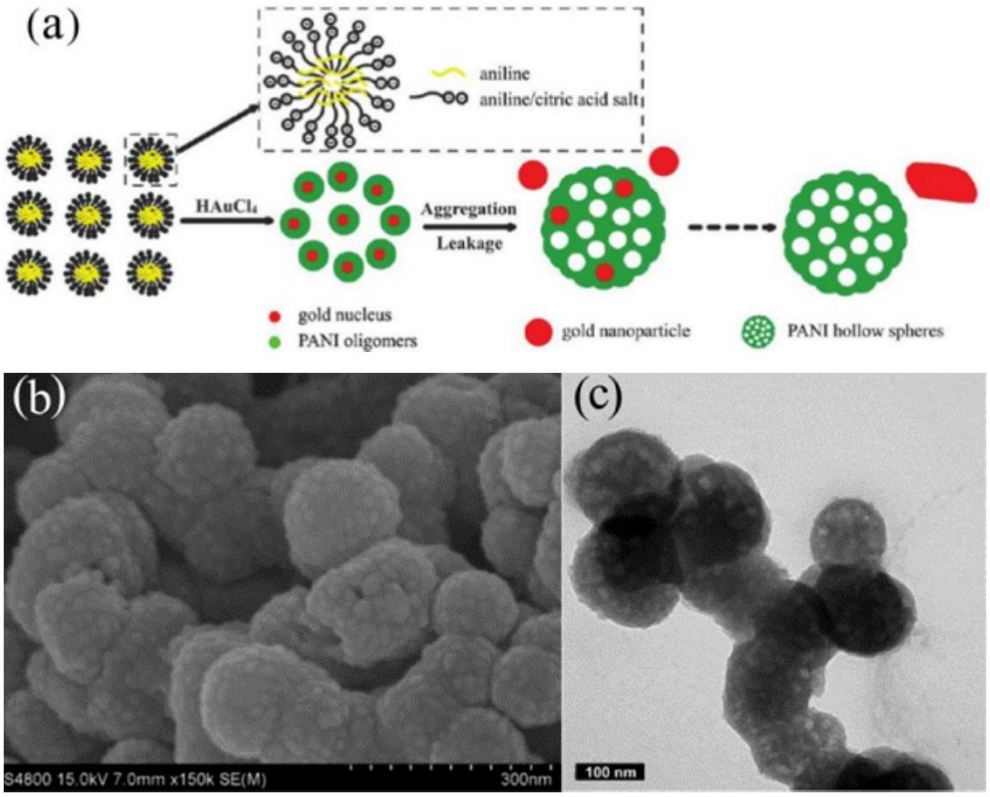

Figure 26

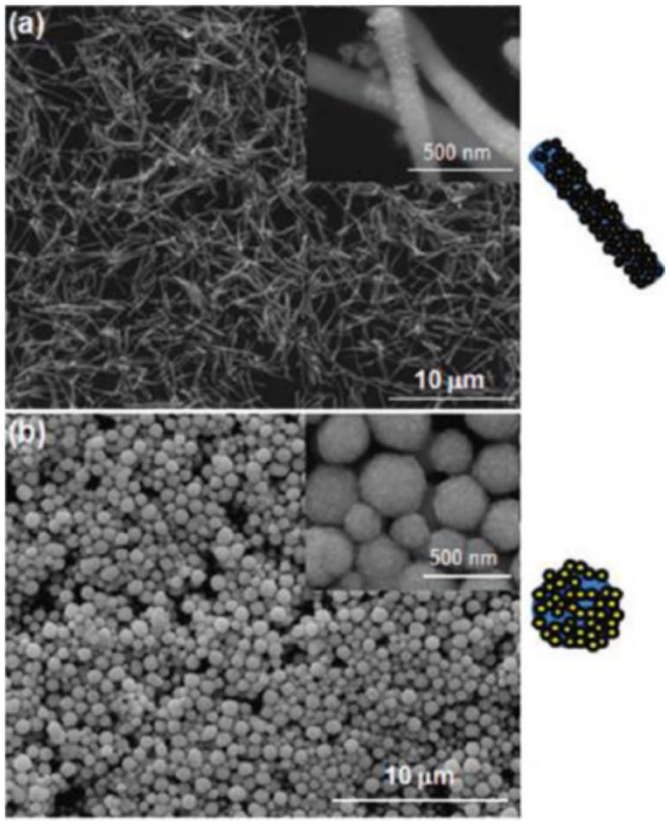

Figure 27

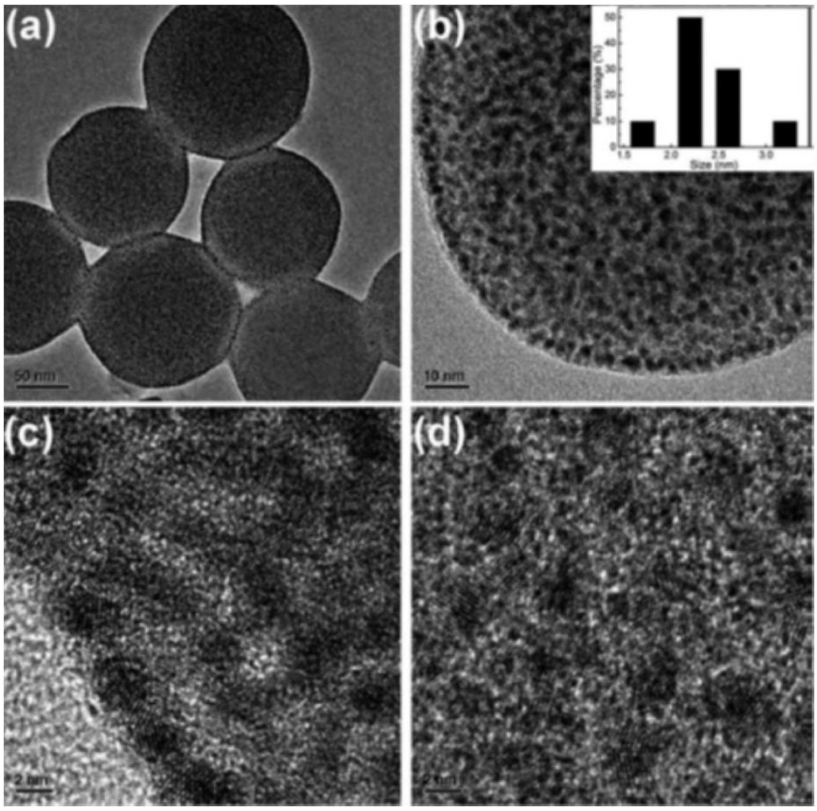

Figure 28

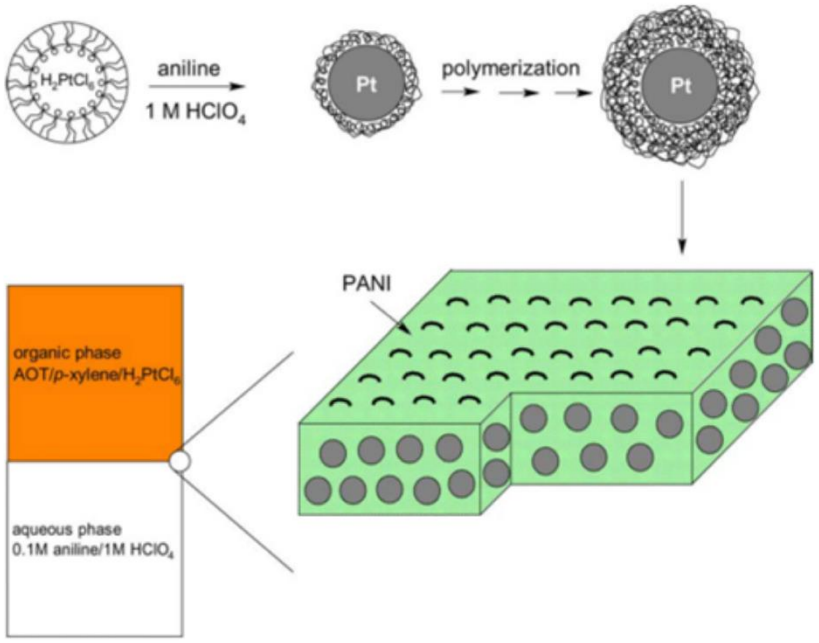

Figure 29

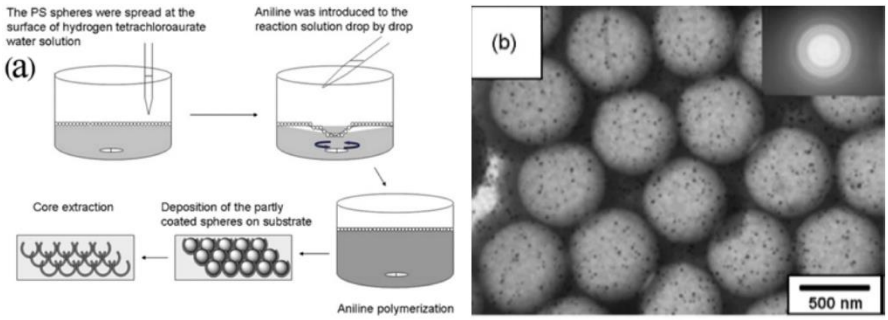

Figure 30

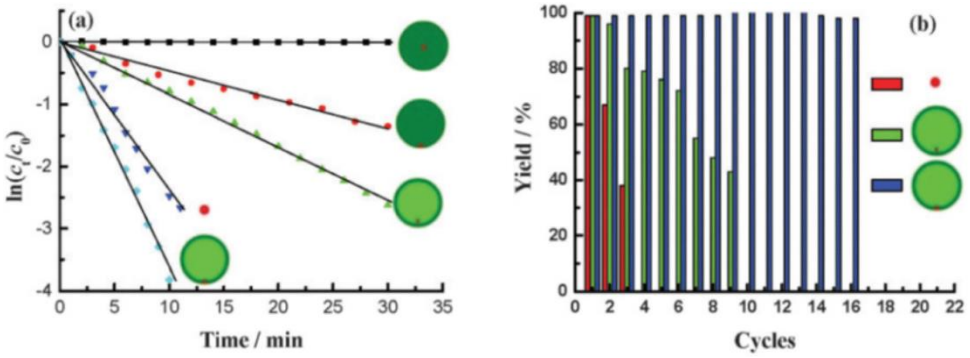

Figure 31

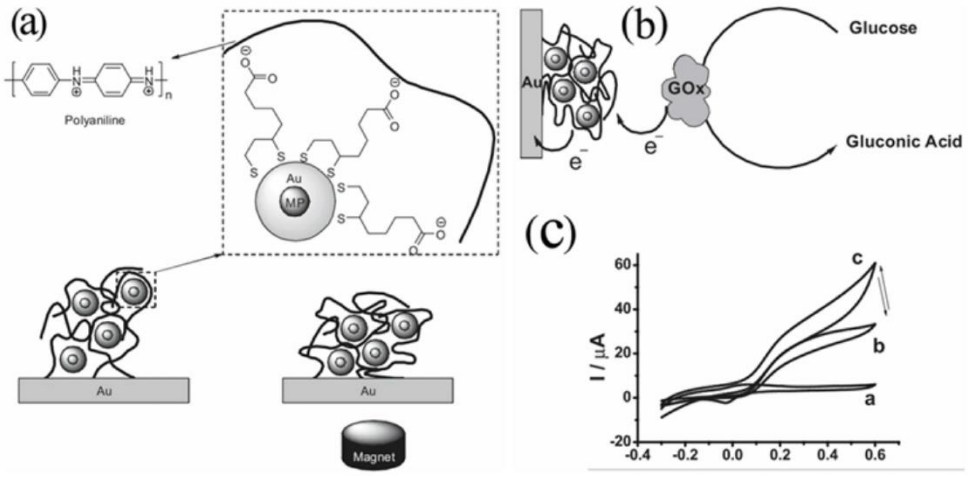

Figure 32

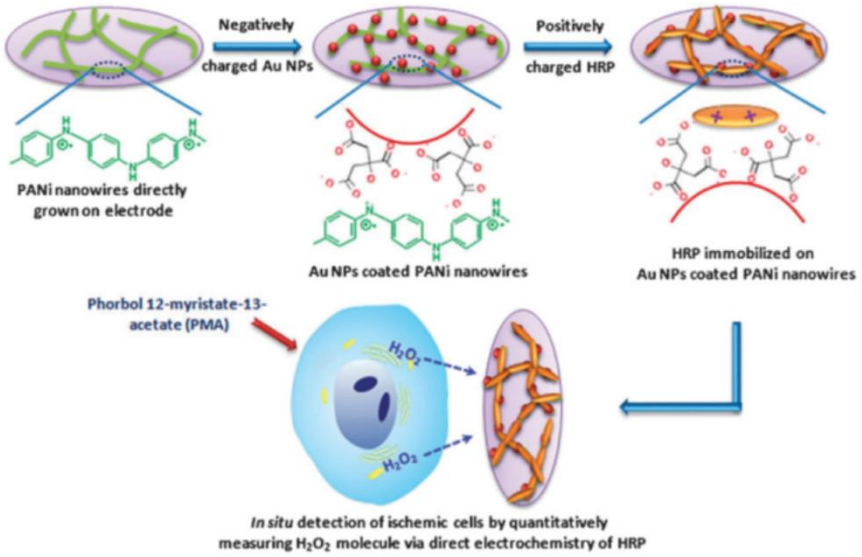

Figure 33

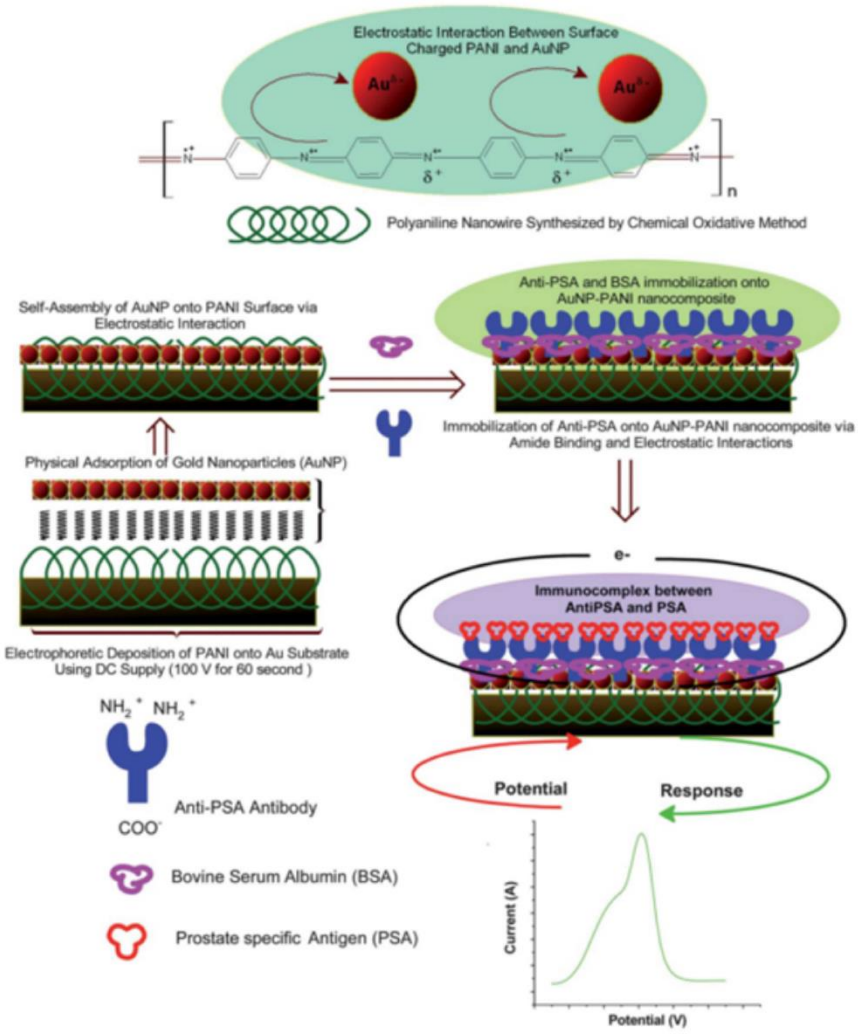

Figure 34

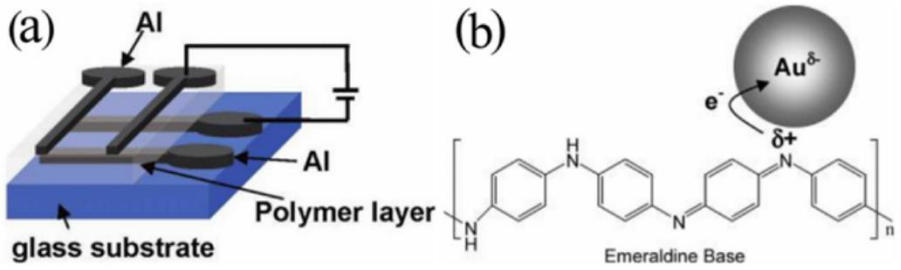

Figure 35

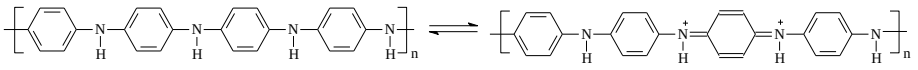

Leucoemeraldine Emeraldine salt (1)

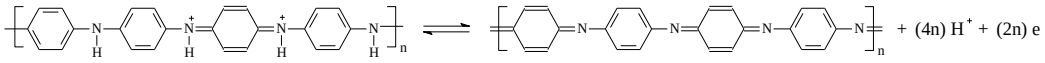

Emeraldine salt Pernigraniline (2)

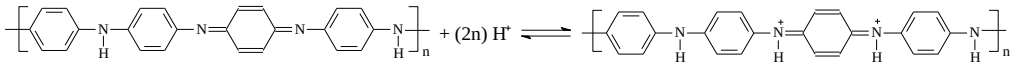

Emeraldine base Emeraldine salt (3)

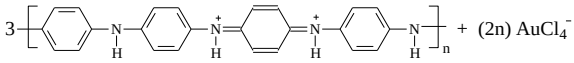

Emeraldine salt

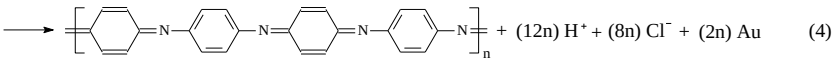

Pernigraniline (4)

Table 1 A comparison of different strategies involved in the synthesis of CP-NMNP hybrids.

Methods	Feature	Advantage	Limitation
CPs and NMNPs	Simple mixing of pre-synthesized CPs and NMNPs	Pre-designed size and morphology of CPs and NMNPs	Tedious process, weak interactions, possible aggregation of individual components
CPs and noble metal ions	*In situ* reduction of noble metal ions by CPs	Controllable geometry of CP-NMNP hybrids with pre-designed size and morphology of CPs	Weak control over size and amount of NMNPs
Monomers and NMNPs	*In situ* oxidative polymerization of monomers in the presence of NMNPs	Pre-designed size and morphology of NMNPs with controllable CPs thickness	Limited hybrid configuration of typical core-shell nanostructures
Monomers and noble metal ions	Simultaneous formation of CPs and NMNPs	Simple, economic and environmentally friendly process with diverse hybrid configurations and compact interactions between CPs and NMNPs	Lack in rational control over size and morphology of individual components and hybrids